

JOURNAL OF THE  
**Electrochemical  
Society**

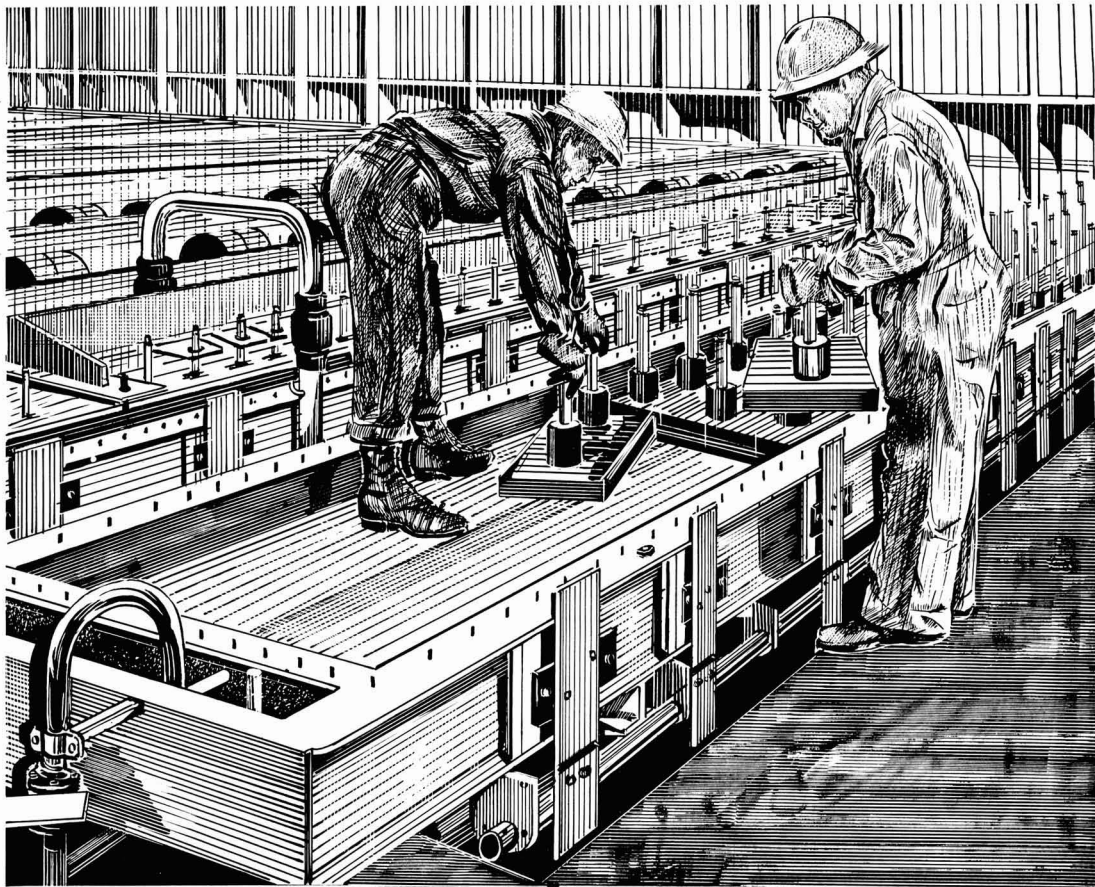
Vol. 105, No. 10

October 1958

LIBRARY  
OCT 9 1958  
N C E I

แผนกห้องสมุด วิศวกรรมศาสตร  
คณะวิศวกรรมศาสตร์





## Preview of production

Top efficiency of high capacity mercury cells depends upon the special abilities of the men who build and maintain them.

Another vital factor in high productivity is the efficiency of GLC Anodes which are "custom made" for individual cell requirements.

**FREE**—This illustration of cell maintenance has been handsomely reproduced with no advertising text. We will be pleased to send you one of these reproductions with our compliments. Simply write to Dept. J-10.

ELECTRODE  
**GLC**<sup>®</sup>  
DIVISION

**GREAT LAKES CARBON CORPORATION**

18 EAST 48TH STREET, NEW YORK 17, N.Y. OFFICES IN PRINCIPAL CITIES

## EDITORIAL STAFF

R. J. McKay, Chairman, Publication Committee  
Cecil V. King, Editor  
Norman Hackerman, Technical Editor  
Ruth G. Sterns, Managing Editor  
U. B. Thomas, News Editor  
H. W. Salzberg, Book Review Editor  
Natalie Michalski, Assistant Editor

## DIVISIONAL EDITORS

W. C. Vosburgh, Battery  
Milton Stern, Corrosion, I  
R. T. Foley, Corrosion, II  
T. D. Callinan, Electric Insulation  
Abner Brenner, Electrodeposition  
H. C. Froelich, Electronics  
D. H. Baird, Electronics—Semiconductors  
Sherlock Swann, Jr., Electro-Organic, I  
Stanley Wawzonek, Electro-Organic, II  
John M. Blocher, Jr., Electrothermics and Metallurgy, I  
A. U. Seybolt, Electrothermics and Metallurgy, II  
N. J. Johnson, Industrial Electrolytic  
C. W. Tobias, Theoretical Electrochemistry, I  
A. J. deBethune, Theoretical Electrochemistry, II

## REGIONAL EDITORS

Howard T. Francis, Chicago  
Joseph Schulein, Pacific Northwest  
J. C. Schumacher, Los Angeles  
G. W. Heise, Cleveland  
G. H. Fetterley, Niagara Falls  
Oliver Osborn, Houston  
Earl A. Gulbrandsen, Pittsburgh  
A. C. Holm, Canada  
J. W. Cuthbertson, Great Britain  
T. L. Rama Char, India

## ADVERTISING OFFICE

ECS  
1860 Broadway, New York 23, N. Y.

## ECS OFFICERS

Sherlock Swann, Jr., President  
University of Illinois, Urbana, Ill.  
W. C. Gardiner, Vice-President  
Olin Mathieson Chemical Corp., Niagara Falls, N. Y.  
R. A. Schaefer, Vice-President  
Cleveland Graphite Bronze Div., Clevite Corp., Cleveland, Ohio  
Henry B. Linford, Vice-President and Interim Secretary  
Columbia University, New York, N. Y.  
Lyle I. Gilbertson, Treasurer  
Air Reduction Co., Murray Hill, N. J.  
Robert K. Shannon, Executive Secretary  
National Headquarters, The ECS, 1860 Broadway, New York 23, N. Y.

# Journal of the Electrochemical Society

OCTOBER 1958

VOL. 105 • NO. 10

## CONTENTS

### Editorial

University Teaching and Research..... 206C

### Technical Papers

- Lead-Acid Storage Batteries; Changes in Positive Active Material Density during Various Conditions of Service. *J. F. Dittmann and J. F. Sams*..... 553 ✓  
Self-Discharge Reactions in Lead-Acid Batteries. *P. Ruetschi and R. T. Angstadt*..... 555 ✓  
The Reduction of Passive Films by Hydrogen Diffusion through Steel. *R. T. Davis, Jr., and T. J. Butler*..... 563  
An Investigation of Chemical Variables Affecting the Corrosion of Copper. *W. D. Robertson, V. F. Nole, W. H. Davenport, and F. P. Talboom, Jr.*..... 569  
Some Observations on the Effect of the Interaction of Tantalum with Oxygen, Nitrogen, and Hydrogen. *R. Bakish*..... 574  
Room Temperature Tarnishing of Silver in Bromine and Iodine. *J. L. Weininger*..... 577  
Selective Oxidation of Al from an Al-Fe Alloy. *R. E. Grace and A. U. Seybolt*..... 582  
Particle Size and Efficiency of Electroluminescent Zinc Sulfide Phosphors. *W. Lehmann*..... 585  
Gold in Silicon. *G. Bemski and J. D. Struthers*..... 588  
Technique for Preserving Lifetime in Diffused Silicon. *S. J. Silverman and J. B. Singleton*..... 591  
Bonding Materials for Making Contacts to p-Type Silicon. *D. R. Mason and J. C. Sarace*..... 594  
Electrolytic Reduction of Cyanamide, II. The Nature of the Reduction of Cyanamide and Formamidine. *K. Odo, E. Ichikawa, K. Shimogai, and K. Sugino*..... 598  
The Measurement of Magnetic Fields in Aluminum Reduction Furnaces. *J. H. Kent*..... 603  
Destruction of Cyanide Wastes by Electrolytic Chlorination. *J. T. Byrne, W. S. Turnley, and A. K. Williams*..... 607

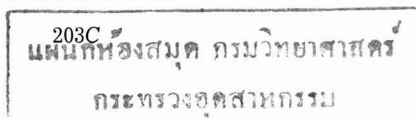
### Brief Communication

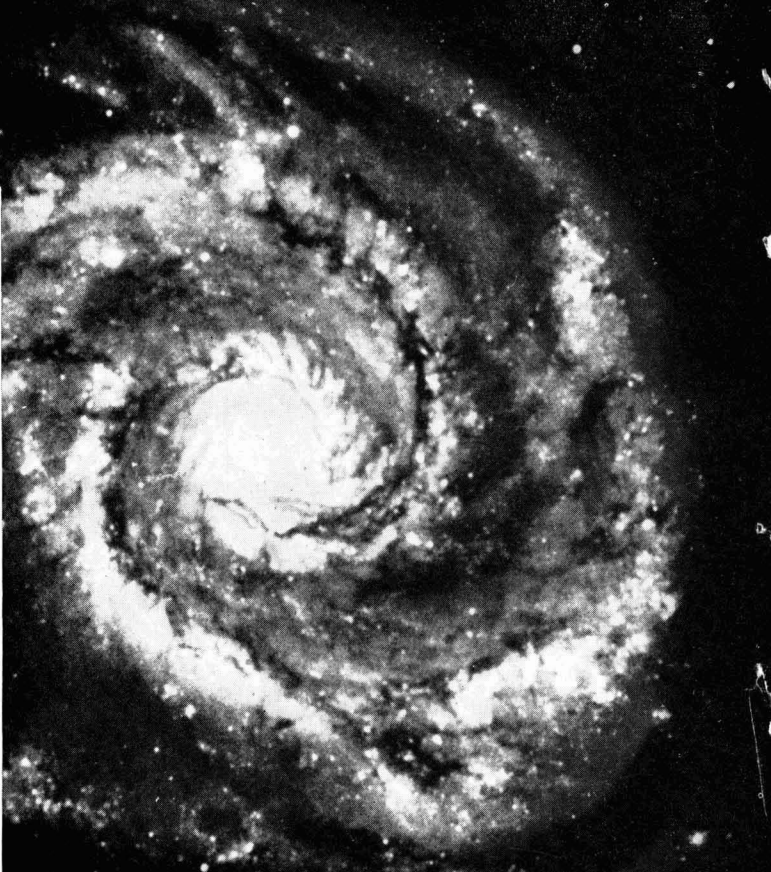
"Reaction of Hydrogen with Uranium." *W. M. Albrecht and M. W. Mallett*..... 610

### Current Affairs

- Report on the Second Congress of the European Corrosion Federation, Frankfurt, June 5-8, 1958. *R. Bakish*..... 209C  
Section News ..... 212C News Items ..... 216C  
Division News ..... 213C Literature from Industry ..... 217C  
Letter to the Editor ..... 213C Announcements from Publishers ..... 219C  
Committees of The ECS, 1958-1959 ..... 214C Employment Situation ..... 219C  
Personals ..... 215C ECS Future Meetings ..... 612

Published monthly by The Electrochemical Society, Inc., from Manchester, N. H., Executive Offices, Editorial Office and Circulation Dept., and Advertising Office at 1860 Broadway, New York 23, N. Y., combining the JOURNAL and TRANSACTIONS OF THE ELECTROCHEMICAL SOCIETY. Statements and opinions given in articles and papers in the JOURNAL OF THE ELECTROCHEMICAL SOCIETY are those of the contributors, and The Electrochemical Society assumes no responsibility for them. Noneductible subscription to members \$5.00; subscription to nonmembers \$18.00. Single copies \$1.25 to members, \$1.75 to nonmembers. Copyright 1958 by The Electrochemical Society, Inc. Entered as second-class matter at the Post Office at Manchester, N. H., under the act of August 24, 1912.





# Announcing

# GRACE SILICON

(ultra-high purity)

Whether you make or use silicon devices, a new standard of quality is now available to you through Grace—leader in chemical research and development.

Grace Silicon, manufactured by the Pechiney process, has an extremely low boron content as well as over-all ultra-high purity.

Other characteristics of Grace Silicon include uniform quality as verified by some of the nation's leading electronic manufacturers.

Wherever a semi-conductor of top quality is desired for rectifiers, transistors, diodes—get in touch with GRACE ELECTRONIC CHEMICALS, INC., at PLaza 2-7699 in Baltimore.

**GRACE ELECTRONIC CHEMICALS, INC.**

101 N. Charles St., Baltimore, Maryland



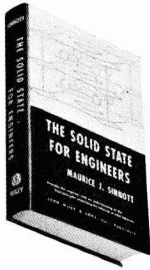
Subsidiary of W. R. GRACE & CO.



## 1. THE SOLID STATE FOR ENGINEERS

By MAURICE J. SINNOTT,  
University of Michigan

An accurate and convenient reference for problems concerning the choice and use of solid materials. Examines the ultimate structure of matter. Discusses the thermodynamic stability of solid structures, the rates at which changes occur between various states, and the important subjects of nucleation and growth. Includes: a factual survey of metallic, ionic, covalent, and molecular solids; a study of the electron and zone theories; optical and surface properties; and new information on luminescence, phosphorescence, and similar phenomena.

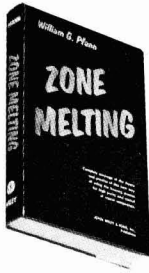


1958      522 pages      325 illus.      \$12.50

## 2. ZONE MELTING

By WILLIAM G. PFANN,  
Bell Telephone Laboratories

All the information you need to plan a zone melting process, or to decide whether one is feasible. Covers both theory and practice, and spells out the potentialities of crystallization methods as yet unexploited for controlling the purity and precise composition of metals. Covers: Normal Freezing and the Distribution Coefficient; Theory, Techniques, and Applications of Zone Refining; Continuous Zone Refining; Zone Leveling and Single Crystal Growth; Methods of Perturbing the Concentration; and Temperature-Gradient Zone Melting. A publication in the *Wiley Series on the Science and Technology of Materials*: J. H. Hollomon, Advisory Editor.



1958      236 pages      Illus.      \$7.50

## 3. CERAMIC FABRICATION PROCESSES

Edited by W. D. KINGERY, M.I.T.  
With 22 contributors.

Chock full of helpful information on ceramic research, development, and production. Based on lectures given at the 1956 M.I.T. Special Summer Program in Ceramics, the book combines scientific understanding with practical experience in these areas: Slip Casting; Pressure Fabrication; Plastic Forming; Drying and Firing; Some Special Processes; and Ceramic Microstructures. A *Technology Press Book*, M.I.T.



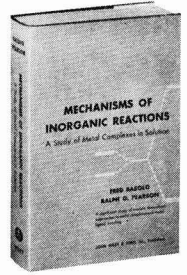
1958      235 pages      Illus.      \$9.50

## 4. MECHANISMS OF INORGANIC REACTIONS

A Study of Metal Complexes in Solution

By FRED BASOLO and  
RALPH G. PEARSON,  
both of Northwestern University

The newest theories on the dynamic, mechanistic aspects of the chemical reactions of coordination compounds. Explores recent advances in the mechanisms of substitution reactions of metal complexes, oxidation-reduction reactions, and metal ion catalysis. Applies the crystal field theory of metal-ligand bonding to problems associated with reactivity and mode of reaction metal complexes.

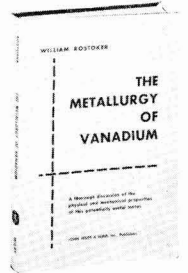


1958      426 pages      Illus.      \$11.75

## 5. THE METALLURGY OF VANADIUM

By WILLIAM ROSTOKER,  
Armour Research Foundation

An up-to-date progress report on this interesting metal. Explores its potential usefulness, and provides a comprehensive treatment of its extraction, properties, and processing. A handy reference for those who seek new materials for special applications. A publication in the *Wiley Series on the Science and Technology of Materials*: J. H. Hollomon, Advisory Editor.



1958      185 pages      \$8.50

## 6. PROGRESS IN SEMICONDUCTORS

Volume II

Edited by ALAN F. GIBSON, P. AIGRAIN, and  
R. E. BURGESS

The latest information on important aspects of semiconductor research by 13 top authorities.

1957      280 pages      Illus.      \$10.50

Send for your 10-day ON-APPROVAL copies of these books. Mail this coupon NOW!

JOHN WILEY & SONS, Inc.

440 Fourth Ave., New York 16, N. Y.

JES-108

Please send me a copy of the book(s) circled below to read and examine ON APPROVAL. Within 10 days I will either return the book(s), and owe nothing, or I will remit the full purchase price(s), plus postage.

1      2      3      4      5      6

Name .....

Address .....

City ..... Zone ..... State .....

SAVE POSTAGE! Check here if you ENCLOSE payment, in which case we will pay postage. Same return privilege, of course.



## University Teaching and Research

*I*N 1940, the Federal Government spent about \$15,000,000 for scientific research at colleges and universities; in 1958 the corresponding figure is close to \$500,000,000 (NSF Report 58-10, available from Superintendent of Documents, U. S. Government Printing Office, Washington, D. C., for 40¢). Of this sum, \$60,000,000 is for new facilities and major equipment, \$175,000,000 for University-operated research centers (such as the various National Laboratories), \$265,000,000 for research and development in the regular academic departments. It is estimated that as much as two-thirds of all research funds spent by institutions of higher learning in the United States today comes from the Federal Government. There is, of course, danger that the source of funds can steer the direction of research undesirably, and efforts are made to study this possibility and to avoid pressure except in the case of specific problems.

Much of the research in the last category mentioned above is carried out by advanced students under faculty supervision. Since only a fraction of the funds is allotted to "basic" research, the faculties must decide which problems can earn degree credit. Unlucky is the student who must work on one project for a living, do additional research for a thesis. At least, with Government contracts and grants, with fellowships and other funds provided by industry and private endowment, as well as the need for advanced students in teaching, the science major need not go hungry during his graduate career. In fact, there is keen competition for Ph.D. candidates and post-doctoral fellows, as witnessed by the departmental bulletin boards and by the office files.

There is great danger that too much faculty effort is being drained away from *teaching*. After all, the primary function of a college or university is to teach students at all levels, not just at the research level, and there is great need for devoted teachers who give proper care and attention to their undergraduate lectures, recitations, and laboratories. What has become of the "career instructor" who did little or no publishable research, but who was the mainstay of the undergraduate courses? It is a distinct mistake to hire *all* new faculty members with the bait of "directing research." W. E. Caldwell has protested<sup>1</sup> that too much chemistry teaching is in the hands of graduate students or even seniors. Student teaching assistants are extremely useful but, for their own good and that of their students, the planning and supervision, the equipment, supplies, unknowns, examinations, and whatnot, should be in the hands of experienced, responsible, full-time, faculty members.

Perhaps the above is just another way of saying that the tremendous expansion in scientific development since 1940 has made it impossible, even with all the inducements at the higher levels, to produce sufficient trained personnel to maintain the pace. Efforts are being made to apply the stimulating needle in the secondary and even the primary schools, but it will be several years before the results are evident.

—CVK

<sup>1</sup> *Chemical and Engineering News*, May 5, 1958.

## THE SARGENT

# LABORATORY RECORDER

(Patents Pending)

An automatic, self-balancing potentiometric recorder which measures voltages or current and graphically records these variables as a function of time.



Designed and Manufactured by  
E. H. SARGENT & CO.

**Style:** Vertical strip chart recorder, designed for laboratory bench operation. Assembly of three individual, separable, and self contained units; viz., control panel assembly, amplifier and power supply chassis, and chart and pen drive chassis unit.

Automatic null balancing potentiometric system with standard cell standardization by panel control, conventional chopper-amplifier method with special Sargent high gain amplifier and high stability Sargent bridge power supply using combined or alternate dry cells and mercury cells. Use of the latter obviates need for standardization over very long periods.

**Ranges:** Multiple full scale ranges selected by panel range switch as follows: 1.25, 2.5, 5, 12.5, 25, 50, 125, 250, 500, 1250, 2500. All ranges are made direct reading as full scale deflection in millivolts, milliamperes, or microamperes by use of an associated units selector switch. All 33 scales provide true potentiometric measurement. An additional series of the same eleven ranges in terms of volts is provided by an additional selector switch position, this series using a divider input with an impedance of one megohm.

True potentiometric measurements are thus provided to a maximum of 2.5 volts, higher voltages only being measured through a divider.

**Accuracy:** 0.1% or 20 microvolts, whichever is greater.

**Chart:** Width, 250 mm; length, 120 feet. Ruling rational with all ranges on a decimal basis. Indexed for reference. Graduated steel scale provides for any necessary correction of calibration. Two-position writing plate, 15° or 40° from vertical.

**Chart Drive:** Forward drive recording, reverse drive re-

- **MULTI-RANGE—40 ranges.**
- **MULTI-SPEED—9 standard chart speeds with provision for optional 1-5 range multiplication or 5-1 range reduction.**
- **VOLTAGE OR CURRENT RECORDING—for measurement of voltage or current or any other variable which can be translated to voltage or current signals.**
- **FLEXIBILITY OF APPLICATION**
- **DESIGNED FOR BENCH OPERATION**

ording, magnetic brake eliminating coasting when stopped and free clutch position with separate provision for rapid non-synchronous drive.

Recording speeds of  $\frac{1}{3}$ ,  $\frac{1}{2}$ , 1,  $1\frac{1}{2}$ , 2,  $2\frac{3}{4}$ , 4, 8, and 12 inches per minute, selected by interchange of two gears on end of chassis.

Free clutch or neutral drive at the rate of approximately 20 feet per minute in either direction for rapid scanning of recorded information, chart reroll, or chart positioning.

Recording either by automatic take-up on roll or with free end chart and tear off.

Synchronous switching outlet for automatic synchronization of external devices with recording.

**Pen Speed:** 1 second full scale. Other speeds can be provided on special order with change of motors.

**Bridge:** Special Sargent specification. Provision for coupled transmitting potentiometer for output to integrating circuits, etc.

**Damping:** Dynamics controlled with single panel knob adjustment of amplifier gain.

**Dimensions:** Width,  $21\frac{1}{2}$  inches; depth, 13 inches; height, 24 inches; weight, about 75 pounds.

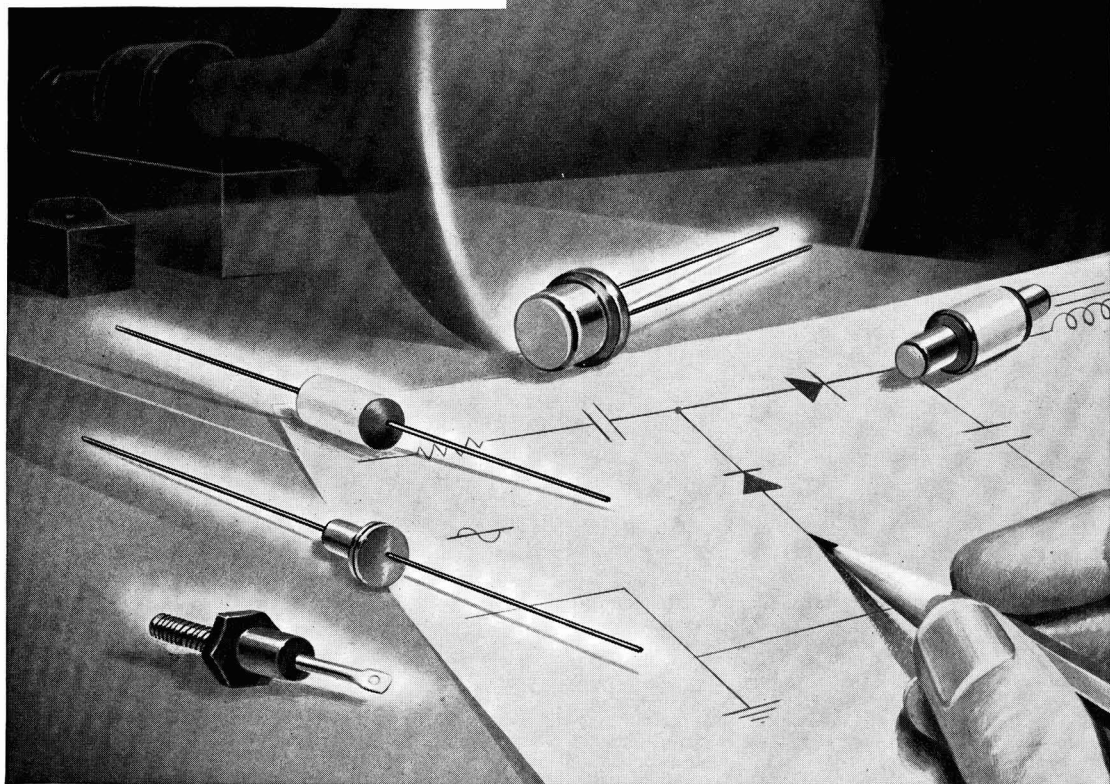
**S-72150 RECORDER — Potentiometric, Sargent** Complete with two S-72165 chart rolls; two each S-72175 pens; red, blue and green; one S-72176 wet ink pen, input cable assembly; synchronous switch cable assembly; plastic dust cover; spare ring for take-up mechanism; spare pen drive cable assembly; and fuses. For operation from 115 volt, A.C. single phase, 60 cycle circuits. . . . . **\$1725.00**

# SARGENT

SCIENTIFIC LABORATORY INSTRUMENTS • APPARATUS • SUPPLIES • CHEMICALS

E. H. SARGENT & COMPANY, 4647 W. FOSTER, CHICAGO 30, ILLINOIS  
DETROIT 4, MICH. • DALLAS 35, TEXAS • BIRMINGHAM 4, ALA. • SPRINGFIELD, N. J.

## NEWS ABOUT SILICON DEVICES



Reverse current:  $10^{-7}$  amp. Rectification ratio: 10,000,000:1

## Now... new efficiency for TV power supplies with dependable diodes of Du Pont Hyperpure Silicon

More efficient power supplies . . . savings in space and weight . . . important reasons why TV manufacturers are replacing conventional rectifying systems with silicon diodes. Today, several types of silicon diodes and rectifiers are readily available for TV circuits. TV manufacturers have tested silicon rectifiers and report no noticeable change in output voltage under continuous load conditions over long periods of time. Sil-

con components can operate in ambients from  $-65^{\circ}$  to  $150^{\circ}$  C. They maintain excellent electrical stability and resist aging.

**Silicon components** have high shock and vibration limits. They are up to 99% efficient in units operated at 60 cps. and require little maintenance. Silicon cells permit a rectification ratio as high as 10 million to 1—almost negligible reverse conductance. Silicon bridges are

available with ratings from 1 to 1,000 amperes and more than 600 volts rms.

**Note to device manufacturers:** You can produce silicon transistors, rectifiers and diodes of the highest quality with Du Pont Hyperpure Silicon. It's now available in three grades for maximum efficiency and ease of use . . . with a purity range of 3 to 11 atoms of boron per billion. Technical information on crystal growing is available from Du Pont . . . pioneer producer of semiconductor-grade silicon.



### NEW BOOKLET ON DU PONT HYPERPURE SILICON

You'll find our new, illustrated booklet about Hyperpure Silicon helpful and interesting—it describes the manufacture, properties and uses of Du Pont Hyperpure Silicon. Just drop us a card for your copy. E. I. du Pont de Nemours & Co. (Inc.), Pigments Department, Silicon Development Group, Wilmington 98, Delaware.

(This offer limited to United States and Canada.)

PIGMENTS DEPARTMENT



**HYPERPURE  
SILICON**

BETTER THINGS FOR BETTER LIVING  
. . . THROUGH CHEMISTRY

# Lead-Acid Storage Batteries

## Changes In Positive Active Material Density During Various Conditions of Service

J. F. Dittmann and J. F. Sams

*Research Laboratories, The Eagle-Picher Company, Joplin, Missouri*

### ABSTRACT

Observations made on the lead-acid battery indicate that changes occur in the apparent density of the positive active material during service. To determine the extent of these density changes, measurements have been conducted during all usual conditions of testing. The apparent density of the positive active material has been found to decrease regardless of active material shedding. This finding appears to explain many of the observed performance characteristics of the lead-acid battery.

When observing the performance characteristics of many batteries tested under various conditions, it became evident that changes were occurring in the apparent density of the positive active material during the life of the battery. To determine the extent of these changes, density determinations were conducted periodically on positive plates during their life on each of the SAE cycling, overcharge and Emark tests, during storage, and in SLI service. Fundamental performance and life characteristics of batteries subjected to these various tests have been presented (1).

### Experimental

All data accumulated in this study were obtained from standard 15 plate 100 amp-hr battery assemblies which were tested on the various life tests. Prior to life testing, density determinations were made on representative positive plates from each group of batteries before formation, after formation, and after completion of six initial cycles.

The method used for conducting density determinations on a battery plate has been described by Dittmann and Harner (2). Briefly, the procedure is as follows: data for calculating apparent  $PbO_2$  density are obtained by weighing the dry battery plate, filling the pores of active material with water, and determining the full plate volume by water displacement through use of a specially designed apparatus. The plate is again dried and weighed after first removing approximately two-thirds of its material. A second volume measurement is conducted as before on the partially filled plate. Weight and volume values are obtained by differences and used to calculate apparent density. The method has sufficient accuracy to obtain suitable values for comparison.

Starting with positive plates of known  $PbO_2$  density, changes were observed by means of measurements made on representative plates periodically during the various recognized life tests (1). The consolidated data appearing in Fig. 1 are presented

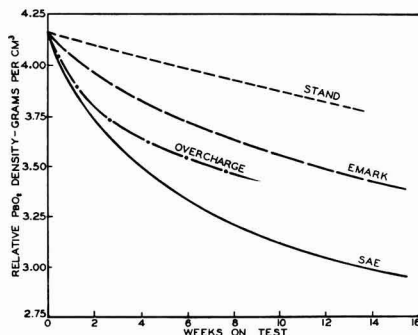


Fig. 1. Decrease in apparent  $PbO_2$  density of positive plates during various conditions of testing.

as indicative rather than absolute because it is evident that other conditions such as temperature, original  $PbO_2$  density, grid metal and grid design, type of oxide, etc., may alter the degree of density change.

### Discussion

Perhaps the most important finding disclosed by data in Fig. 1 is the fact that the apparent density of the positive active material was found to decrease regardless of conditions of testing or of the extent of positive active material shedding. More specifically it is noted that the degree of change in  $PbO_2$  density is greatest for batteries subjected to the SAE "deep" cycling test. Positive plates subjected to overcharging and to the "shallow" cycling Emark test were found to decrease somewhat less in density. The fact that active material of positive plates decreased in density upon storage in sulfuric acid is also of significance. In summarizing, it may be stated that the apparent density of the active material of positive plates is caused to decrease by deep cycling, by shallow cycling, by overcharging, and by storage in sulfuric acid.

Of further significance is the fact that these characteristic decreases in  $PbO_2$  density can be related to

all fundamental causes of failure commonly observed in the lead-acid battery regardless of conditions of service.

For example, the act of positive material shedding in deep cycling services can be explained simply by the fact that, as positive active material decreases in density and expands and the active material alternates between lead peroxide and lead sulfate, the crystalline bonds are disrupted causing the material to fall or be washed free from the plate.

In overcharge and shallow cycling service conditions, shedding of positive material normally does not occur because there is little or no disruption of the  $PbO_2$  bonds by formation of lead sulfate. However, the act of overcharging a battery in absence of cycling also causes an appreciable decrease in  $PbO_2$  apparent density, and since no appreciable shedding of material occurs, the active material must expand. This expansion exerts pressures on the grid frame and its members, causing them to break at weak points, particularly as the grid becomes weakened by electrolytic corrosion. The result is a continued loss in positive plate conductivity as the plate disintegrates.

It is recognized that the grid frame and its members also are caused to expand by products of electrolytic corrosion, and this process also contributes to ultimate positive plate disintegration. It has become evident from these investigations that the expanding forces exerted by positive active material and by products of grid corrosion are the major, if not the most important cause of battery failure in services characterized by overcharging. This is substantiated by the fact that, after a positive plate has failed by disintegration as a result of overcharging, shallow cycling, or storage, it will still contain anywhere from 50% to 80% of its original weight of grid metal.

Further evidence of the effect of  $PbO_2$  expansion on positive plate disintegration is disclosed by the condition of positive plates as revealed in Fig. 2. Batteries of identical assembly, but containing positive active material at various densities, were subjected to four weeks of SAE overcharge testing. Plate No. 7, Fig. 2, contained active material lowest in initial  $PbO_2$  density and was characterized by the lack of grid frame breakage. Likewise, Plate No. 8, although showing signs of complete deterioration,

was in better condition than No. 9 which was highest in  $PbO_2$  density. The effect of stresses applied to the grid by expanding  $PbO_2$  and its subsequent disintegration was also reflected by the much lower capacity output of the No. 9 plate. The appearance and condition of these plates would appear to be conclusive evidence that other factors than grid corrosion were at play. Since all plates represented in Fig. 2 were subjected to the same number of ampere-hours of overcharge, it follows that each should have developed the same amount of grid corrosion. Therefore, the obvious differences in plate appearance and degree of disintegration must be related to stresses exerted by expanding  $PbO_2$  and/or other factors.

Positive plates subjected to overcharging or SLI service often warp and buckle causing wear to separators that results in battery failure. The mechanism by which a positive plate is caused to warp or buckle can, likewise, be explained by considering reduction in positive active material density during service. Seldom, if ever, is a positive plate prepared with equal distribution of paste on both sides, nor is all paste in any one plate always of the same density. Under these conditions the active material expands unequally causing stresses to be applied more in one direction than in another. As growth continues, the plates warp or buckle with the concavity toward the side of lesser active material expansion.

It is known that a lead-acid battery has a greater ampere-hour capacity after activated storage than before. This fundamental increase in capacity resulting from activated storage prior to testing was first reported by Harner and Chubb in 1935 (3). The phenomenon may be explained by consideration of changes occurring in the  $PbO_2$  density during storage in sulfuric acid. As is apparent from data recorded in Fig. 1, the positive plates of a battery allowed to stand in storage for no more than a one-month period will decrease substantially in  $PbO_2$  density. The increase in capacity efficiency which accompanies a decrease in positive  $PbO_2$  density would explain in part, if not entirely, the reason for the observed increase in capacity which occurs as a result of storage.

A lead-acid battery in automobile service is normally subjected to shallow cycling, to overcharging, and to many hours of idleness, all of which have been shown to cause a decrease in positive active material density. From these considerations, positive plates subjected to SLI service would be expected to reveal density changes similar to those obtained upon Emark and overcharge testing. Measurements made on positive plates removed from car service disclose this to be true. Therefore, it may be concluded that stress applied to grids by expanding positive active material is a major contributing cause of failure in batteries placed in automobile service.

### Conclusions

The active material density of formed positive plates of the lead-acid battery decreases substan-

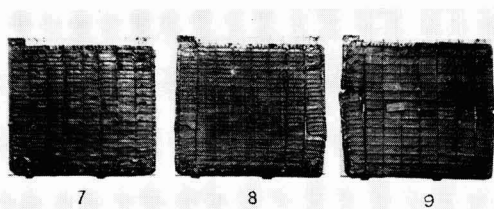


Fig. 2. Effect of  $PbO_2$  expansion on positive plate disintegration.

Results of four weeks SAE overcharge testing

Positive plate No.	7	8	9
Original $PbO_2$ density	4.03	4.27	4.64 g/cm <sup>3</sup>
Final $PbO_2$ density	3.54	3.78	4.09 g/cm <sup>3</sup>
Final capacity efficiency	1.31	1.09	0.49 amp-hr/28.35g

tially and progressively when subjected to deep cycling, shallow cycling, overcharging, activated storage, or automobile service. It appears that this reduction in positive active material density with service exerts a marked influence on battery performance characteristics and on the ultimate failure of the positive plate.

Manuscript received Jan. 27, 1958. This paper was prepared for delivery before the Buffalo Meeting, Oct. 6-10, 1957.

Any discussion of this paper will appear in a Discussion Section to be published in the June 1959 JOURNAL.

#### REFERENCES

1. J. F. Dittmann and H. R. Harner, *This Journal*, **101**, 533 (1954).
2. J. F. Dittmann and H. R. Harner, "Starting and Lighting Batteries," No. 7 in a Series, "Paste Preparation and Plate Control," The Eagle-Picher Company (1956).
3. H. R. Harner and M. F. Chubb, *Trans. Electrochem. Soc.*, **68**, 309 (1935).

## Self-Discharge Reactions In Lead-Acid Batteries

Paul Rüetschi and R. T. Angstadt

*Research Department, The Electric Storage Battery Company, Philadelphia, Pennsylvania*

#### ABSTRACT

A theoretical and experimental analysis of the self-discharge of lead-acid batteries shows that seven different reactions contribute to the process. The rate of each has been determined. It is shown that positive plate self-discharge is due primarily to a reaction between  $\text{PbO}_2$  and grid metal. The rate of this reaction decreases with increasing acid concentration because of the passivating action of the  $\text{PbSO}_4$  layers formed. The passivating action is decreased by the presence of antimony in the grid, producing pores in the  $\text{PbSO}_4$  layers and providing further access of the electrolyte to the grid. At low acid gravities antimony compounds become almost insoluble and can act as passivators decreasing the reaction between grid metal and  $\text{PbO}_2$ . Other self-discharge reactions in positive plates are the decomposition of water by  $\text{PbO}_2$  with evolution of oxygen and the oxidation of separator material in contact with  $\text{PbO}_2$ . Oxidation of hydrogen, coming from the negative plates, occurs at immeasurably small rates.

Self-discharge of the negative plates is due to the reaction between  $\text{H}_2\text{SO}_4$  and lead, producing  $\text{H}_2$  and  $\text{PbSO}_4$ . This reaction is slow in absence of foreign substances because of the high hydrogen overvoltage on lead. However, contamination of the negatives with antimony decreases the hydrogen overvoltage and greatly accelerates the self-discharge of negative plates. Furthermore, negative plates are self-discharged by oxygen dissolved in the electrolyte. The rate of reduction of oxygen is so fast on a lead electrode in sulfuric acid that the reaction is diffusion controlled.

Self-discharge, also referred to by the terms "open circuit loss," "local action," and "sulfation," of lead-acid batteries has received a great deal of attention in the past, especially in connection with standby batteries for telephone systems, with the storage of charged automobile batteries, and with special applications where the evolution of gas may be hazardous.

Battery engineers are accustomed to relate self-discharge mainly to the negative plates. It is interesting to note, however, that Vinal (1) early pointed out that self-discharge also occurs in the positive plates. He found that negative plates sulfated faster with increasing acid concentration, whereas self-discharge of the positive plates decreased with increasing acid concentration (2). He determined self-discharge rates by the method of weighing plates and this has the disadvantage of difficultly interpretable results because the weighings are made in solution and buoyancy corrections are necessary. These corrections may be different for different self-discharge reactions (see Eqs. [1] and [2]). Therefore, a correct interpretation of the

weight figure is not possible without knowing the relative rate of each of the two reactions. Vinal regarded positive plate self-discharge as the result of a reaction which is the same as the cell reaction of lead acid batteries according to the double sulfation theory (3, 4). The same reaction was considered by Lander (5, 6). Positive plates sulfate faster than the negative plates in new batteries (7, 8). The influence of forming temperature on self-discharge of positive plates has also been studied (7). It had been noted before by Hatfield and Brown (9) that, on cycling test, there is an increase in the shedding of positive active material with decrease in the forming temperature. At higher temperatures, formation is more complete and less "apparent  $\text{PbO}$ " is left in the plates. Self-discharge of the positive plates decreased with increasing forming temperatures. Greenburg and Caldwell (7) attributed 50% of the self-discharge rate of positives to direct sulfation of  $\text{PbO}_2$  accompanied by oxygen liberation, 25% to a "potential difference reaction" between grid metal and  $\text{PbO}_2$ , and 25% to sulfation of "apparent  $\text{PbO}$ ." Increasing temperature caused higher

corrosion of the positive grids during formation and therefore an increase in antimony transfer to the negatives and higher self-discharge of the negatives (9).

Lander (10) found the self-discharge of the positive plate to occur at rates comparable to negative plate self-discharge. His experiments were made with cells which had previously received some overcharge and cycling. Lander suggests that the self-discharge of the positive plate is due primarily to oxidation of the Sb phase in the grid.

The self-discharge reaction occurring in the negative plate has usually been assumed to be an attack on Pb by  $H_2SO_4$  with  $H_2$  evolution. Contamination of the negative plate with Sb catalyzes this reaction to a high degree (11-15). A great deal of work on the self-discharge of lead-acid batteries and especially the influence of temperature on self-discharge has been done by Zachlin (16, 17), but most of his work has been concerned with full size cells and not with single positive or negative plates. In the present paper a detailed discussion of the various self-discharge reactions and a determination of their relative rates is presented.

### Experimental

Single positive plates, single negative plates, and three-plate cells with one positive and two negatives were placed in electrolytes whose gravities and temperatures were kept constant to  $\pm 0.002$  g/cm<sup>3</sup> and  $\pm 0.5^\circ C$ , respectively. All experiments were performed at  $35^\circ C$  unless otherwise noted. The specific gravities were adjusted at  $26.7^\circ C$ . Plates were analyzed for sulfate after 2, 4, 8, and 16 weeks. All the cells had a large excess of electrolyte, one single plate or a three-plate cell being placed in a jar with 1000 cc  $H_2SO_4$  of a given gravity. The separators used were microporous rubber separators unless stated to the contrary. The positive plates had a capacity of 7.2 amp-hr at the 5 hr rate. The grids were 13.35 cm high, 10.6 cm wide and 0.17-0.18 cm thick. Positive and negative plates had identical dimensions. The composition of the grid alloys used in this study are given in Table I (18). Bismuth, iron, and nickel are not shown in the table but were all in the usual low range and without significance for this study.

The paste for the positive plates was prepared using 80% gray oxide and 20% red lead. The mix

was made with 51 cc of water and 21 cc of  $H_2SO_4$  (sp gr 1.400) per 453 g of active material. The negative paste contained 95% gray oxide and 5% 232 W (National Lead Company) and the mix was made using 51 cc of water and 25 cc of  $H_2SO_4$  (sp gr 1.400) per 453 g of active material.

Positive plates were set at room temperature and humidity for 44 hr and at completion of this time sprayed, drained, piled, and aged for 4 days. The negative plates were set for 30 hr at  $51.7^\circ C$  in 90% humidity, air dried, and stored 3 days before use.

Plates with a given grid alloy were always formed against plates with the same grid alloy, the formation procedure being conventional, namely, 18 hr with 2 amp per positive plate in 1.070 sp gr acid in 11-plate cells. Then the cells were dumped and re-filled and the acid adjusted to 1.250 sp gr, using a 5 hr mixing charge with 2 amp per 11-plate cell. All cells were then given one cycle consisting of a 5-hr discharge at 7.2 amp and a 9-hr charge at 5.0 amp. The cells were then taken apart and single-plate and three-plate cells were built. In the three-plate units, negative and positive plates had the same grid alloy. In order to study the influence of the separators on the rate of self-discharge, single plates covered on both sides with a separator were also placed in electrolytes of constant gravity. Three different separator types were studied, paper (phenolic-bound), spun glass with inert backing, and microporous rubber. Some of these experiments were made using electrolytes dosed with various amounts of  $Sb_2(SO_4)_3$  in order to investigate the filtration action of the separators. Finally, active material was knocked out of formed plates with Sb-free grid alloy and placed in electrolytes of various gravities at constant temperature. The formation of sulfate was followed by analysis after 2, 4, 8, and 16 weeks. By this procedure the reaction of isolated active material with  $H_2SO_4$  could be studied.

Samples of the active material of the plates were taken after the indicated time periods by removing the plates from the electrolyte, punching out a number of pellets of active material, grinding the active material in a mortar, and washing with water. The material was then filtered and dried. A 2-g sample of the dry material was boiled for 1 hr in a solution of 15-g of  $Na_2CO_3$  in 100 cc of water. The solution was filtered, made acidic with HCl, and boiled to remove  $CO_2$ . Finally, the sulfate was precipitated with 20 cc of a 15% solution of barium chloride. The barium sulfate was collected in a Gooch crucible by filtration and dried over a burner at red heat until the weight was constant.

### Results

The weight percentage of lead sulfate of washed and dried samples expresses the total amount of  $SO_4$  in the form of  $PbSO_4$ . That means that any  $SO_4$  present in the form of  $(SbO_2)_2SO_4$  or in the form of basic lead sulfates appears as  $PbSO_4$ . A detailed analysis of each self-discharge product would have been more rigorous, but, since  $PbSO_4$  is the major self-discharge product, no considerable error is introduced. The results given below allow the ap-

Table I. Analysis of the lead alloys used (in % per weight)

Alloy No.	Sb	As	Sn	Ag	Cu	Ca	Al	Se	Te
1	4.80	0.28	0.16	0.008	0.008	—	—	—	—
2	4.80	0.23	0.03	0.003	0.025	—	—	—	—
3	5.76	0.48	0.51	0.122	0.003	—	—	—	—
4	2.58	0.045	0.0001	0.004	0.010	—	—	—	—
5	3.36	0.03	1.66	0.008	0.003	—	—	0.026	—
6	—	—	—	—	—	0.082	0.006	—	—
7	—	—	—	—	—	0.070	0.010	—	—
8	4.20	0.11	0.62	0.161	0.040	—	—	—	0.040
9	4.26	0.47	0.51	0.106	0.005	—	—	—	—
10	4.20	0.03	4.36	0.003	0.008	—	—	—	—
11	—	—	—	—	—	—	—	—	—
12	—	—	—	—	—	0.066	—	—	—

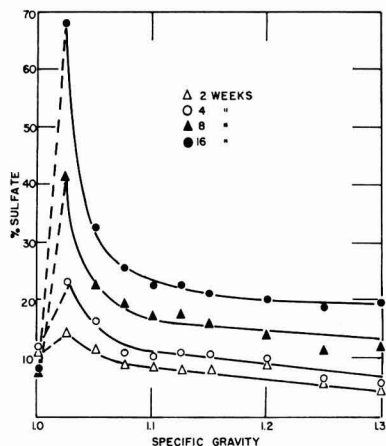


Fig. 1. Self-discharge of a single positive plate with grid alloy No. 6 at 35°C.

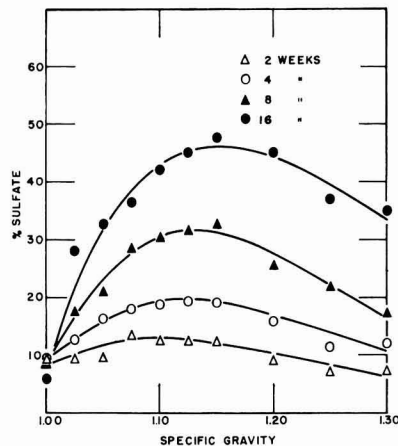


Fig. 3. Self-discharge of a single positive plate with grid alloy No. 3 at 35°C.

proximate determination of the rate of any self-discharge reaction occurring in lead-acid batteries.

The rate of self-discharge of positive plates with various grid alloys and in the absence of separators and negative plates is illustrated in Fig. 1 to 4. The self-discharge has a pronounced maximum at a gravity of about 1.100 for plates with Pb-Sb grid alloys and at a gravity of about 1.025 for plates with Pb-Ca-Al grid alloys. The maximum is shifted toward higher gravities with increasing Sb content in the grid. The maximum also seems to be displaced slightly toward higher gravities with increasing time. The results show that for the acid gravity range used in batteries the self-discharge of the positive plates increases with decreasing acid gravity. The sulfate figures for these positive plates are of the same order of magnitude as figures for negative plates for the same time periods as shown below. The PbSO<sub>4</sub> percentage shown for plates in sp gr 1 reflects the amount of H<sub>2</sub>SO<sub>4</sub> retained in the plates when they were transferred from the forming electrolyte.

Figure 5 shows the influence of the grid alloy on positive plate self-discharge. The plots show that the reaction rate is almost independent of the sulfate content in the plates for sulfate percentages below approximately 30%. The positive plates containing Sb in the grid undergo self-discharge at a higher rate than plates with Sb-free grid alloys. Figures 6 and 7 give the rates of self-discharge reactions in positive plates under various conditions.

The rate of the self-discharge reaction of isolated positive active material depends on the acid gravity as shown by Fig. 8. The rate of the reaction between PbO<sub>2</sub> and H<sub>2</sub>SO<sub>4</sub> increases with increasing acid concentration.

Figure 9 shows the influence of one cycle on the rate of self-discharge of single positive plates and Fig. 10 shows the influence of grid alloy on positive plate self-discharge in 3-plate cells. The negatives and the positives in each 3-plate cell had identical grid compositions. The differences between the sulfate figures are due to differences in the reaction between the grid and the active material.

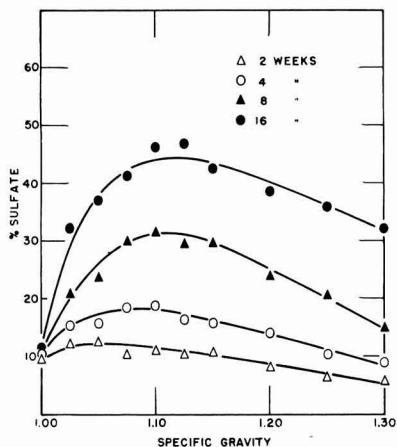


Fig. 2. Self-discharge of a single positive plate with grid alloy No. 9 at 35°C.

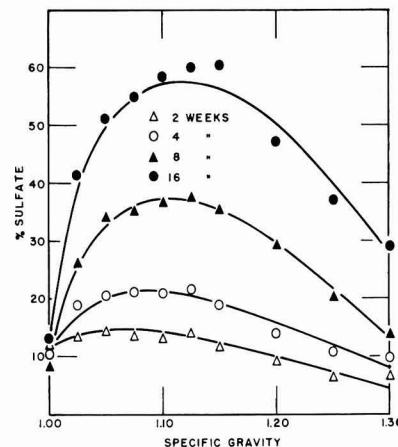


Fig. 4. Self-discharge of a single positive plate with grid alloy No. 4 at 35°C.

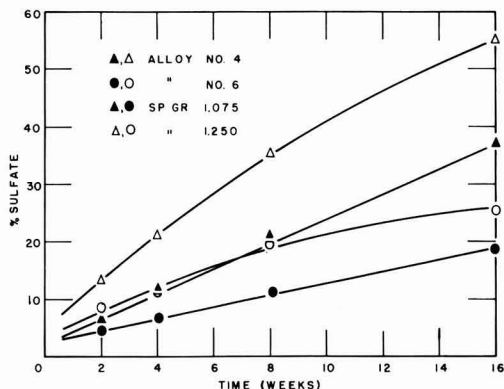


Fig. 5. Rate of self-discharge of single positive plates (grid alloy No. 4 and No. 6) in 1.250 sp gr acid and 1.075 sp gr acid at 35°C.

The results on self-discharge of negative plates are given in Fig. 11 to 15. Figure 11 shows only a small difference in self-discharge between single plates with Sb-free grids and plates with up to 4% Sb in the grids. Figure 12 and 13 illustrate the rate of the self-discharge reactions for negative plates in varying environmental conditions. Here, the open circle corresponds to the self-discharge of a single negative plate in the absence of separators and positive plates, the solid circle to the sulfation of negative plates covered on both sides with separators, the solid triangle to the self-discharge of the negative plate in 3-plate cells. The steep curve was obtained on bubbling oxygen gas through the electrolyte continuously. Enormous self-discharge rates are observed under these conditions.

Figure 14 shows the influence of different separators on negative plate self-discharge. These results were obtained with single negative plates covered with separators on both sides. A series of these plates was also placed in electrolyte dosed with 0.1 g/l and 1 g/l  $\text{Sb}_2(\text{SO}_4)_3$ . The presence of Sb in electrolyte accelerates negative plate self-discharge tremendously. With 1 g/l the plates without separators are 80% discharged in 4 days. In these experiments it could actually be observed how the

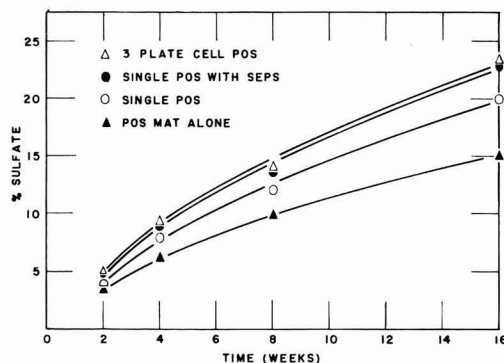


Fig. 6. Rates of self-discharge for positive plates (grid alloy No. 6) in 1.250 sp gr acid at 35°C. ▲ active material alone; ○ single positive plate; ● single positive plate with separators; △ positive plate in 3-plate cell.

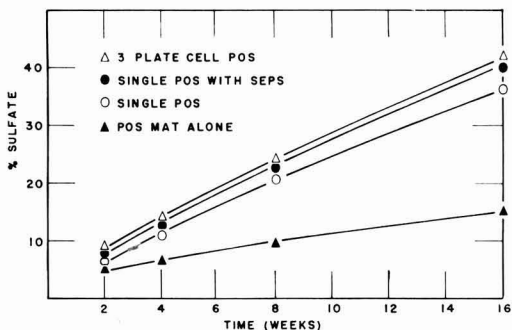


Fig. 7. Rates of self-discharge for positive plates (grid alloy No. 9) in 1.250 sp gr acid at 35°C. ▲ active material alone; ○ single positive plate; ● single positive plate with separators; △ positive plate in 3-plate cell.

Sb was plated on the negative plate causing increased self-discharge. The separators decrease the rate of diffusion of Sb and oxygen toward the negative plate and decrease, therefore, negative plate self-discharge.

Figure 15 shows the self-discharge of negative plates in 3-plate cells. It is interesting to note (see also Fig. 12) that negatives in Sb-free assemblies in 3-plate cells have a smaller rate of self-discharge than single Sb-free negative plates because of the protecting action of the separators against oxygen diffusion. Negatives in 3-plate cells with grid alloys of high Sb-content and particularly alloys of high corrodibility (alloy No. 4) show a higher rate of self-discharge than single negatives containing the same grid alloy because of Sb-transfer from the positives to the negatives, overcoming the benefit due to the presence of separators.

## Discussion

A large series of  $\text{PbO}_2$  determinations on active material samples after 0, 2, 4, 8, and 16 weeks open-circuit stand showed that the sum of the  $\text{PbSO}_4$  and  $\text{PbO}_2$  percentages never added up to 100%. There was always a deficit of 5-10%. This deficit has sometimes been called "apparent  $\text{PbO}_2$ ." However, the oxygen deficit is only partially due to actual

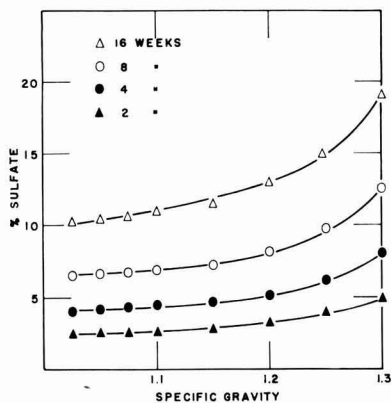


Fig. 8. Self-discharge of positive active material alone as a function of the acid gravity.

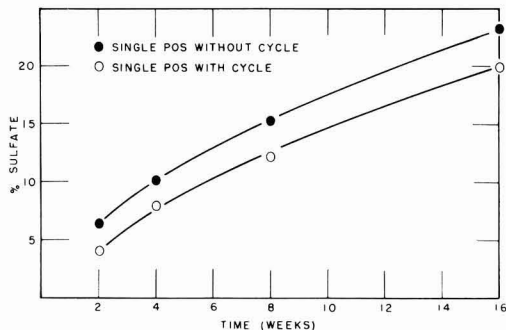


Fig. 9. Rate of self-discharge of positive plates (alloy No. 6) in sp gr 1.250  $H_2SO_4$ , showing the effect of one cycle following formation.

existence of  $PbO$ . It must be kept in mind that the lead dioxide lattice always has an oxygen deficiency (19-21). The electrical conductivity of lead dioxide is very high, approaching that of metallic conductors. The oxygen deficiency produces free electrons and is responsible for high conductivity. The conductivity would be expected to increase with increasing deficit in oxygen (22). However, Kittel's thermodecomposition studies show that the conductivity decreases with increasing amount of missing oxygen, due to the formation of a new insulating compound (23). This new compound is subject to fast sulfation (24). It is not established, however, if the same compound exists in incompletely formed positive plates.

In this study all the positive plates were formed under exactly the same conditions (temperature, current rate, amount of charge) in order to form the plates to approximately the same degree of completeness. It was observed that the sulfate on freshly formed positive plates was always below 1%, using any formation procedure, but the amount of  $PbO_2$  varied greatly with different formation procedures, from 88 to 95%. The rate of sulfation of positive active material in the absence of grids, separators, and negative plates increases slightly with increasing acid concentration (Fig. 8). The fact that the curves do not tend toward zero at sp gr 1.0 suggests that the sulfate ion is taking part only indirectly in

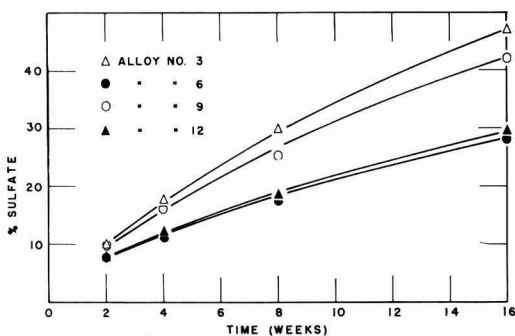


Fig. 10. Influence of the grid alloy on positive plate self-discharge in 3-plate cells (1 positive and two negatives) with sp gr 1.250  $H_2SO_4$ .

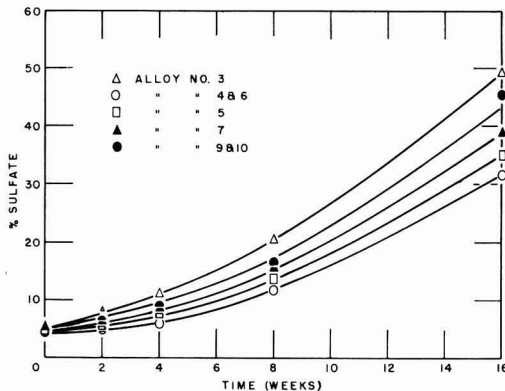


Fig. 11. Self-discharge of single negative plates in  $H_2SO_4$ , sp gr 1.250 at 35°C.

the reaction. Formation of persulfate  $S_2O_8^{2-}$  requires a potential of +2.01 (25), whereas the potential of the  $PbSO_4/PbO_2$  couple is only 1.685 v. Persulfate is unstable in sulfuric acid and decomposes with formation of oxygen and hydrogen peroxide (26). The water-hydrogen peroxide couple has a potential +1.77 v. However, the oxygen couple in acid solution ( $O_2 + 4H^+ + 4e = 2H_2O$ ) has a potential of only +1.229 v. This shows that persulfate and hydrogen peroxide will not be formed on a positive electrode during open-circuit stand, and that oxygen must be the reaction product.

The question of whether the oxygen evolved in the over-all self-discharge reaction



comes from the  $H_2O$  in the solution or the  $PbO_2$  could be answered by oxygen isotope studies. Reaction [1] is responsible for the self-discharge of isolated positive active material, and its speed can be evaluated from Fig. 6 and 7 (the curve marked with the solid triangle) and from Fig. 8. The free energy of reaction [1] is -21030 cal.

It can be shown that the oxygen content of the positive active material is related to the rate of self-discharge. Figure 9 shows a comparison of rates of

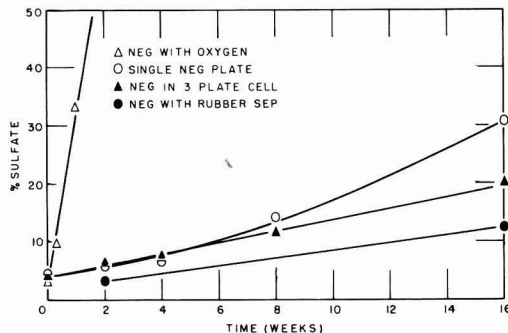


Fig. 12. Self-discharge of a negative plate (grid alloy No. 6) in  $H_2SO_4$ , sp gr 1.250 at 35°C. O single negative plate; ● negative plate with separators; ▲ negative plate in 3-plate cell; △ negative plate in  $H_2SO_4$  saturated with oxygen.

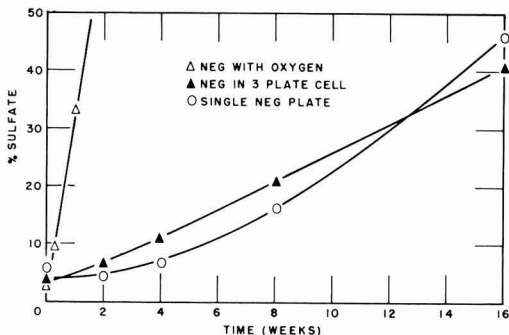


Fig. 13. Self-discharge of a negative plate (grid alloy No. 9) in  $H_2SO_4$ , sp gr 1.250 at  $35^\circ C$ . O single negative plate;  $\blacktriangle$  negative plate in 3-plate cell;  $\triangle$  negative plate in  $H_2SO_4$ , saturated with oxygen.

self-discharge between two positives of identical grid alloy (No. 6) and which were formed in series, but one plate was discharged at the 5-hr rate for 5 hr following formation and recharged, and the other plate was not cycled. Both were left to self-discharge in 1.250 sp gr acid at  $35^\circ C$  with analysis made at the indicated time intervals. The analysis on these plates prior to self-discharge (after formation and one cycle for the cycled plate and after formation for the uncycled plate) showed both plates to have less than 0.5%  $PbSO_4$ , but the uncycled plate analyzed 92%  $PbO_2$ , whereas the cycled plate analyzed 94%  $PbO_2$ . Although these plates show a very low and nearly identical  $PbSO_4$  concentration, the difference in  $PbO_2$  content indicates a difference in amounts of "apparent  $PbO$ ," that is, a lack of oxygen. The plate with the higher percentage of  $PbO_2$  was observed to have the lower rate of self-discharge. Thus, formation of the positives should be as complete as possible to reduce stand loss. The amount of "apparent  $PbO$ " is reduced by increasing temperature during formation or by cycling after formation.

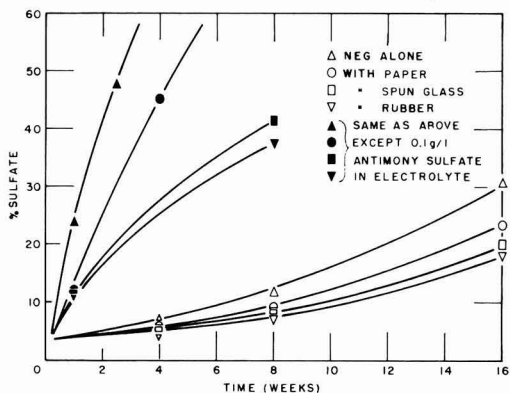


Fig. 14. Influence of the separator on self-discharge of single negative plates,  $\triangle$  no separator,  $\Delta$  microporous rubber,  $\square$  spun glass with inert backing,  $\circ$  paper (phenolic-bound), in  $H_2SO_4$ , sp gr 1.250 at  $35^\circ C$ . The self-discharge rates in  $H_2SO_4$ , sp gr 1.250 at  $35^\circ C$ , dosed with 0.1 g  $Sb_2(SO_4)_3$  per liter are shown with black symbols.

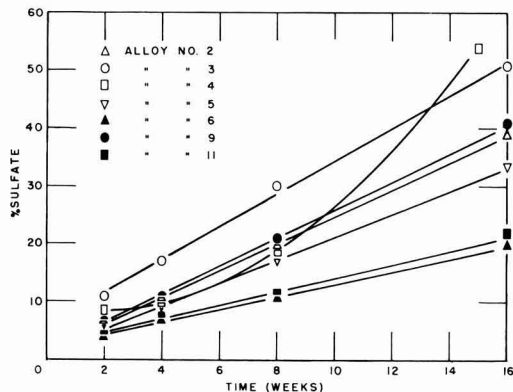
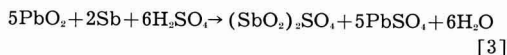
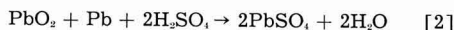


Fig. 15. Rate of self-discharge of negative plates in 3-plate cells.

If the positive active material is in contact with a lead or lead-antimonial grid, the following self-discharge reactions occur:



Reaction [2] corresponds to the discharge reaction of a lead acid cell according to the double sulfation theory. Comparing Fig. 1 with Fig. 2-4, or Fig. 6 with Fig. 7 it can be seen that reaction [2] is relatively slow in the absence of Sb in acid gravities above 1.10 and does not contribute much to the over-all rate of self-discharge. Reaction [2] involves a  $\Delta F$  of  $-92,300$  cal and would tend to proceed spontaneously. Fortunately, the electrolyte has only very limited access to the lead metal and formation of lead sulfate passivates the reaction on the exposed areas. With increasing dilution of the acid, the solubility of lead sulfate increases as shown in Fig. 16 [data from (27)] and the passivating action of lead sulfate decreases (28-31). This situation is illustrated schematically in Fig. 17. The area of metallic lead exposed to the electrolyte is polarized anodically by the presence of  $PbO_2$  to a value 2 v more positive than its reversible potential. Therefore, the lead would tend to dissolve spontaneously under formation of  $Pb^{2+}$  or  $Pb^{4+}$  ions. The driving force for this reaction would even be expected to increase with increasing acid gravity since the potential of the positive electrode becomes more posi-

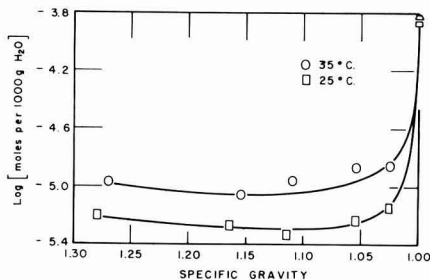


Fig. 16. Solubility of lead sulfate in sulfuric acid. [Data from (28)].

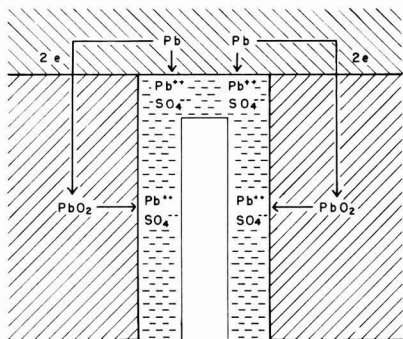


Fig. 17. Schematic diagram of the self-discharge process in a pore of a positive plate with an antimony-free grid.

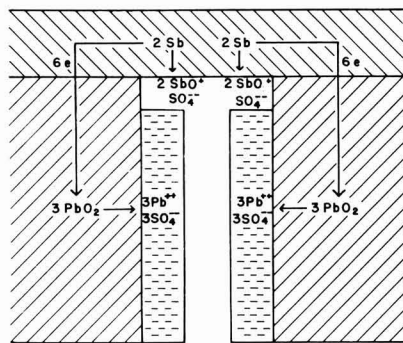


Fig. 18. Schematic diagram of the self-discharge process in a pore of a positive plate with an antimonial-lead grid.

tive at higher acid gravities. This follows from the thermodynamics of the PbO<sub>2</sub>/PbSO<sub>4</sub> electrode.

The potential of the cell



has been measured by Hamer (32) and Harned and Hamer (33). The electromotive force is given by the equation

$$E = E_0 + \frac{0.05916}{2} \log a_{\text{H}^+}^2 \times a_{\text{SO}_4^{2-}} - \frac{0.05916}{2} \log a_{\text{H}_2\text{O}}^2$$

or

$$E = E_0 + \frac{0.05916}{2} \log m_{\pm}^2 + \frac{0.05916}{2} \log f_{\pm}^2 - \frac{0.05916}{2} \log a_{\text{H}_2\text{O}}^2$$

where  $m_{\pm}$  and  $f_{\pm}$  are the mean molality ( $m_{\pm}^2 = m_{\text{SO}_4^{2-}}$ )<sup>1/3</sup> and the mean stoichiometric activity coefficient, respectively, of the sulfuric acid. At 25°C,  $E_0$  equals 1.685 v. The values for the activity coefficients have been determined with fair accuracy by others (34-41).

Delahay, Pourbaix, and Van Rysselberghe (42, 43) calculated the potential of the positive electrode as follows

$$E = 1.655 - 0.0886 \text{ pH} + 0.0295 \log a_{\text{H}_2\text{SO}_4}$$

and

$$E = 1.712 - 0.1182 \text{ pH} + 0.0295 \log a_{\text{SO}_4^{2-}}$$

The potential of the positive electrode increases,

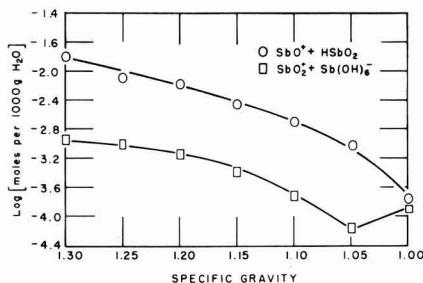


Fig. 19. Solubility of antimony sulfates in sulfuric acid

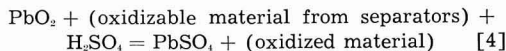
therefore, with increasing acid gravity. Nevertheless, the rate of self-discharge (anodic dissolution of Pb at the exposed areas) decreases with increasing acid concentration, due to increased passivation.

Figure 18 illustrates schematically how, in a plate with an antimonial-lead grid, the Sb may enter into the self-discharge reaction with the positive active material to form (SbO<sub>3</sub>)<sub>2</sub>SO<sub>4</sub> and (SbO<sub>5</sub>)<sub>2</sub>SO<sub>4</sub>, which are more soluble than PbSO<sub>4</sub>. This greater solubility of the Sb corrosion products creates holes or pores in the passivating layer of PbSO<sub>4</sub>, and permits the self-discharge reaction between the Pb metal of the grid and the active material to continue. Figures 2 to 4 show that self-discharge in antimonial positives increases with increasing acid gravity up to a gravity of 1.1, then decreases with increasing acid gravity. This behavior can be explained by the relative solubilities of PbSO<sub>4</sub> and (SbO<sub>3</sub>)<sub>2</sub>SO<sub>4</sub>.

Figure 19 shows the solubility of SbO<sup>3+</sup> + HSO<sub>4</sub><sup>-</sup> + Sb(OH)<sub>6</sub><sup>-</sup> (total amount of trivalent Sb) and of SbO<sub>5</sub><sup>2+</sup> + Sb(OH)<sub>6</sub><sup>-</sup> (total amount of pentavalent Sb) as a function of acid gravity at 25°C. The data for trivalent Sb have been obtained in this laboratory. The values plotted for pentavalent Sb have been calculated from Ref. (44). For the acid gravity range used in storage batteries the solubility of both tri- and pentavalent Sb increases with increasing acid gravity. This opposite effect in the passivating action between the corrosion products of Pb and Sb leads to the maximum observed in Fig. 2-4. At high acid gravities, protection is due to PbSO<sub>4</sub>; at low acid gravities protection is due to corrosion products of Sb. The potential-pH diagram (44) shows that pentavalent Sb will be formed preferably in the corrosion self-discharge process in positive plates.

The amount of self-discharge due to reactions [2] or [3] can be evaluated from the plots shown in Fig. 6 and 7. For positive plates without Sb in the grid alloy, the superposition of reaction [1] and [2] leads to the sulfate figures shown with the curves of Fig. 1 and with the curve marked with the open circle in Fig. 6.

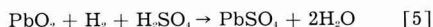
From Fig. 6 and 7 it can be concluded that the reaction



is responsible for a slight amount of positive self-discharge. The self-discharge of the positive plates can be reduced by using separators most resistant to

oxidation. The reaction can be minimized by reducing the contact area between separators and positive plates and by the use of a small number of relatively thick plates.

In 3-plate cells, positive plate self-discharge is practically the same as with single positive plates in contact with separators. The very small difference could be due to the presence of negative plates. These evolve hydrogen on open circuit which could diffuse toward the positive plates and reduce the active material, according to the equation

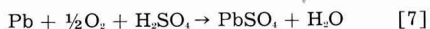


The electrochemical oxidation of hydrogen on  $\text{PbO}_2$  is, however, reaction controlled and extremely small. The solubility of hydrogen in  $\text{H}_2\text{SO}_4$  solutions is quite low and decreases with increasing acid concentration (45). The rate of the oxidation of hydrogen has been studied recently by Frumkin (46, 47), on platinum electrodes. Similar studies for lead dioxide electrodes in this laboratory indicate that hydrogen is reduced at practically immeasurably small rates on these electrodes. The adsorption of  $\text{SO}_4^{2-}$  ions on the  $\text{PbO}_2$  electrode probably inhibits the reaction.

The rate of self-discharge of single negative plates in the absence of separators and positive plates is of the same order of magnitude as the rate of self-discharge of positive plates. Antimony present in the grids of the negative plates accelerates the rate of self-discharge. However, the increase in self-discharge due to Sb in the negative grids is smaller than expected and only becomes important for high Sb concentrations. The self-discharge reaction



is catalyzed by the presence of Sb which has a much lower hydrogen overvoltage than Pb. This fact is especially evident from Fig. 14 which also shows that microporous rubber is the best separator for low self-discharge batteries. The rate of diffusion of Sb toward the negative plate is decreased in the presence of separators. The presence of the separators also decreases the rate of negative plate self-discharge in the absence of Sb. This is due to an inhibition of the diffusion of oxygen toward the negative plates. Oxygen discharges the negative plates according to the reaction:



This reaction is diffusion controlled since the electrochemical reduction of oxygen at the potential of the negative electrode ( $-0.356$  v) is quite fast (48-53). This is also evident from the curves with the open triangles in Fig. 12 and 13.

The solubility of oxygen in  $\text{H}_2\text{SO}_4$  solutions decreases slightly with increasing acid concentration (45). Nevertheless, the self-discharge of the negative plates normally increases with increasing acid concentration due to reaction [6].

The electromotive force of the cell



is given by

$$E = E_0 - \frac{0.05916}{2} \log a_{\text{H}^+}^2 a_{\text{SO}_4^{2-}}$$

or

$$E = E_0 - \frac{0.05916}{2} \log m^{\pm 2} - \frac{0.05916}{2} \log f^{\pm 2}$$

The potential of the Pb/PbSO<sub>4</sub> electrode can be expressed by

$$E = -0.300 - 0.0295 \text{ pH} - 0.0295 \log a_{\text{H}_2\text{SO}_4}$$

and

$$E = -0.356 - 0.0295 \log a_{\text{SO}_4^{2-}}$$

This leads to the conclusion that the potential of the Pb/PbSO<sub>4</sub> electrode is practically independent of pH (31, 42).

The self-discharge of negative plates in 3-plate cells is higher than that of single negative plates covered with separators, even if the positive plate has an Sb-free grid alloy. This could be due to oxygen released from the positive plates according to reaction [1] and subsequent reduction of this oxygen according to reaction [7].

Tests with full size starter batteries with lead antimonial grids have shown that the Sb concentration in the negative active material increases from 0.003% to 0.012% during standard container formation. A further transfer of Sb takes place during open-circuit stand. The concentration of Sb in the positive active material increases from 0.002% to 0.10% during formation, whereas the concentration of Sb in the formation electrolyte never rises above 0.004 g/l. Similar conclusions have been reached recently by experiments with radioactive tracer techniques (54).

From the analysis given in the present paper it can be concluded that seven different self-discharge reactions take place in a lead-acid battery. The rate of each reaction can be determined separately.

#### Acknowledgment

The authors would like to thank Mr. C. G. Grimes, Director of Research of the Electric Storage Battery Company, for permission to publish this paper.

Manuscript received Jan. 20, 1958. This paper was prepared for delivery before the Cleveland Meeting, Sept. 30-Oct. 4, 1956.

Any discussion of this paper will appear in a Discussion Section to be published in the June 1959 JOURNAL.

#### REFERENCES

1. G. W. Vinal, "Storage Batteries," pp. 120-141, John Wiley & Sons, Inc., New York (1940).
2. C. Drotschmann, "Bleiakkumulatoren," pp. 34, 35, Verlag Chemie, G.M.B.H., Weinheim, Bergstrasse (1951).
3. W. H. Beck and W. F. K. Wynne-Jones, *Trans. Faraday Soc.*, **50**, 136 (1954).
4. W. H. Beck and W. F. K. Wynne-Jones, *ibid.*, **40**, 147 (1954).
5. J. J. Lander, *This Journal*, **98**, 220 (1951).
6. W. H. Power, S. W. Rabideau, R. A. Kern, R. T. Pierce, and J. J. Lander, Naval Research Lab. Report P-2G08, Washington (1947).
7. R. H. Greenburg and B. P. Caldwell, *Trans. Electrochem. Soc.*, **80**, 71 (1941).
8. R. H. Greenburg and J. A. Orsino, National Lead Co. Research Lab. Publication No. 219-50, Brooklyn (1950).

9. J. E. Hatfield and O. W. Brown, *Trans. Electrochem. Soc.*, **72**, 361 (1937).
10. J. J. Lander, *This Journal*, **99**, 339 (1952).
11. H. E. Haring and U. B. Thomas, *Trans. Electrochem. Soc.*, **68**, 293 (1935).
12. J. T. Crenell and A. G. Milligan, *Trans. Faraday Soc.*, **27**, 103 (1931).
13. J. W. R. Byfield, *Trans. Electrochem. Soc.*, **79**, 259 (1941).
14. H. E. Haring and U. B. Thomas, *ibid.*, **68**, 293 (1935).
15. C. G. Fink and A. J. Dornblatt, *ibid.*, **79**, 269 (1941).
16. A. C. Zachlin, *ibid.*, **82**, 365 (1942).
17. A. C. Zachlin, *ibid.*, **92**, 259 (1947).
18. H. Stoertz, (to the Electric Storage Battery Co.) U. S. Pat. 2,678,340 and 2,678,341 (1954).
19. M. Le Blanc and E. Eberius, *Z. physik. Chem.*, **A160**, 69 (1932).
20. A. Bystrom, *Arkiv Kemi, Mineralogi Geol.*, **20A**, 1 (1945).
21. T. Katz and R. Faivre, *Bull. Soc. Chim. France*, **16**, D124 (1949).
22. U. B. Thomas, *J. (and Trans.) Electrochem. Soc.*, **94**, 42 (1948).
23. A. Kittel, Beiträge zum Mechanismus der Elektrischen Leitung in PbO<sub>2</sub> und Se, Diss. Prag, Czechoslovak. (1944).
24. P. Ruetschi and B. D. Cahan, *This Journal*, **105**, 369 (1958).
25. W. M. Latimer, "Oxidation Potentials," p. 78, Prentice-Hall, Inc., New York (1953).
26. I. M. Kolthoff and I. K. Miller, *J. Am. Chem. Soc.*, **73**, 3055 (1951).
27. A. Seidell, "Solubilities," p. 1414, D. Van Nostrand Co., Inc., New York (1953).
28. W. H. Beck, R. Lind, and W. F. K. Wynne-Jones, *Trans. Faraday Soc.*, **50**, 1249 (1954).
29. J. Jones, R. Lind, and W. F. K. Wynne-Jones, *ibid.*, **50**, 972 (1954).
30. W. H. Beck, J. Jones, and W. F. K. Wynne-Jones, *ibid.*, **50**, 1249 (1954).
31. B. N. Kabanov, D. I. Leikis, and E. I. Krepakova, *Doklady Akad. Nauk*, **98**, 989 (1954).
32. W. J. Hamer, *J. Am. Chem. Soc.*, **57**, 9 (1935).
33. H. S. Harned and W. J. Hamer, *ibid.*, **57**, 33 (1935).
34. S. Shankman and A. R. Gordon, *ibid.*, **61**, 2370 (1939).
35. R. H. Stokes, *ibid.*, **69**, 1291 (1947).
36. J. E. Kunzler and W. F. Giauque, *ibid.*, **74**, 3472 (1952).
37. R. H. Stokes, *Trans. Faraday Soc.*, **44**, 295 (1948).
38. A. Grollman and J. C. W. Frazer, *J. Am. Chem. Soc.*, **47**, 712 (1925).
39. E. Glueckauf and G. P. Kitt, *Trans. Faraday Soc.*, **52**, 1074 (1956).
40. C. N. Deno and R. W. Taft, *J. Am. Chem. Soc.*, **76**, 244 (1954).
41. E. W. Hornung and W. F. Giauque, *ibid.*, **77**, 2744 (1955).
42. P. Delahay, M. Pourbaix, and P. Van Rysselberghe, *This Journal*, **98**, 57 (1951).
43. J. Van Muylder and M. Pourbaix, Proc. of the 6th Meeting of the International Committee for Electrochemical Thermodynamics and Kinetics, Poitiers (1954).
44. A. L. Pittman, M. Pourbaix, and N. de Zoubov, *This Journal*, **104**, 594 (1957).
45. A. Geffcken, *Z. physik. Chem.*, **49**, 268 (1904).
46. A. Frumkin, *Z. Elektrochem.*, **59**, 807 (1955).
47. A. Frumkin and E. A. Aikazyan, *Doklady Akad. Nauk, SSSR*, **100**, 315 (1955).
48. M. J. Joncich and N. Hackerman, *J. Phys. Chem.*, **57**, 674 (1953).
49. S. A. Siver and B. N. Kabanov, *Zhur. Fiz. Khim.*, **1**, 53 (1948).
50. F. Tödt, *Chemiker Ztg.*, **74**, 254 (1950).
51. H. Grubitsch, *Monatsh. Chem.*, **83**, 549 (1952).
52. P. Delahay, C. L. Pillon, and D. Perry, *This Journal*, **99**, 414 (1952).
53. P. Delahay and L. J. Stagg, *ibid.*, **99**, 547 (1952).
54. W. Herrmann and G. Pröpstl, *Z. Elektrochem.*, **61**, 1154 (1957).

## The Reduction of Passive Films by Hydrogen Diffusion through Steel

R. T. Davis, Jr., and T. J. Butler

*Applied Research Laboratory, U. S. Steel Corporation, Monroeville, Pennsylvania*

### ABSTRACT

An experimental technique is described wherein the diffusion of hydrogen through a steel specimen is followed by electrode-potential measurements. In this technique, one surface of the specimen is exposed to acid and the other surface to a sodium dichromate solution. As the hydrogen produced by acid attack at the steel surface diffuses to the other surface, the potential of the surface in contact with the Na<sub>2</sub>Cr<sub>2</sub>O<sub>7</sub> solution changes with time, and changes of potential ranging from 300 mv to 900 mv are observed. It is believed that the observed potential changes result from the reduction of the dichromate-produced passive film by diffused hydrogen. The effect of variations in steel composition and thickness, acid composition and concentration, and sodium dichromate concentration on the phenomenon is reported.

It is generally recognized that steel is usually permeable to hydrogen under conditions favorable to the formation of atomic hydrogen (1), i.e., high temperature, acid corrosion, or cathodic charging. When corrosion occurs on all surfaces of a steel specimen, the metal eventually becomes saturated with hydrogen. When only one surface is exposed to the corroding acid, hydrogen diffuses through the

specimen and is liberated at the unexposed metal surfaces. A number of methods have been used by various workers to determine the quantity of hydrogen dissolved in steel specimens, viz., degassing techniques (2, 3) and vacuum fusion (4, 5). The permeability of hydrogen in steel has been investigated by gas-solubility (2) and gas-diffusion measurements (6, 7).

Table I. Composition of various steels used in hydrogen diffusion studies

Specimen designation	Composition, per cent											
	C	Mn	P	S	Si	Cu	As	N	Ni	Cr	Mo	Al
A†	0.071	0.38	0.009	0.036	0.001	0.014	0.011	0.002	*	*	*	*
B	0.078	0.38	0.010	0.036	0.001	0.010	0.010	0.009	*	*	*	*
C	0.050	0.28	0.005	0.028	0.001	0.046	0.009	0.003	*	*	*	*
D	0.074	0.30	0.005	0.036	0.001	0.038	0.013	0.004	*	*	*	*
S	0.088	0.49	0.006	0.023	0.002	0.055	0.010	0.002	*	*	*	*
F	0.100	0.34	0.006	0.040	0.001	0.073	0.015	0.004	*	*	*	*
H-1115	0.21	0.82	0.013	0.026	0.032	0.10	0.002	*	0.03	0.036	0.009	0.006
H-1234	0.20	0.72	0.009	0.023	0.063	0.042	0.006	*	0.03	0.022	0.018	0.006

\* Not reported.

† Pairs A, B; C, D; and S, F were from the same heats of steel; members of each pair were processed in a slightly different manner. The three sets of pairs were obtained from three different Corporation mills.

Several years ago, during studies of acid corrosion of steel and hydrogen diffusion into and through steel, it was observed that the potential of the surface of a steel plate exposed to a sodium-dichromate solution changed from a cathodic (passive) potential to an anodic (active) potential when the other surface of the plate was exposed to a corrosive medium. From this we concluded that the hydrogen which diffused through the plate apparently reduced the passive surface formed by reaction with the dichromate solution. Because this phenomenon appeared to be a useful method for studying hydrogen diffusion and passive films, further research work was undertaken. We are reporting here the results of studies on the effect of variations in (a) steel composition and thickness, (b) the nature and concentration of the corroding medium, and (c) passivating conditions, on the time-potential phenomenon.

Several workers have studied the reaction of diffused hydrogen with various liquid substances or solutions (8-10) and have measured the potential of the exit surface exposed to various solutions (11, 12). However, until recently, only Uhlig (13, 14) had described this phenomenon. He used the phenomenon as a means of studying passivation reactions with iron-chromium alloy surfaces and was not particularly interested in studying hydrogen diffusion. Recently, Amiot (15) studied this phenomenon and reported results somewhat similar to but not as complete as those reported here.

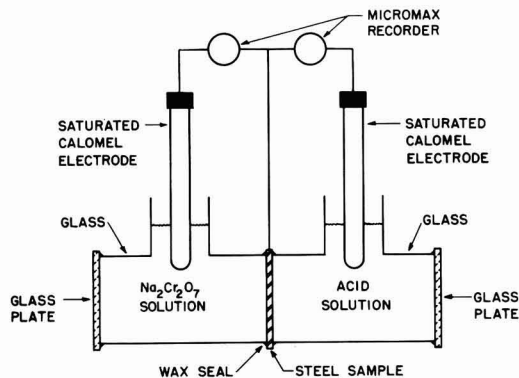


Fig. 1. Diffusion cells

## Experimental

**Steel.**—One set of specimens consisted of samples of tin-plate-gauge steel (approximately 0.25 mm thick) that had been obtained from several different sources. The other set of specimens consisted of samples of low-carbon steel (AISI C1020) that had been machined to various thicknesses ranging from 2.54 mm to 25.4 mm. The chemical compositions of the steel specimens are shown in Table I. The tin-plate steels had been box annealed. The prior processing history of the AISI C1020 steels is not known. From an examination of the microstructure of Sample H-1235 it is believed to have been annealed.

**Solution.**—All solutions were prepared from reagent-grade chemicals dissolved in distilled water. Unless otherwise specified, the corroding acid was 2N H<sub>2</sub>SO<sub>4</sub>, and the passivating solution was 0.05M Na<sub>2</sub>Cr<sub>2</sub>O<sub>7</sub>. Acid solutions containing a sulfite promoter were 0.01M Na<sub>2</sub>SO<sub>3</sub> in 2N H<sub>2</sub>SO<sub>4</sub>, and were freshly made prior to use.

**Instrumentation.**—All measurements of potential were made relative to the saturated calomel electrode (Leeds & Northrup Model 1199-31). The electrode potentials were recorded either on a six-point L&N Micromax Recorder that records the points at 1-min intervals, or on a L&N Speedomax Recorder having a strip speed of 10 in./min.

**Cell construction.**—Figure 1 shows a diagrammatic sketch of the cells in which the potentials were measured. The glass cells were made of 28 mm (OD) tubing, and each cell held about 30 cc. The steel samples were affixed to the cell by a wax seal (beeswax and rosin mixture). The steel acted as one electrode. Saturated calomel reference electrodes were inserted into the necks of either or both of the cells.

**Method of measurement.**—The cell unit was assembled as shown in Fig. 1. Sodium dichromate solution was poured into one of the cell compartments, the calomel electrode was inserted into the solution, and the whole unit was placed in a constant-temperature oven maintained at 40°C. The potential of the steel surface exposed to the dichromate solution was recorded as a function of time. When this potential became constant, usually after several hours, acid was poured into the other cell, and the measurement of the potential in the dichromate cell was continued. In some experiments, the potential of the

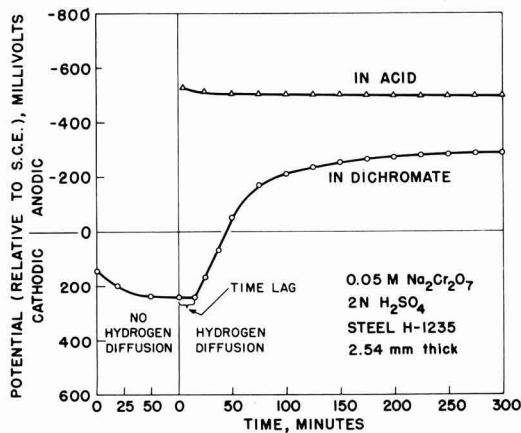


Fig. 2. Typical time-potential relation

surface exposed to the acid was also recorded as a function of time.

#### General Description of the Phenomenon

The initial potential of the steel surface exposed to the dichromate passivating solution is cathodic (Fig. 2). With continued exposure to the passivating solution, the steel surface becomes more cathodic and finally, after several hours, exposure, reaches a cathodic potential of several hundred millivolts. Upon addition of acid to the adjacent cell, the potential of the passive surface remains constant for a time and then changes rapidly in the anodic direction. After a few hours, the potential of the passive surface becomes several hundred millivolts anodic, approaching in some instances a potential approximating that of the normal hydrogen overvoltage on steel.<sup>2</sup> The potential of the surface exposed to acid does not change appreciably with time.

<sup>1</sup> All potential designations in this paper are with respect to the saturated calomel electrode.

<sup>2</sup> "Normal hydrogen overvoltage on steel" as used in this paper is the potential approximating that observed when steel corrodes in an acid solution. See, for example, Fig. 2.

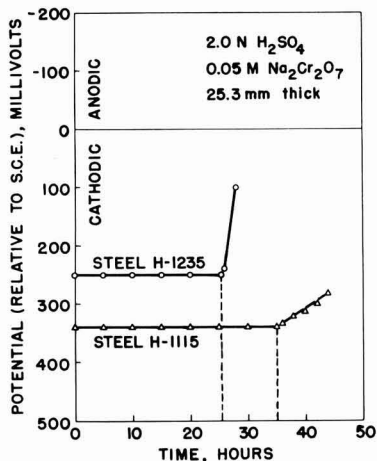


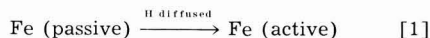
Fig. 3. Time-potential plots for two steels of same nominal composition (AISI C1020).

Table II. Time-lag values for tin-plate steels

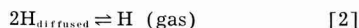
Steel	Thickness (mm)	Time-lag,* sec
A	0.235	9.6
B	0.237	9.7
C	0.238	10.3
D	0.240	13.7
S	0.256	7.5
F	0.248	18.5

\* Charging medium 2N H<sub>2</sub>SO<sub>4</sub>. Detecting medium 0.05M Na<sub>2</sub>Cr<sub>2</sub>O<sub>7</sub>.

The reactions taking part in the phenomena described above are undoubtedly complex. Acid attack on the nonpassivated side produces hydrogen, some of which remains atomic in character and diffuses through to the passivated side. Here two reactions are possible: reduction of the passivating film on the metal surface by the diffused hydrogen, with a consequent change in surface potential



or recombination of the diffused hydrogen to form gaseous molecular hydrogen



There is reason to believe that reaction [1] does occur (see later). Uhlig (13) interpreted the potential change as a result of an increase in thermodynamic "activity" of the iron and chromium components of his alloys caused by the presence of the diffused hydrogen in the lattice system. We do not believe that this is as logical an explanation as the one we proposed, which is in agreement with the suggestion made by Hoar in a discussion of Uhlig's work (13). This phenomenon is affected by variations in experimental conditions in the following manner.

#### Effect of Steel Composition

Figure 3<sup>3</sup> presents the results of measurements made under uniform conditions for two different steel specimens of the same nominal steel type (AISI C1020) but of slightly different chemical composition. It is observed that the time-lag (time elapsing between initiation of corrosive attack and the break in the time-potential curve) is greater for one steel than for the other steel, and also that the slope is much greater for one steel than for the other. There is also a difference in the initial cathodic passive potential; however, this difference does not appear to affect the time-lag of the steel and apparently is related to nonuniform surface preparations.

Figure 4 presents the results of measurements made on six different tin-plate-gauge steel samples. Here the time-lag is so short (about 15 sec) that it does not appear in the figure. However, the time-lags have been determined by using the Speedomax recorder, and they are presented in Table II. Apparently, the nature of the steel significantly affects the shape of the time-potential curves and the time-lag value.

<sup>3</sup> Unless otherwise indicated, the zero of the time scale on all figures refers to the time at which acid was added to the cell.

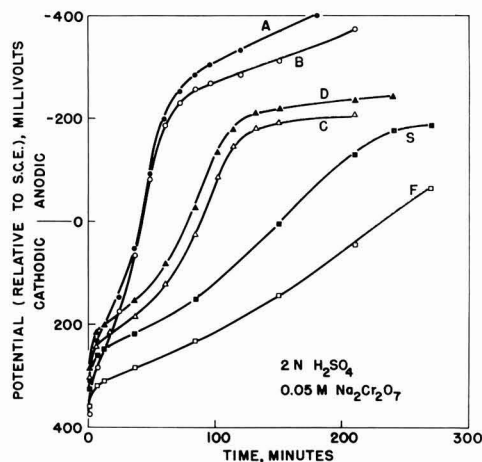


Fig. 4. Time-potential relation for tin-plate steels

It has not been possible to determine which factors, with respect to steel composition or processing history, influence these results. However, there are several ways in which variations in steel composition could effect the phenomena. For example, the chemistry of the steel can influence the rate of corrosion attack and thus increase or decrease the rate at which hydrogen is reduced at the surface. Moreover, the presence of certain alloying elements or metal impurities at the surface can catalyze or poison the recombination or surface-diffusion reactions and thus influence the ratio of hydrogen diffused to gaseous hydrogen released (effused) at the surface. Separate studies of this ratio will be made at a later date to help clarify this point.

It is also possible that variations in the steel composition or degree of mechanical work influence the rate of hydrogen diffusion, and indeed, this has been reported (2). Likewise, variations in steel composition may affect the passivation reaction in the dichromate solution and the reduction of the passive film at the dichromate-steel surface.

#### Effect of Steel Thickness

The effect of steel thickness was investigated with two different steels and with thickness variations ranging from 2.5 mm to 25.4 mm. Figure 5 shows

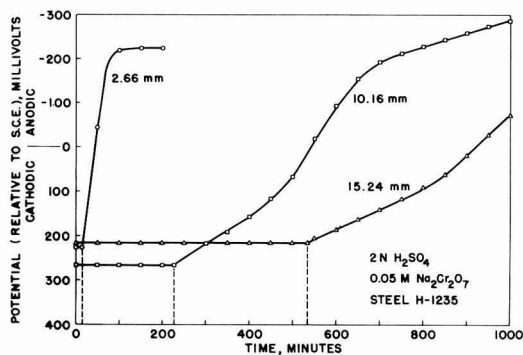


Fig. 5. Effect of sample thickness on time-potential relation

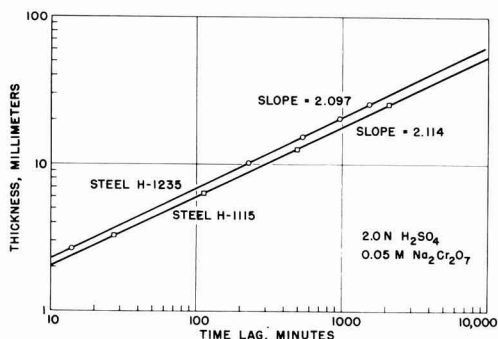


Fig. 6. Plot of thickness vs. time-lag

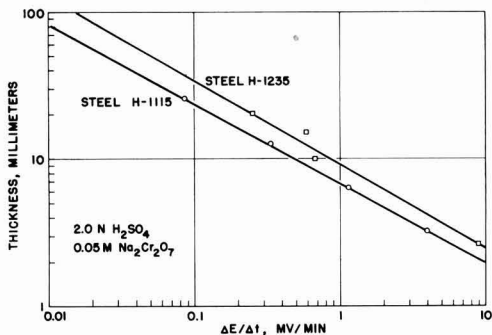
that as the thickness ( $d$ ) of the steel increases the time-lag increases. A plot of the logarithm of the time-lag vs. the logarithm of thickness for the two steels investigated is shown in Fig. 6, where a straight-line relationship is observed. The lines for the two steels are parallel and have a slope of approximately 2.10. If the time-lag data are plotted against the square of thickness,  $t$  vs.  $d^2$ , the deviation from linearity at the smaller thicknesses cannot be detected. However, calculation of  $k$  of the equation  $t = kd^2$  for the various sets of time-lag—thickness data shows that the  $k$  is not a true constant (see Table III).

It was also observed (Fig. 5) that the initial slope of the time-potential curve decreased with increasing specimen thickness. A plot of  $\log(dE)/(dt)$  vs.  $\log d$  is shown in Fig. 7. The lines for the two steels are nearly parallel and have a slope of approximately  $-1.8$ .

These data indicate that the time-lag is related to the thickness of the steel by the relation  $t = kd^{2.10}$  (see Table III). If it is assumed that the time-lag is a measure of the time required for hydrogen to diffuse through the specimen and appear at the steel-dichromate surface, then these results are in accord with classical diffusion theory, which would predict that the time should be proportional to the thickness squared. Whether the difference between the observed exponent 2.10 and the theoretical exponent of 2.00 is real or due to experimental error is

Table III. Time-lag vs. thickness for steel samples H-1115 and H-1235

Thickness, $d$ (mm)	Time lag, $t$ (min)	$k_1 = \frac{t}{d^2}$	$k_2 = \frac{t}{d^{2.1}}$
<i>Sample H-115</i>			
3.22	27	2.60	2.31
6.32	113	2.83	2.35
12.60	492	3.12	2.34
25.3	2100	3.29	2.35
<i>Sample H-1235</i>			
2.66	14	1.97	1.80
5.08	53	2.03	1.74
10.2	228	2.19	1.74
12.7	350	2.19	1.68
15.2	536	2.32	1.77
20.7	961	2.23	1.72
25.2	1527	2.41	1.72

Fig. 7. Plot of thickness vs.  $\Delta E/\Delta t$ 

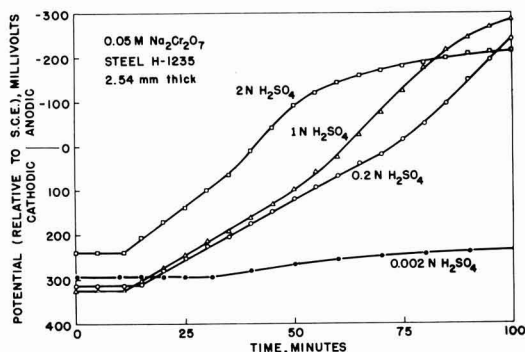
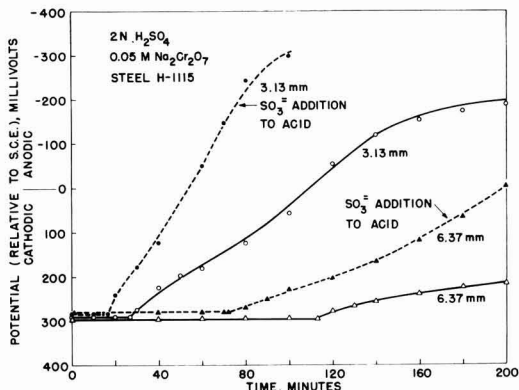
not known. Indeed, it is likely that the time-lag does not correspond to the time required for the appearance of the hydrogen but perhaps to the time required for the rate of hydrogen arrival at the surface to reach a certain value.

If the change in potential  $\Delta E$  is assumed to be proportional to the quantity,  $Q$ , of hydrogen which has diffused through the steel plate, then  $\Delta E/\Delta t$  should be proportional to  $dQ/dt$ . However, classical diffusion theory predicts  $dQ/dt$  to be inversely proportional to the thickness,  $d$ , of the membrane or thus, by analogy,  $\Delta E/\Delta t$  should be proportional to  $d^{-1}$  rather than  $d^{-1.8}$  as found experimentally. Apparently  $\Delta E/\Delta t$  is not proportional to the quantity of hydrogen passed through the steel, a relation which is perhaps too simple to have expected anyway. Thus, there is no explanation at this time for the  $\Delta E/\Delta t = kd^{-1.8}$  relationship.

#### Effect of Acid Variations

The effect of variations in sulfuric acid concentration is shown in Fig. 8. Note that a 1000-fold change in acid concentration markedly influences the shape of the time-potential curves. As the acid concentration decreases, the time-lag increases, and  $\Delta E/\Delta t$  also decreases slightly. This is in agreement with the concept that at lower acid concentrations the rate of steel corrosion, and consequently the rate of hydrogen diffusion, decreases.

Other investigators have shown that the addition of certain compounds to the acid solution increases the rate at which hydrogen enters steel (2, 14). One

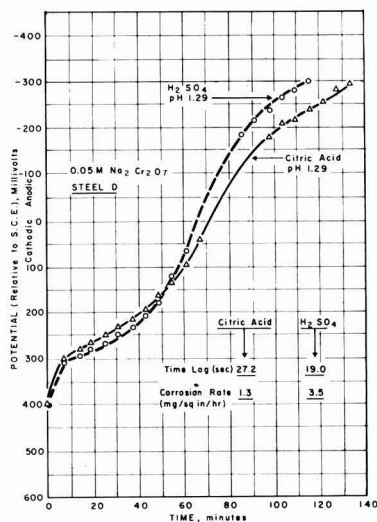
Fig. 8. Effect of variation of charging acid ( $H_2SO_4$ ) concentration on time-potential relation.Fig. 9. Effect of  $SO_3^{2-}$  promoter action on time-potential relation.

such compound is sodium sulfite. The effect of its addition to the corroding acid on the time-potential curve is shown in Fig. 9. The addition greatly decreases the time-lag and increases  $\Delta E/\Delta t$ . Preliminary corrosion rate studies indicate that the presence of the sulfite increases the corrosion rate, but the change in time-lag with sulfite addition is not necessarily proportional to the change in corrosion rate.

The effect of using citric acid instead of sulfuric acid as the corroding medium is shown in Fig. 10 for the case of solutions of equal pH (1.29). Although the time-potential curves are similar when recorded over several hours, the time-lag for the sulfuric acid experiment is considerably shorter than for the citric acid experiment (19.0 vs. 27.2 sec) and the corrosion rate with sulfuric acid is almost three times greater than with citric acid.

#### Effect of Variations in Passivating Solution

Figure 11 illustrates the changes that occurred when the concentration of the dichromate solution

Fig. 10. Effect of variation in acid composition ( $H_2SO_4$  vs. citric) at equal pH on time-potential relation.

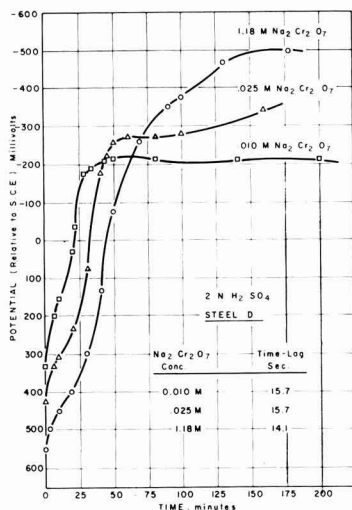


Fig. 11. Effect of variation in detecting solution ( $\text{Na}_2\text{Cr}_2\text{O}_7$ ) concentration on time-potential relation.

was varied from 0.01M to 1.18M. As the concentration of sodium dichromate increases, the initial  $\Delta E/\Delta t$  decreases; however, the time-lag remains relatively constant.

In addition to the use of sodium dichromate as a passivating solution, experiments are under way in which concentrated nitric acid, mercurous nitrate, and sodium hydroxide solutions are used as passivating agents; however, these experiments are not complete and will be reported at a later time.

### General Discussion

On the basis of the results described above, we believe that the electrode potential of the steel surface exposed to the dichromate solution is changing because of a surface reaction. The potential change does not appear to be related to the increase in dissolved hydrogen in the metal lattice or to diffusion through the lattice.

This surface reaction appears to be the reduction of the passive iron-oxide film. When this reaction occurs even to a slight extent, the surface can consist of three types of areas: the passive iron-oxide area, a reduced-iron area, and a reduced-iron area concentration-polarized by a gaseous hydrogen film. Thus, the electrode potential of the surface is no longer that of the passive iron oxide. As time proceeds, the reduced-iron area tends to increase; however, its rate of increase is influenced by the rate of passivation in the dichromate solution. Moreover, the presence of the polarizing gaseous hydrogen film on the surface tends to prevent the dichromate ions from reaching the reduced iron surface. Thus, the initial or early slope of the time-potential curve is determined by (a) the rate at which the hydrogen diffuses through the metal (see Fig. 5), and (b) the rate of passivating reaction, i.e., dichromate concentration (see Fig. 11). The final potential of the sys-

tem is determined by whether the hydrogen-diffusion rate is rapid enough to completely overshadow the passivation rate, in which case the final potential is that of the normal hydrogen overvoltage on the steel surface. This actually occurs, for example, when sodium sulfite is used as a promotor, Fig. 9, or with certain steels, Fig. 4. If the hydrogen-diffusion rate is not sufficient to overshadow the passivation rate, eventually a dynamic equilibrium condition is reached wherein a constant fraction of the surface exists as a passive film and another fraction as a hydrogen polarized iron electrode. In this situation, the potential becomes steady at some value less than that of the normal hydrogen overvoltage. Numerous incidences of this have been observed (see, for example, Fig. 4 and 11). As further evidence that an equilibrium exists, it was noted that, if the acid solution is completely removed or neutralized with sodium hydroxide, the potential of the surface in the dichromate solution changes in the cathodic direction. It has also been observed that, if the corrosion reaction lowers the strength of the corroding medium, the potential in the dichromate solution will pass through a maximum.

This technique should be useful in studies of the effect of corrosion inhibitors and accelerators on hydrogen diffusion and the nature of surface passivation reactions.

### Acknowledgment

Mr. John Burke assisted in making many of the experimental measurements described above, and his assistance is gratefully acknowledged.

Manuscript received March 4, 1958. This paper was prepared for delivery before the Cleveland Meeting, Sept. 30-Oct. 4, 1956.

Any discussion of this paper will appear in a Discussion Section to be published in the June 1959 JOURNAL.

### REFERENCES

1. T. S. Fuller, *Trans. Am. Electrochem. Soc.*, **36**, 113 (1919).
2. L. S. Darken and R. P. Smith, *Corrosion*, **5**, 1 (1949).
3. T. D. McKinley, *This Journal*, **102**, 117 (1955).
4. R. A. Heaton, *Vacuum*, **2**, 115 (1952).
5. D. J. Carney, J. Chipman, and N. J. Grant, *J. Metals*, **188**, 397 (1950).
6. C. A. Edwards, *J. Iron Steel Inst. London*, **110**, 9 (1924).
7. T. N. Morris, *J. Soc. Chem. Ind., London*, **54**, 7T (1935).
8. L. D. McGraw, et al., National Advisory Committee for Aeronautics, Technical Note 2696, April 1952; Technical Note 3164, March 1954.
9. M. J. N. Pourbaix, "Thermodynamics of Dilute Aqueous Solutions," p. 95, Edward Arnold and Co., London (1949).
10. J. Bernard and P. H. Albert, *Compt. rend.* **224**, 45 (1947).
11. H. Fisher and H. Heiling, *Z. Elektrochem.*, **54**, 184 (1950).
12. J. A. Bagotskaya and A. N. Frumkin, *Doklady Akad. Nauk, SSSR*, **92**, 979 (1953).
13. H. H. Uhlig, *Trans. AIME*, **140**, 387 (1940).
14. H. H. Uhlig, N. E. Carr, and P. N. Schneider, *Trans. Electrochem. Soc.*, **79**, 111 (1941).
15. P. Amiot, L'Institut de Recherches de la Siderurgie, Series A, **158**, 57, April 1957.

# An Investigation of Chemical Variables Affecting the Corrosion of Copper

W. D. Robertson,<sup>1</sup> V. F. Nole, W. H. Davenport, and F. P. Talboom, Jr.<sup>2</sup>

Chase Brass and Copper Company, Waterbury, Connecticut

## ABSTRACT

In the presence of excess oxygen the corrosion rate of copper is a linear function of hydrogen ion concentration for each of three anions ( $\text{SO}_4^-$ ,  $\text{Cl}^-$ ,  $\text{C}_2\text{H}_3\text{O}_2^-$ ). The rate is not a simple function of anion concentration, and the concentration dependence varies with pH. The effect of  $\text{CO}_2$  is negligible. The temperature dependence of the rate, at constant oxygen concentration, for both chloride and sulfate solutions, is

$$\text{Rate} = A e^{-10000/RT}$$

The corrosion rate of copper in open solutions saturated with air goes through a maximum in the range  $71^\circ\text{--}77^\circ\text{C}$ .

The corrosion rate of copper has been determined in dilute aqueous salt solutions, under conditions in which an attempt was made to maintain a constant, predetermined electrolyte composition throughout the test period. This was accomplished by passing solutions continuously through the corrosion vessel at a rate such that the corrosion rate was independent of the solution flow rate.

Previous investigations of the rate of solution of Cu in  $\text{H}_2\text{SO}_4$  (1) and in ammonia (2) served a similar purpose by providing a large excess of reactants in a closed system. However, the present technique of a flowing system was adopted, in preference to a closed system, to avoid a significant increase in soluble corrosion products which affect the rate (3) and, at the same time, to supply an excess of reactants to the surface at a constant concentration.

The chemical variables investigated included anion concentration and type (sulfate, chloride, and acetate), hydrogen ion concentration, oxygen, free carbon dioxide, and temperature.

## Experimental Procedure

**Material.**—The material selected for the testing program was phosphorous deoxidized copper containing 0.025% phosphorus, less than 0.01% zinc, less than 0.002% iron and nickel, and less than 0.005% lead. Test specimens were prepared from cold rolled sheet, 0.032 in. thick, milled to 3.000 x 0.740 in. All edges and corners were rounded (approximate radius of curvature 0.016 in.) using an abrasive belt with No. 180 emery paper.

Prior to testing, specimens were prepared by hand scrubbing with water and pumice, rinsed in hot water, and dried immediately. Then they were weighed to the nearest tenth of a milligram and placed under test in a reproducible manner so that comparable films were formed on all specimens during the brief atmospheric exposure.

Subsequent to testing, specimens were cleaned electrolytically (4) in 5%  $\text{H}_2\text{SO}_4$  containing approximately 2 ml/liter of an organic inhibitor (Rordine No. 77) for a period not exceeding 1.5 min at a current density of 0.2 amp/cm<sup>2</sup> with a Pt anode. This procedure successfully removed corrosion products without affecting the remaining metallic specimen. The specimens were then dried and again weighed to the nearest tenth of a milligram.

All plotted points are the arithmetic average of at least two determinations, and, in general, reproducibility was about  $\pm 10\%$ .

**Corrosion cell.**—To maintain constant composition of the solution a test cell of the form shown in Fig. 1 was adopted. A continuous supply of solution was fed to the bottom of the cell through the center tube at 230 ml/hr, which was established by experiment as approximately twice the rate at which corrosion varied significantly with solution flow rate. The solution was carried up the side arm by the airlift, mixed with solution in the tube, and aerated; the solution then passed over the specimens, and

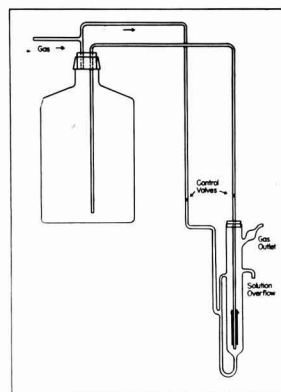


Fig. 1. Corrosion testing cell arranged for continuous renewal of solution and aeration.

<sup>1</sup> Yale University, New Haven, Conn., Consultant.  
<sup>2</sup> Present address: U. S. Navy, 224 8th St., N.H.A. #1, Honolulu 18, T.H.

excess solution overflowed at the top. The pH of the air-saturated solution remained constant to  $\pm 0.1$  unit, and the concentration of soluble Cu increased from zero to  $3 \times 10^{-3}M$  at pH 1.6, and from zero to  $8 \times 10^{-3}M$  at pH 6 in 48 hr.

**Preparation of solutions.**—All solutions were prepared in 10-gal quantities with laboratory distilled water and reagent grade chemicals. In the case of the chloride or sulfate ions, HCl or  $H_2SO_4$  was added to the water until the desired pH was attained. By the addition of the proper sodium salt, the anion concentration was adjusted to the required value. With the acetate ion, the proper anion concentration was first obtained with acetic acid and then sodium hydroxide was added until the required pH was attained. Chloride, sulfate, and acetate concentrations were determined subsequently by titration.

**Gas atmosphere.**—When a gas atmosphere other than air was required, the gas was bubbled through the stock bottle of test solution for a period of not less than 12 hr, which was found to be sufficient to saturate the solution. During the test, gas was passed over the previously saturated solution to maintain saturation and through the corrosion cell via the gas lift. In the case of air, the solution was presaturated with air, from which  $CO_2$  was removed by calcium hydroxide and the  $CO_2$  free air was bubbled through the cells. The flow of gas to the side arm of the corrosion cell was maintained at 400 ml/min for all tests. Oxygen availability to the corroding surface was controlled by varying the partial pressure of  $O_2$  in the gas mixture.

Gas saturation at higher temperatures was performed in the same manner. Oxygen concentrations at the various temperatures were obtained from available data (5, 6) which were verified by chemical analysis. Analyzed concentrations were found to be in agreement with the reported data.

Gases used in testing, other than air, were oxygen, carbon dioxide, mixtures of oxygen and nitrogen, and mixtures of oxygen and carbon dioxide. These gases were obtained in cylinders of commercial grade. When mixtures of gases were desired, composition was defined with flowmeters and dissolved oxygen concentrations in the solutions were

determined by analysis, using a modified Winkler method.

**Temperature.**—The temperature dependence of corrosion rate was determined by immersing cells in an oil bath controlled to  $\pm 0.3^\circ C$ . The test solution was admitted to the cell, and the selected gas atmosphere passed through the cell in the usual manner. Upon reaching the desired temperature, the test was initiated by placing the specimens in the cell and starting the flow of solution through the cell.

Experiments involving different oxygen concentrations, defined by oxygen solubility under 1 atm of air at each temperature (the usual practical case), and experiments at constant oxygen concentration at all temperatures were performed. In the former experiments, air alone was bubbled through the cell so that the solution reached saturation with respect to oxygen in air at the temperature of the experiment.

To obtain a measure of the temperature dependence of corrosion of copper at constant oxygen concentration, tests were run with an oxygen concentration determined by the oxygen solubility at  $82^\circ C$ . From the oxygen solubility curve and chemical analysis it was found that the test solution contained 2.56 ppm ( $8 \times 10^{-5}M$ ) dissolved oxygen from the air at  $82^\circ C$ . The oxygen concentration at this temperature was taken as the constant concentration, and oxygen and nitrogen in proper proportions were used to provide 2.56 ppm oxygen at all lower temperatures. All other tests, except those designed specifically to study temperature effects, were run at room temperature.

### Experimental Results

**Time dependence.**—Tests were conducted to determine whether corrosion rates were constant in time. Chloride and sulfate solutions of different anion concentrations, each at a pH of 2, 3, and 6 were investigated. Typical data are presented in Fig. 2.

The results of these tests show that corrosion is linear in time under the present conditions of surface preparation, constant solution composition, and pH. This was in spite of the fact that visible corrosion films are formed in the pH range of 6 to 3, but no film is evident at pH 2. On the basis of these results the exposure time chosen for subsequent tests was arbitrarily set at 48 hr.

**Anion concentration.**—Figure 3 shows the dependence of corrosion rate on sulfate and chloride concentrations at pH 2 and pH 6; at pH 2 it is impossible to extend the investigation to the low anion concentrations attainable at pH 6. Obviously, the dependence of corrosion rate on the type and concentration of anion is extremely complicated, and more extensive and detailed investigations will be necessary to separate the different factors. Almost certainly a single explanation cannot cover adequately all the observed variations.

**Dependence of corrosion rate on pH and oxygen concentration.**—The effect of pH on the corrosion rate of Cu in chloride, sulfate, and acetate solutions is shown in Fig. 4. For sulfate and acetate solutions the logarithm of corrosion rate is seen to be a linear

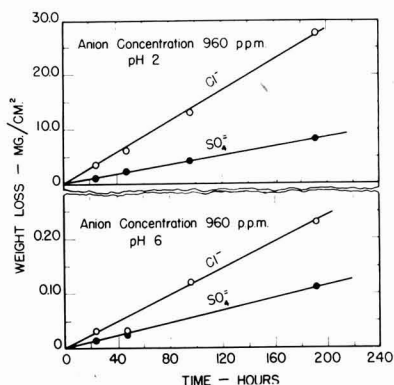


Fig. 2. Corrosion of Cu at  $20^\circ C$  as a function of time in chloride and sulfate solutions saturated with air at a pH of 2 and 6.

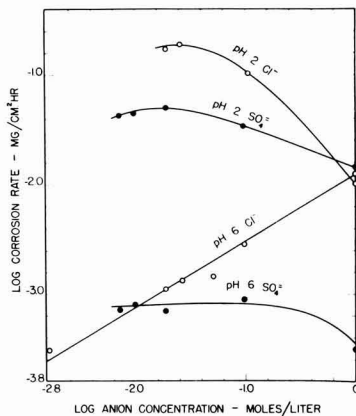


Fig. 3. Corrosion of Cu at 20°C as a function of chloride and sulfate concentration at a pH of 2 and 6, air saturation.

function of pH. In chloride solutions, below a pH of 3, the deviation from linearity is attributable to insufficient oxygen. In Fig. 5 the dependence of corrosion rate on oxygen concentration is seen to be significant in chloride solutions below pH 3. In this range corrosion rate appears to become almost independent of pH at a level defined by the oxygen partial pressure.

*Effect of carbon dioxide.*—Before investigating the effect of CO<sub>2</sub> concentration, it was necessary to determine the significance of oxygen in combination with CO<sub>2</sub>. A series of experiments were conducted in sulfate and chloride solutions at pH 2, 3, and 6, saturated with free CO<sub>2</sub> in the absence of oxygen. The resulting negligible corrosion rate showed that oxygen, or an oxidizing agent, is necessary, and also that CO<sub>2</sub>, by itself, does not cause corrosion of Cu.

In accordance with the preceding results, it was necessary to combine the CO<sub>2</sub> with various constant oxygen concentrations. Two constant oxygen concentrations were chosen: saturation with air (8 ppm O<sub>2</sub>) and the concentration resulting from saturation with oxygen (40 ppm O<sub>2</sub>).

The results are shown in Fig. 6. At pH 6 the corrosion rate appears to increase with an increase in

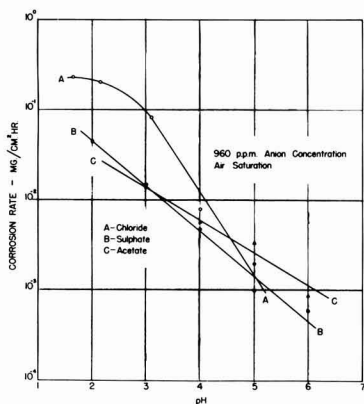


Fig. 4. Logarithm of corrosion rate of Cu at 20°C as a function of pH in sulfate, acetate, and chloride solutions.

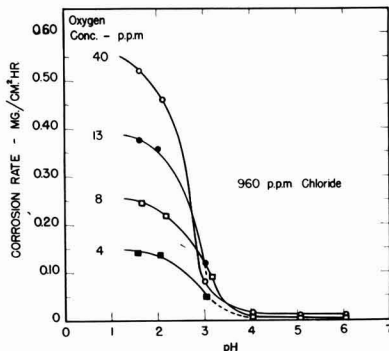


Fig. 5. Dependence of corrosion rate of Cu at 20°C on pH in a chloride solution.

CO<sub>2</sub>, but this apparent increase is probably due to the difficulty of maintaining a constant pH of 6 with CO<sub>2</sub> in an unbuffered solution. At a pH of 3 the corrosion rate apparently decreases with small concentrations of CO<sub>2</sub> and then becomes essentially independent of the CO<sub>2</sub> concentration.

The lack of significant effect of CO<sub>2</sub> on the corrosion rate does not contradict general experience. In an unbuffered solution, the addition of CO<sub>2</sub> produces an increase in hydrogen ion concentration. In the present experiments, this increase is eliminated and it is demonstrated that CO<sub>2</sub>, as such, has little or no effect on the corrosion rate.

*Effect of temperature.*—Figure 7 shows the dependence of corrosion rate on temperature at a pH

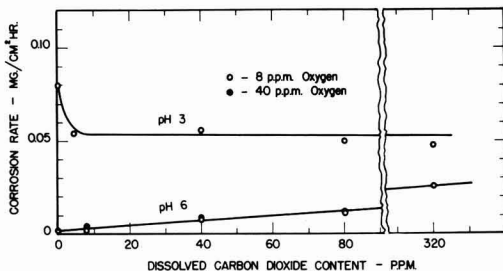


Fig. 6. Corrosion of Cu at 20°C as a function of CO<sub>2</sub> concentration.

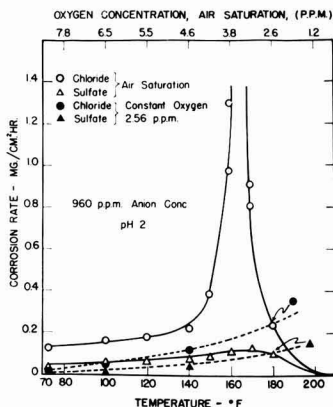


Fig. 7. Dependence of corrosion rate of Cu on temperature in chloride and sulfate solutions at a pH of 2.

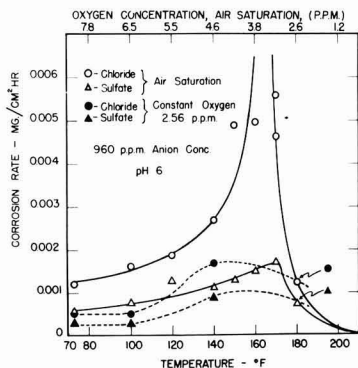


Fig. 8. Dependence of corrosion rate of Cu on temperature in chloride and sulfate solutions at a pH of 6.

of 2, in sulfate and chloride solutions (a) in equilibrium with air and (b) at constant oxygen concentration. The effect of temperature at a pH of 6, in chloride and sulfate, is shown in Fig. 8.

At a pH of 6 and a pH of 2, and constant chloride concentration of 960 ppm Cl<sup>-</sup>, the corrosion rate goes through a very high maximum between 160° and 170°F (71°-77°C) in an open system. At constant sulfate concentration a maximum also appears but the corrosion rate does not become catastrophic. In both cases oxygen concentration is decreasing with temperature as shown.

The effect of temperature at constant oxygen concentration (2.56 ppm O<sub>2</sub>) is also shown in Fig. 7 and 8. The lower rates are, of course, due to lower oxygen concentrations at all temperatures. In sulfate and chloride solutions at pH 6 and at the low oxygen concentration, the corrosion rates are extremely low and the data are correspondingly uncertain, but the data indicate that a maximum rate persists in the higher ranges of temperature. Subsequent tests were made in this range and the data were verified. At pH 2, the corrosion rate is shown as increasing uniformly with temperature; however, as a result of the considerations below, it is possible that a maximum may also be found in a narrow range of temperature near 71°C, where data are lacking.

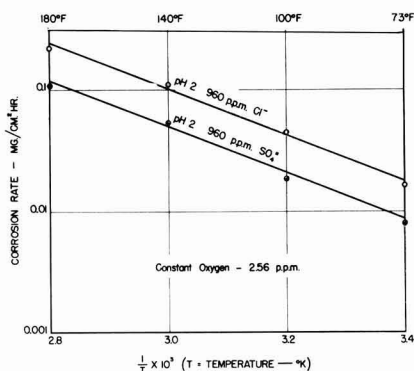


Fig. 9. Corrosion rate of Cu as a function of reciprocal absolute temperature.

## Discussion

*Time dependence.*—Since the corrosion rate at room temperature was found to be constant in time in both sulfate and chloride solutions at each pH level, it appears that the growth of visible films in time does not significantly affect the rate (which is characteristic of each ion type and pH level).

Weeks and Hill (7) have shown that the rate diminishes from a high initial value to a constant rate after about 1 min in acid chloride solutions. However, in the latter experiments, a higher order of sensitivity was employed and, while oxide films were substantially removed prior to immersion, it is possible, as suggested by those authors, that the rapid solution of traces of oxide may account for the high initial rate. In the present experiments, no attempt was made to eliminate air-formed films, and the results show that films formed during the subsequent corrosion process do not significantly affect the rate which is constant from zero time. Since a linear dependence on time was obtained in both acid and near neutral solutions, it appears that the results are quite general.

*Hydrogen ion concentration.*—If it is assumed that corrosion rate is proportional to hydrogen ion concentration, then, in accordance with the definition of pH:

$$\log \text{rate} = -k \text{pH} + \text{constant} \quad [1]$$

The experimental data obtained in sulfate, acetate, and chloride solutions, Fig. 4, are in accordance with this relationship, except in chloride solutions below pH 3 where the system appears to be under oxygen control. A similar departure from linearity was observed by Weeks and Hill (7) at a lower pH. Figure 5 shows that the limiting rate is approximately proportional to the oxygen concentration which is consistent with a limiting rate defined by the diffusion-controlled transport of oxygen from the solution to the metal interfaces.

Since hydrogen ions are not reduced by the oxidation of Cu, under the present conditions, the linear dependence of corrosion rate on hydrogen ion concentration requires some explanation. Weeks and Hill (7) and Hill (8) have proposed the following net reaction for the rate-determining step:



It was assumed that oxygen is first adsorbed from solution to form an "oxidized site," followed by reaction with a hydrogen ion to form the cuprous ion and the peroxide ion. The results of the present investigation appear to be generally in accord with this mechanism.

*Chloride and sulfate dependence.*—With respect to the relatively high rates observed in chloride solutions, compared with sulfate solutions, certain negative conclusions may be drawn, but the detailed mechanism is still not clear. Perhaps it should be emphasized that these data were obtained with a constant anion concentration at each pH.

In the apparent absence of rate-limiting films, particularly at pH 2, the penetrating properties of chloride ions, as demonstrated with Al and passi-

vated Fe, do not seem to have any obvious function. Furthermore, at the lower pH, the rate decreases with increasing chloride concentration, approximately parallel with the decreasing rate in sulfate solutions and the decrease is considerably larger than can be accounted for by decreasing oxygen solubility. At pH 6, the rate does increase with chloride ion concentration and it may be that film penetration is involved. However, there is no other evidence of a rate-limiting film and, since chloride ion does not appear to be involved in the net reaction, its function is not obvious.

**Temperature dependence.**—Analysis of the temperature dependence of corrosion rate can be rigorously applied only to conditions of constant oxygen concentration. However, the data obtained in air-saturated open systems is of considerable practical significance, i.e., the existence of a catastrophic phenomenon that appears in a temperature range around 71°C in chloride solution.

In conformity with general kinetic theory, the temperature dependence of reaction rate is written:

$$\text{Rate} = A \exp(-E/RT) \quad [3]$$

and, accordingly, log Rate is shown as a function of reciprocal temperature in Fig. 9 for constant oxygen and a pH of 2. Obviously the data are in complete accord with the relationship; the apparent activation energy,  $E$ , is 9000 cal/mole and is the same for both chloride and sulfate solutions. It may be significant that the observed activation energy for this process, involving the reduction of oxygen, lies in the range of values observed (9) for the reduction of hydrogen ions on Pt and Pd, 6000-11500 cal/mole. Furthermore the activation energy is the same in both chloride and sulfate solutions which, again, indicates that the temperature dependence of rate is associated with a process common to both types of solution.

It is evident in Fig. 8 that at pH 6 and constant oxygen concentration the data do not conform to a simple exponential function of temperature. Assuming that the temperature dependence, as such, is exponential, the increased rate must be attributed to some extraneous factor, probably associated with the form of the corrosion products.

The presence of such an extraneous factor is indicated by the catastrophic rates observed in the open systems, particularly in the presence of chloride. After correcting for oxygen concentration, the observed rapid increase in rate in the temperature range of 62°-71°C is much greater than can be ac-

counted for in terms of the exponential temperature dependence alone.

### Conclusions

1. The corrosion rate of Cu at room temperature is constant in time in chloride and sulfate solutions, in the range of pH 2-6, and the rate does not appear to be limited by the growth of corrosion product films.

2. In air-saturated solutions of constant anion concentration, corrosion rate is a linear function of hydrogen ion concentration except in chloride solutions at a pH less than 3, where the increasing rate is limited by the diffusion of oxygen.

3. Corrosion rate is a complex function of chloride and sulfate concentration which varies with pH in solutions of constant anion concentration.

4. In an open system, at equilibrium with air, the corrosion rate rises to a maximum between 71°-77°C. When oxygen concentration is constant at all temperatures, the rate in both chloride and sulfate solutions at pH 2 may be expressed as:

$$\text{Rate} = A e^{-9000/RT} \text{ (mg cm}^{-2} \text{ hr}^{-1}\text{)}$$

### Acknowledgments

The authors wish to thank D. K. Crampton and H. L. Burghoff for their interest and suggestions concerning this investigation and to acknowledge the assistance of S. Banisky and other members of the Research and Development Dept. of the Chase Brass and Copper Co.

Manuscript received Sept. 10, 1956. This paper was prepared for delivery before the Cleveland Meeting, Sept. 30-Oct. 4, 1956.

Any discussion of this paper will appear in a Discussion Section to be published in the June 1959 JOURNAL.

### REFERENCES

1. C. Y. Lu and W. F. Graydon, *Can. J. Chem.*, **32**, 153 (1954).
2. J. Halpern, *This Journal*, **100**, 421 (1953).
3. R. J. Agnew, J. K. Truitt, and W. D. Robertson, *Ind. Eng. Chem.*, **50**, 649 (1958).
4. A.S.T.M. Standards, 1946, Part 1-B, Nonferrous Metals, p. 800, Appendix I.
5. F. N. Speller, "Corrosion Causes and Prevention," 3rd Ed., p. 167, Fig. 39, McGraw-Hill Book Co., Inc., New York (1951).
6. "Handbook of Chemistry and Physics," 37th Ed., 1955-1956, p. 1606, Chemical Rubber Publishing Co., Cleveland, Ohio (1955).
7. J. R. Weeks and G. R. Hill, *This Journal*, **103**, 203 (1956).
8. G. R. Hill, *ibid.*, **100**, 345 (1953).
9. F. P. Bowden and J. N. Agar, *Ann. Rept. Chem. Soc.*, **34**, 107 (1937).

# Some Observations on the Effect of the Interaction of Tantalum with Oxygen, Nitrogen, and Hydrogen

R. Bakish<sup>1</sup>

*Sprague Electric Company, North Adams, Massachusetts*

## ABSTRACT

Experiments and results on the interaction of tantalum with O<sub>2</sub>, N<sub>2</sub>, and H<sub>2</sub> are presented. The {100} is shown to be the habit plane of the segregation of the reaction products which appear to be Ta<sub>2</sub>O<sub>5</sub>, TaN, and βTaH, respectively.

The role of the gas-metal interaction on the fracture behavior of single crystals has been evaluated. The observed {100} and {110} cleavage-type fractures as induced by this interaction are discussed and a hypothesis to explain occurrence advanced. Markings observed on cleavage faces are described.

The interaction of tantalum with oxygen, nitrogen, and hydrogen has been studied in some detail by a number of investigators (1-4). Several aspects of this interaction have been completely neglected, however, and an attempt to cover some of these gaps is made with this communication.

High-purity Ta in sheet and wire form from Fansteel Metallurgical Corporation (0.03 C max, 0.03 Fe max, 99.9+ Ta) was used in this investigation. Observations were made both on fine grain material and on sheet single crystals of about 0.01 in. thickness grown by strain annealing.

## Experimental Procedures and Results

Standard x-ray powder techniques were used in conjunction with the ASTM card index for the identification of compounds formed. The same technique applied to wires from which the surface reaction product was removed was also used for the identification of product of internal gas-metal reaction, i.e., the crystallographic precipitate of the oxide, nitride, or hydride, as the case might be.

All orientations were determined from Laue back-reflection photographs and stereographic analysis in accordance with standard procedures (5). Determination of the orientation of the habit plane of the internal precipitation of the gas-metal compounds were carried out as follows: two surfaces with known angular relations were ground on crystals of known orientation, and the angles made by the planes of the precipitates with the common edge were measured. This information was then plotted stereographically and analyzed using a standard projection, in accordance with standard procedures (6).

Standard metallographic techniques were applied in this study, and a solution of H<sub>2</sub>SO<sub>4</sub> (95%), HNO<sub>3</sub> (70%), and HF (48%) in ratio (5:2:2) was used as the etchant.

### *Effect of Oxygen*

Oxygen was introduced into the specimen by oxidation in air at 750°C for 1 hr and, depending on the

thickness of the material studied, complete conversion of the metal to oxide or partial conversion of the surface with internal precipitation was produced. Oxidation in pure oxygen leads in essence to the same end results even though at apparently higher rates. This fact and the inability to detect x-ray evidence of presence of TaN in specimens oxidized in air tends to indicate lack of reaction between the Ta and the N<sub>2</sub> of the air.

Possibility of dissolution of small amounts of N<sub>2</sub> is not precluded but, if present, it does not seem to affect the crystallographic factors studied. X-ray data indicate that the oxide formed is Ta<sub>2</sub>O<sub>5</sub>. It precipitates on the {100} planes of the bcc lattice, as has been discussed in detail elsewhere (7).

Single crystals oxidized in air or in O<sub>2</sub> for periods between 20 min to 1 hr are extremely brittle; in several cases, dropping a crystal to a cement floor from a distance of about 3 ft was sufficient to produce excessive cracking and disintegration along certain planes. Measurements of these elements of cleavage-type fracture revealed that oxygen-embrittled Ta single crystals cleave on the {110} and {100} planes within the error of measurement of 2°.

When noncrystallographic brittle fracture was produced in crystals by bending normal to random direction, one could always detect facets parallel to the {110} and the {100} cleavage planes on the fracture surface.

Examination of cleavage surfaces revealed the presence of markings. These are quite varied at different areas of cleaved {110} and {100} planes in a crystal and also in {110} and {100} planes in different crystals. No specific pattern associated with either of these two cleavage faces was established, yet certain patterns seemed to be characteristic and constantly appeared alone or in combinations in the large number of {100} and {110} cleavage planes examined. The most common ones are seen in Fig. 1-3.

### *Effect of Hydrogen*

Hydrogen was introduced into the Ta both by annealing in H<sub>2</sub> at 700°C for periods up to 24 hr, de-

<sup>1</sup> Present address: Rare Metals Division, CIBA Limited, Basle, Switzerland.

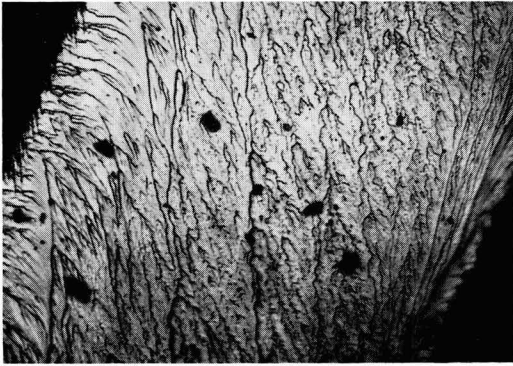


Fig. 1. Typical cleavage markings. Magnification 500X before reduction for publication.

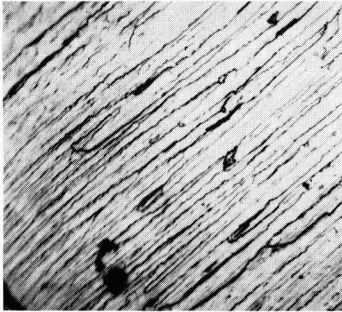


Fig. 2. Typical cleavage markings. Magnification 500X

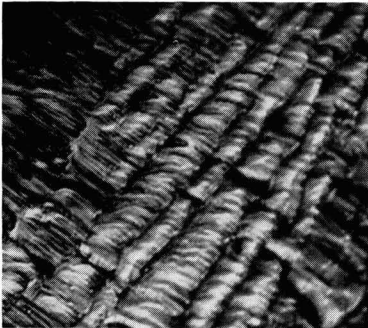


Fig. 3. Typical cleavage markings. Magnification 2000X

pending on the extent of hydrogenation needed, and also by cathodic charging at room temperature at a current density of 0.5 amp/in.<sup>2</sup> in a solution consisting of 90% HNO<sub>3</sub> (70%) and 10% HF (48%). The cathodic charging was used for the study of the effect of H<sub>2</sub> on fracture properties and for comparison with the behavior of material in which H<sub>2</sub> was introduced at high temperature.

The product of the hydrogen-tantalum reaction also precipitates on the {100} planes. The compound believed to be segregating on the {100} plane is the  $\beta$ -tantalum hydride (8). This precipitation of the hydride produces distortion in the Ta which manifests itself in warping of the specimen. A polycrystalline specimen showing the crystallography dependent  $\beta$ -TaH precipitation can be seen in Fig. 4.

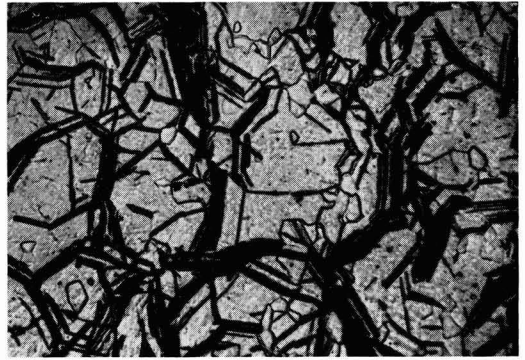


Fig. 4.  $\beta$ -TaH precipitate in fine-grained Ta sheet. Treatment, 24 hr, 700°C in H<sub>2</sub>. Magnification 500X before reduction for publication.

Hydrogen introduced into Ta as indicated leads to cleavage-type fracture on bending. Here the {100} and the {110} type of cleavage are both observed, with the {100} type seemingly predominant.

Hydrogen introduced into Ta by cathodic charging under conditions stated above also produces room temperature embrittlement and cleavage fracture on bending. The predominant cleavage here seems to be of the {110} type; rarely was the {100} cleavage detected. Examination of cleavage faces revealed essentially the same features already referred to when discussing oxygen-induced cleavages.

#### Effect of Nitrogen

Nitrogen was introduced in the specimen by annealing in nitrogen atmosphere at 750°C. Nitrogen-tantalum reaction seems to proceed at relatively slow rates at this temperature. Five-hour nitriding was the minimum time needed for sufficient precipitation for habit-plane determination in the single crystals used, but 24-hr treatment was actually used.

The formation of the nitride in the metal must be connected with a substantial volume change, as the nitrided specimens invariably show a substantial amount of distortion and warping. Figure 5 shows the appearance of the surface of a single-crystal specimen which was nitrided for 24 hr at 750°C.



Fig. 5. Surface nitride (dark material) and distortion resulting from nitride precipitation on the (100) planes on a single crystal of Ta after 24 hr at 750°C in N<sub>2</sub> atmosphere. Magnification 500X before reduction for publication.

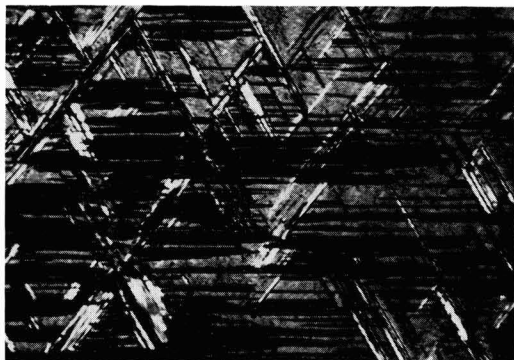


Fig. 6. Nitride platelets on a polished surface viewed under polarized light. Specimen treated as in Fig. 5. Magnification 500X before reduction for publication.

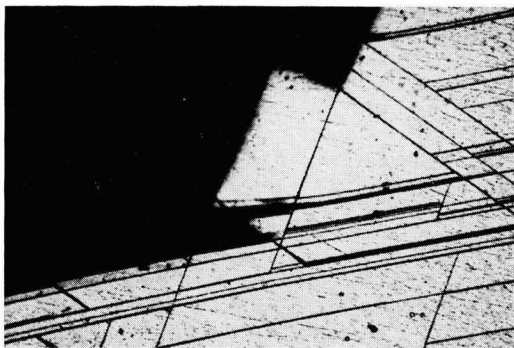


Fig. 7. Fracture associated with the nitride-metal interface

Observe the relief on the surface on the sites of nitride precipitation. No uniform nitride cover seems to be formed; however, bulk nitride formed at different locations is clearly visible. On metallographic polishing of the specimen normal to exposed surface and examination with polarized light, one can see that nitride platelets which form are anisotropic (Fig. 6). The habit plane of precipitation is  $\{100\}$ . The structure of the nitride is not known, and no study of structure was performed; in comparison with other data on tantalum nitride in the literature (9), however, it is quite likely that the compound formed both on the surface and internally on the  $\{100\}$  plane is of the composition TaN.

Cleavage fracture on nitrogen-embrittled Ta in the terms of the treatments described previously was always found associated with a visible precipitate. It apparently does not take place prior to segregation of the nitride phase, and it occurs along the metal-nitride interface on the  $\{100\}$  plane. Figure 7 shows the type of fracture that occurs associated with this nitride-tantalum interface, and the Laue back reflection shows a typical  $\{100\}$  pattern that one obtains from these cleavage faces associated with the metal-nitride interfaces. No  $\{110\}$  cleavage was observed in nitrogen-embrittled Ta.

#### Discussion of Results

The gas-metal compounds resulting from the interaction of Ta with  $O_2$ ,  $N_2$ , and  $H_2$  all precipitate on

the  $\{100\}$  planes of the bcc lattice. The location of the precipitate coincides with the most widely spaced atoms of this lattice. There is identity in the crystallographic factors involved in this interaction, but substantial differences exist in the kinetics of reaction of each of these three gases with the Ta.

The occurrence of cleavage-type fracture in pure Ta induced by impact at low temperature has already been discussed (10). The results of this study indicate the strong effect that  $O_2$ ,  $N_2$ , and  $H_2$  have in modifying this fracture behavior. The evidence presented tends to support the contention here advanced that the  $\{100\}$  type cleavage induced both by  $H_2$  and  $O_2$  must be connected with the early stages of precipitation on this plane and a direct consequence thereof. In the case of  $N_2$ , it takes place at a considerably later stage of precipitation and is associated with the nitride-metal interface. The  $\{100\}$  cleavage is the minor cleavage in high-purity Ta (10). The  $\{110\}$  cleavage is the major cleavage observed in Ta at low temperature (10); the  $\{110\}$  is also the predominant slip plane in this metal (11). The observance of this type of cleavage at room temperature under the conditions described must be a direct consequence of the presence of  $O_2$  and  $N_2$  in solid solution. These gases in solid solution then reduce the ductility of the Ta crystals and make it possible to produce behavior which in pure Ta takes place at  $-196^\circ\text{C}$  at room temperature. No  $\{110\}$  cleavage was observed in material that was treated with  $N_2$ .

Markings of identical appearance as those observed and described for oxygen-embrittled Ta were also observed in hydrogen-embrittled Ta. No satisfactory hypothesis explaining their formation is advanced. It is believed, however, that they result from the interaction of the cleavage plane and screw dislocations in the crystals. Their appearance is apparently influenced by the rate and direction of the crack leading to cleavage.

#### Conclusions

It has been shown that the habit plane of the precipitation of oxide, nitride, and hydride in Ta is  $\{100\}$  and these appear to be  $Ta_2O_5$ , TaN, and  $\beta$ -TaH, respectively.

$\{100\}$  and  $\{110\}$  cleavages result from these gas-metal interactions. The  $\{100\}$  type cleavages appear to be related to the precipitation phenomena while the  $\{110\}$  cleavage seems to be due to gases in solid solution.

#### Acknowledgment

The author wishes to acknowledge the assistance of Miss Nancy Harvin who carried out all x-ray powder work and the identification of the reaction products.

Manuscript received Nov. 4, 1957.

Any discussion of this paper will appear in a Discussion Section to be published in the June 1959 JOURNAL.

#### REFERENCES

1. E. A. Gulbransen and K. F. Andrews, *J. (and Trans.) Electrochem. Soc.*, **96**, 364 (1949).
2. E. A. Gulbransen and K. F. Andrews, *This Journal*, **99**, 6 (1952).

3. E. Geberhardt and Preisdanz, *Plansee Proc.*, 254 (1956).
4. G. Brauer and R. Hermann, *Z. anorg. Chem.*, **244**, 11 (1953).
5. A. B. Greninger, *Trans. AIME*, **17**, 61 (1935).
6. C. S. Barrett, *Structure of Metals*, 40 (1952).
7. R. Bakish, *This Journal*, **105**, 71 (1958).
8. G. Hagg, *Z. physik. Chem.*, **11**, 433 (1930).
9. F. H. Horn and W. T. Ziegler, *J. Am. Chem. Soc.*, **69**, 276 (1947).
10. C. S. Barrett and R. Bakish, *Trans. AIME*, **208**, 122 (1958).
11. R. Bakish, *Acta Met.*, **6**, 120 (1958).

## Room Temperature Tarnishing of Silver in Bromine and Iodine

Joseph L. Weininger

*Research Laboratory, General Electric Company, Schenectady, New York*

### ABSTRACT

Pure silver was tarnished in an atmosphere of iodine and bromine vapor at room temperature. This resulted in impervious halide surface layers, from which tarnishing rates could be deduced by means of a photomicrographic technique. It was found that the parabolic rate law, with diffusion being the rate-determining step, also holds at room temperature. The presence of water vapor reduces the rate of halogenation by a factor of two.

The tarnishing of silver by halogen vapors has attracted much attention. The reason for this interest is the relatively low temperature at which these oxidation reactions proceed and the fact that the halide produced is predominantly an ionic conductor. Hence many interesting conclusions can be drawn from tarnishing experiments (1). Wagner and his school were particularly active in connecting, by theory and experiment, the kinetics of an oxidation reaction with the ionic conductivities of the reaction products, e.g., silver halides in tarnishing reactions.

The present work arose as a problem in solid-electrolyte battery research. In the electric cell Ta(Br<sub>2</sub>)/AgBr/Ag, halogen vapor reacts at the Ta cathode in the presence of a silver anode. The chemical stability of the silver anode is of great importance. One must distinguish between the thermal attack of the halogen on the silver surface, i.e., the tarnishing reaction, and the electrochemical cell reaction, the formation of silver halides. Both processes have the same over-all chemical reaction,



but, whereas the cell reaction is essential for the operation of the cell, the tarnishing reaction is undesirable because it consumes active cell material.

The tarnishing reaction proceeds fairly rapidly at temperatures above 200°C, and experiments performed at high temperatures are described in the literature (2-4). Only few measurements have been reported at lower temperatures and, therefore, tarnishing at room temperature was studied by the following method.

### Experimental Procedure

Jaenicke and co-workers studied the anodic formation of AgCl layers and recrystallization phenomena in aqueous solutions by means of a microscopic technique (5). In the present work, during routine photomicrographic examinations of sections

of tarnished silver foils it was found that very clear reproductions could be obtained at magnification of 500. This formed the basis of an experimental technique in which the course of the tarnishing reaction would simply be followed by the observation of the microscopic increase of the tarnished layer with time.

Silver coupons of "fine" grade, supplied by Handy and Harman Company, were examined.<sup>1</sup> After degreasing and cleaning the coupons were exposed to

<sup>1</sup>The manufacturer's analysis of fine silver is: Ag 99.9+%, Cu 0.05%, Pb 0.004%, traces of Fe and other metals.

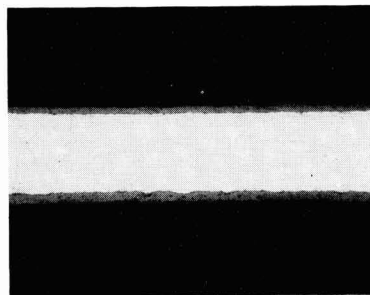


Fig. 1. A 2-mil silver foil after exposure to Br<sub>2</sub> for 7900 sec.  $\Delta x_{\text{Ag}} = 1.0 \mu$ ;  $\Delta x_{\text{AgBr}} = 5.7 \mu$ .

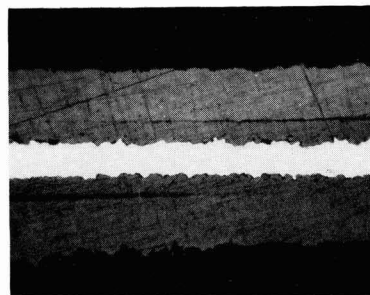


Fig. 2. A 2-mil silver foil after exposure to Br<sub>2</sub> for 1.815  $\times 10^6$  sec.  $\Delta x_{\text{Ag}} = 14.8 \mu$ ;  $\Delta x_{\text{AgBr}} = 43.3 \mu$ .

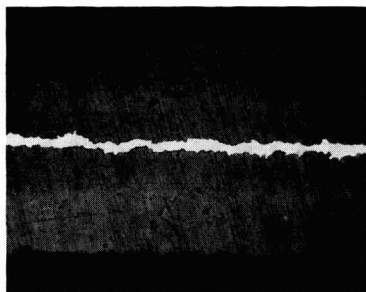


Fig. 3. A 2-mil silver foil after exposure to  $\text{Br}_2$  for  $5.273 \times 10^6$  sec.  $\Delta x_{\text{Ag}} = 22.2 \mu$ ;  $\Delta x_{\text{AgBr}} = 64.0 \mu$ .

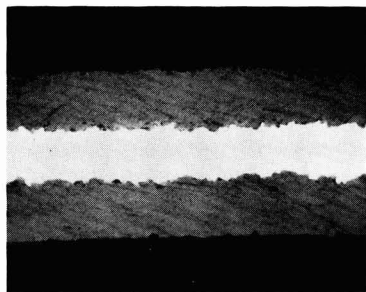


Fig. 4. A 2-mil silver foil after exposure to  $\text{I}_2$  for  $1.492 \times 10^6$  sec.  $\Delta x_{\text{Ag}} = 9.3 \mu$ ;  $\Delta x_{\text{AgI}} = 36.7 \mu$ .

bromine or iodine vapor at room temperature. The coupons were stored in the presence of ordinary illumination in vacuum desiccators which contained an excess of the halogen and drying agent. The desiccators were evacuated so that only the saturated halogen vapor was present. Another series of experiments was performed at 90.14% relative humidity by replacing the desiccant with a saturated aqueous solution of barium chloride. After removal from the halogen atmosphere the samples were mounted in "Selectron," a polyester (prepared from 30% styrene monomer and 70% alkyd resin) which hardens at room temperature. Samples were polished and etched. Only a very slight dichromate etch was permissible. The vertical positioning of the foils in the mount required great care in order to get photomicrographs with truly representative cross-section. Photographs were taken with a flat field objective, at a magnification of 500. For calibration, a microscale and a silver blank were added to each set of photos.

### Experimental Results

Figure 1 through 4 shows the feasibility of the method. The first three are photomicrographs of silver foils with bromide layers. These foils had been exposed to bromine in the absence of water vapor, at room temperature, for increasing periods, approximately 2 hours, 3 weeks, and 2 months, respectively. Figure 4 is an example of a cross section through a silver-silver iodide foil. Exact times of exposure in seconds and changes in the width of silver foil,  $\Delta x_{\text{Ag}}$ , or width of tarnished layers,  $\Delta x_{\text{AgBr}}$  and  $\Delta x_{\text{AgI}}$  in microns are given in the legend of the figures. It may be noted that in Fig. 2 pancake voids were formed at the original location of the silver-

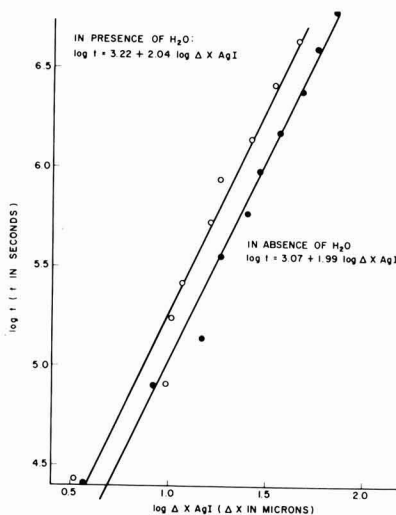


Fig. 5. Tarnishing of silver at room temperature—formation of AgI.

bromine interface (see later). Usually, large voids did not occur. Thus, in Fig. 3 the silver foil was almost completely used up in the formation of silver bromide, but only random pores existed in the halide layer.

When the course of the tarnishing reaction is plotted as the loss of silver thickness ( $\Delta x_{\text{Ag}}$ ) and gain in thickness of the halide ( $\Delta x_{\text{AgX}}$ ) vs. time, the graphs appeared to be parabolic. In Fig. 5 the growth of silver iodide in the presence and absence of water vapor is compared. A slope of 2 for these graphs, from a least square fit, verifies the existence of a parabolic rate law,

$$\frac{d(\Delta x)}{dt} = \frac{k'}{\Delta x}$$

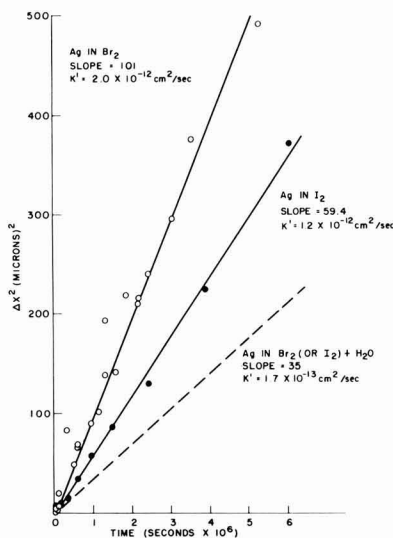


Fig. 6. Rate constants of tarnishing reaction

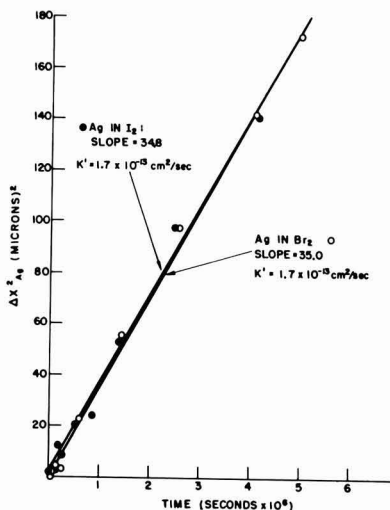


Fig. 7. Rate constants of tarnishing reaction

where  $\Delta x$  is the thickness of the tarnished layer produced in time  $t$  and  $k'$  is the tarnishing or Tam-mann rate constant. If at time  $t = 0$  there is no tarnished layer, then integration of the equation gives  $(\Delta x)^2 = 2k't$ , and  $k'$  can be evaluated from least square fits of plots as in Fig. 6. Here the constants refer to the consumption of silver in bromine and iodine, respectively. The broken line indicates the curves obtained in the presence of water vapor. This is shown in detail in Fig. 7. In water vapor the loss of silver proceeds at about the same rate in either halogen. It should be kept in mind, however, that the room temperature vapor pressures for bromine and iodine are very different and that the rate varies as the square root of the halogen pressures. These are 207 mm for bromine and 0.306 mm for iodine at 25°C. The rational rate constant,  $k$ , is more useful for comparison of different chemical systems because it expresses rates in terms of equivalents, thus:

$$\tilde{n} = w/\tilde{w} = (q \cdot \Delta x \cdot \rho / \tilde{v} \cdot \rho) = q \cdot \Delta x / \tilde{v}$$

where  $\tilde{n}$ ,  $\tilde{w}$ , and  $\tilde{v}$  are the equivalent number, weight, and volume, respectively,  $q$  surface area,  $\rho$  density,  $w$  weight, and  $\Delta x$  thickness of the reaction

product. Hence, introduction of equivalents into the above rate law containing the constant  $k'$  gives:

$$\frac{d\tilde{n}}{dt} = \frac{q}{\tilde{v}} \frac{d(\Delta x)}{dt} = \frac{q}{\tilde{v}} \cdot \frac{k'}{\Delta x} = k \frac{q}{\Delta x}$$

where

$$k = \frac{k'}{\tilde{v}}$$

and  $k$  has the units of equivalents per centimeter per second.

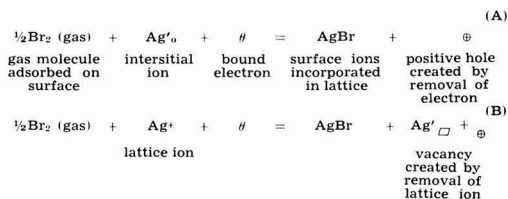
The experimental results are tabulated as rate equations in Table I and rate constants in Table II.

### Discussion

From the eight rate expressions obtained in this investigation one can draw conclusions regarding the mechanism of the reaction, evaluate the rate constants of the tarnishing reaction at room temperature, and gain some insight into the structural features of the halide. As to the precision of the measurements, the probable error in the thickness of the different layers is  $\pm 0.5\mu$  which is considerably smaller than the scatter of the data. The latter must be attributed to random errors in the alignment of the foils in the mount at the time of taking the photomicrograph.

#### Mechanism of the Tarnishing Reaction— Comparison with Higher Temperatures

Consider briefly the case of silver tarnished in a bromine atmosphere. After the initial layer of silver bromide has been formed, its continued growth requires the transport of silver ions to the surface. Interstitial ions are mobile, but originate from lattice positions, therefore the following reactions are equivalent:



Note that Eq. (A) seems to have unbalanced charges. It deals with the removal of a net positive

Table I. Rate equations of tarnishing reaction at room temperature— $\Delta x$  in microns,  $t$  in seconds  $\times 10^6$ 

	H <sub>2</sub> O absent	H <sub>2</sub> O vapor present (90% humidity)
(a) Parabolic relations:		
Bromination	$(\Delta x)^2 = 788 t + 103$	$(\Delta x)^2 = 340 t - 42$
loss of Ag	$(\Delta x)^2 = 101 t + 7.8$	$(\Delta x)^2 = 35.0 t - 0.04$
Iodination	$(\Delta x)^2 = 878 t + 30$	$(\Delta x)^2 = 442 t + 35$
loss of Ag	$(\Delta x)^2 = 59.4 t + 2.7$	$(\Delta x)^2 = 34.8 t + 1.3$
(b) Logarithmic relations:		
Bromination	$\log t = 2.77 + 2.14 \log \Delta x_{\text{AgBr}}$	$\log t = 3.90 + 1.73 \log \Delta x_{\text{AgBr}}$
loss of Ag	$\log t = 3.88 + 2.13 \log \Delta x_{\text{Ag}}$	$\log t = 4.63 + 1.80 \log \Delta x_{\text{Ag}}$
Iodination	$\log t = 3.07 + 1.99 \log \Delta x_{\text{AgI}}$	$\log t = 3.22 + 2.04 \log \Delta x_{\text{AgI}}$
loss of Ag	$\log t = 4.14 + 2.09 \log \Delta x_{\text{Ag}}$	$\log t = 4.41 + 2.02 \log \Delta x_{\text{Ag}}$

Table II. "Rational" tarnishing rate constants (in equiv.  $-\text{cm}^{-1}\text{-sec}^{-1}$ )  
 Temp =  $25 \pm 5^\circ\text{C}$ ,  $P_{\text{Br}_2} = 207 \pm 37$  mm,  $P_{\text{I}_2} = 0.306 \pm 0.016$  mm

	Ag in $\text{Br}_2$	AgBr formation	Ag in $\text{I}_2$	AgI formation
$k_{\text{dry}}$ ( $\text{H}_2\text{O}$ absent)	$4.9 \times 10^{-14}$	$1.3 \times 10^{-13}$	$2.8 \times 10^{-14}$	$1.1 \times 10^{-13}$
$k_{\text{wet}}$ (in presence of $\text{H}_2\text{O}$ vapor, $P_{\text{H}_2\text{O}} = 21.4 \pm 5.5$ mm)	$1.7 \times 10^{-11}$	$5.9 \times 10^{-14}$	$1.7 \times 10^{-14}$	$5.3 \times 10^{-14}$
$k_{\text{dry}}/k_{\text{wet}}$	2.9	2.2	1.6	2.1
Literature:				
Tammann and Koester (6)				
( $P_{\text{Br}_2} = 61$ mm, $T = 20^\circ$ , $\text{H}_2\text{O}$ present)	$10^{-14}$			
Hauffe and Gensch (3)				
( $P_{\text{Br}_2} = 170$ mm)	$1.8 \times 10^{-13}$	(extrapolated from high temp. data)		
Lehovec (7)				
( $p_{\text{I}_2} = 4.3$ mm, $T = 60^\circ$ )				$6.0 \times 10^{-13}$
Wagner (theory) (2)	$10^{-10}$			

charge from the interior (interstitial Ag ion) to the surface. The ion is replaced by a positive hole, and the existence of a corresponding negative charge before and after the removal of the ion is assumed. These ions are very mobile compared to lattice ions, but holes must likewise diffuse to the surface in order that the reaction may proceed. This is the rate-determining step in the mechanism which was postulated and verified experimentally by Wagner at elevated temperatures (2). The slope of the plots of log time vs. log thickness in the present work indicates that the parabolic rate law is also valid at room temperature. It may also be assumed that the mobility of the holes is still rate-determining provided a polycrystalline but impervious layer of halide is formed. Otherwise the mechanism will depend on the gross structure of the deposit. A complication is introduced by the presence of water vapor which reduces the rates of tarnishing by a factor of two. It is known that water vapor adsorbs readily on silver halides, but its role in the tarnishing process is not yet well understood.

#### Rate Constants at Room Temperature

Table II shows a comparison of the rate constants obtained in a dry halogen atmosphere with values given in the literature. Regarding the present measurements the constants obtained from the formation of the halide or loss of silver should be the same for each of the two chemical systems. Actually there is a discrepancy of a factor of three, with the smaller rate constant being obtained from decreases of thickness of silver. Examination of the halide layers, in both cases, showed about 20% porosity of the halide, which would give a corresponding error in the rate constant. This would not account for the total discrepancy, of course, which in view of the simple experimental procedure is not surprising. In fact, comparison of the two values for each system gives a room temperature rate constant that should be more accurate than one order of magnitude. This is confirmed also by comparison with available literature values. The work of Tammann and Koester (6) was performed in an atmosphere saturated with water vapor, which may be responsible for a slightly lower value of the rate constant. In comparison to our data, their constant would also be increased by a factor of two owing to the smaller

pressure of bromine in Tammann's experiment. Hauffe and Gensch (3) performed their experiments in a temperature range  $200^\circ\text{-}400^\circ\text{C}$  with a quartz balance. The agreement of their extrapolated value with our rate constant is remarkable. This is also the case with the iodide determination of Lehovec who used a quartz balance too (7). Calculations of the rate constant based on Wagner's theory of tarnishing (2) depends on the knowledge of the conductivity of the tarnished layer and the transference numbers in it of both species of ions, as well as the transference number of electrons. Following Jost and Weiss (8) the sum of the ionic transference numbers,  $t_1 + t_2 = 0.999$  was assumed and the electronic transference number  $t_3 = 0.001$ . For the conductivity of silver bromide  $2.3 \times 10^{-8}$  ohm $^{-1}$  cm $^{-1}$  was chosen. The latter two values may be considerably in error, and it is therefore not surprising that the calculated rate constant is off by two or three orders of magnitude.

#### Structure of the Halide

Different views exist regarding the structure of an oxide or halide layer on a metal. The Pilling-Bedworth rule states (9) that if the volume of the oxide formed is larger than the volume of the metal, then the surface is free to expand outward, due to an increase in volume, to an extent limited only by its ability to stretch successfully. The mechanical forces on the oxide layer may eventually become great enough to cause a deviation from the parabolic rate law, or even to disrupt the uniform oxide layer. However, Vermilyea (10) has recently postulated a low-temperature mechanism of oxidation in which stresses are absent because reaction takes place only at imperfections of the oxide or halide lattice.

It may be concluded that the room temperature halogenation of silver proceeds between the two above extremes. The halide structure which is formed at room temperature, hence at a lower rate, is at least as uniform as one formed at higher temperatures. This is shown visually, by observation of photomicrographs. However, the halide structure is not perfect and pores are formed. They are located at random in the halide. As mentioned above, an estimate of the porosity based on the photomicrographs is about 20%. In a few cases agglomeration

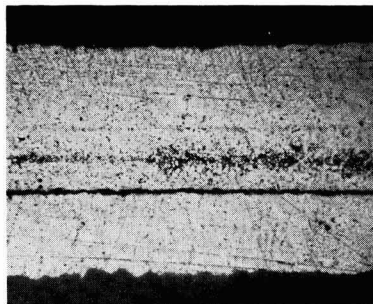


Fig. 8. A 2-mil silver foil after exposure to  $\text{Br}_2$  for  $3.040 \times 10^4$  sec. Silver is completely brominated.

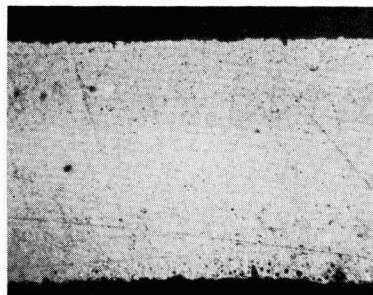


Fig. 9. A 2-mil silver foil after exposure to  $\text{Br}_2$  for  $8.736 \times 10^4$  sec. Silver is completely brominated.

of pores into continuous voids could be observed. There are indications of such pancake pores at the original metal-vapor interface. This is most drastically seen in Fig. 8, in which a silver foil is pictured which had been completely brominated in less time than would have been required by the parabolic rate law. This is however the exception to the usual complete halogenation of a foil as pictured in Fig. 9 where again only random pores exist. It cannot be explained why the occasional silver halide shows continuous pore formation where other identically treated foils do not show this. Birchenall recently pointed out (11) that the formation of porous scales is connected with the plastic properties of oxides and therefore it is possible that some unknown factor may have entered to hinder the plastic flow of the halide in the case where large pores appear. The fact that this may occur in a few samples where a large number of others under identical conditions

do not show it, only serves to point up the complexity of the study and the work that remains to be done.

### Conclusions

1. Tarnishing reactions of silver by iodine and bromine resulted in an impervious halide surface layer which contains up to 20% pores, located at random.
2. The reactions proceed according to parabolic rate law. Rate constants are given for tarnishing, in the absence of water vapor and when it was present to the extent of 90% relative humidity, at room temperature.
3. It is postulated that diffusion of defect-electrons in a direction opposite to that of silver ions, which is the rate-determining step at higher temperature, is also limiting at room temperature.
4. Presence of water vapor reduces the tarnishing rate by about a factor of two.

### Acknowledgment

The author is indebted to Dr. D. L. Douglas of the General Electric Research Laboratory for many helpful discussions. The careful metallographic work, which is the basis of this study, was performed by the Metallography group of the Research Laboratory, General Electric Company.

Manuscript received Nov. 18, 1957. This paper was prepared for delivery before the Buffalo Meeting, Oct. 6-10, 1957.

Any discussion of this paper will appear in a Discussion Section to be published in the June 1959 JOURNAL.

### REFERENCES

1. K. Hauffe, "Reaktionen in und an festen Stoffen," Springer-Verlag, Berlin (1955).
2. C. Wagner, *Z. physik. Chem.*, **B32**, 447 (1936).
3. K. Hauffe and C. Gensch, *ibid.*, **195**, 116 (1950).
4. I. Pfeiffer, K. Hauffe, and W. Jaenicke, *Z. Elektrochem.*, **56**, 728 (1952).
5. W. Jaenicke, R. P. Tischer, and H. Gerischer, *ibid.*, **59**, 448 (1955).
6. G. Tammann and W. Koester, *Z. anorg. u. allgem. Chem.*, **123**, 196 (1933).
7. K. Lehovc, *et al.*, 3rd quarterly report, February 1955, U. S. A. Signal Corps Contract No. DA-36-039-SC-63151.
8. W. Jost and K. Weiss, *Z. physik. Chem. (Frankfurt)*, **2**, 112 (1954).
9. N. B. Pilling and R. E. Bedworth, *J. Inst. Metals*, **29**, 529 (1923).
10. D. Vermilyea, *Acta Met.*, **5**, 492 (1957).
11. C. E. Birchenall, *This Journal*, **103**, 619 (1956).

# Selective Oxidation of Al from an Al-Fe Alloy

Richard E. Grace

Department of Metallurgical Engineering, Purdue University, Lafayette, Indiana

and

Alan U. Seybolt

Research Laboratory, General Electric Company, Schenectady, New York

## ABSTRACT

The selective oxidation of aluminum from a 4.8 wt % Al-Fe alloy was studied with a microbalance at temperatures of 700°-900°C. The oxidizing gas was damp H<sub>2</sub>, with dewpoints ranging from -55° to 0°C. The oxidation product was identified by electron diffraction to be the crystalline spinel,  $\gamma$ -Al<sub>2</sub>O<sub>3</sub>. At 800°C the parabolic oxidation constant was approximately proportional to the 1/7th power of the H<sub>2</sub>O/H<sub>2</sub> gas ratio, and the experimental activation energy for the over-all oxidation reaction with 0°C dewpoint hydrogen gas was 72 kcal/mole.

Oxidation of alloys in damp hydrogen at elevated temperatures has been carried out recently by several investigators, Moreau and Bénard (1) and Seybolt and Alessandrini (2) on Ni-Cr alloys and Fe-Si alloys, respectively. Use of various H<sub>2</sub>O/H<sub>2</sub> gas ratios determined by the vapor pressure of ice at subzero temperatures permits a broad coverage of oxidizing potential at very low effective oxygen pressures. When a binary solid solution is exposed to oxygen pressures which are too low to oxidize the solvent (more noble component), but which are high enough to oxidize the solute, the process is called selective oxidation. In Al-Fe solid solutions there is a wide range of oxygen pressures which permits the selective oxidation of Al without apparently affecting the Fe.

The present study was initiated in order to study the kinetics of the over-all reaction given below:



Gulbransen and Wysong (3) have studied the oxidation of Al in oxygen at various temperatures and oxygen pressures with a quartz microbalance, and the weight gain data reported herein were taken with a similar microbalance of  $\pm 1 \mu\text{g}$  sensitivity. A determination of the structure of the surface oxide films was made by reflection electron diffraction techniques on samples that were cooled to room temperature in the H<sub>2</sub>O/H<sub>2</sub> gas in which they were oxidized.

## Experimental

Samples of a 4.8 wt % Al-Fe alloy which had been vacuum melted from electrolytic materials of 99.99+ % purity and rolled to 0.014-in. sheet were cut with 5 cm<sup>2</sup> surface area. The small rectangular specimens were polished through 00 paper by hand and then washed with an 80% acetone -20% toluene degreasing solution. The samples were desiccated for 2-5 days before use. No chemical etching or polishing was attempted because it was felt that selective etching might take place or a foreign sur-

face film might be produced. The specimens were hung on an 0.002-in. nichrome wire from one arm of a quartz microbalance in the apparatus shown schematically in Fig. 1. The system was usually flushed out overnight at room temperature with dry hydrogen (-196°C dewpoint) before the run was started. During a run the damp gas was preheated to temperature in a quartz spiral around the specimen before it was introduced into the furnace. Weight gains were followed by measuring the shift in the quartz beam away from a fixed quartz pointer with a telemicroscope. A change of 0.001 cm shift was equivalent to 1  $\mu\text{g}$ , and an individual reading could be made to  $\pm 0.2 \mu\text{g}$ . The definition of the starting time for a run was arbitrarily chosen to be about 15 min after the wet hydrogen was admitted to the furnace. During this brief interval the microbalance beam oscillated, making readings erratic. While it is impossible to determine exactly the oxygen uptake of the samples during heating in the first 15 min of any run, an estimate of 2-3  $\mu\text{g}$  oxygen/cm<sup>2</sup> has been made. Microbalance readings were made regularly over several hours and typical

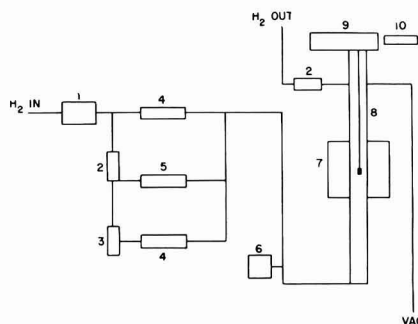


Fig. 1. Schematic representation of oxidation apparatus. 1, copper catalyst; 2, flowmeter; 3, water saturator; 4, cold trap; 5, gas mixer; 6, McLeod gauge; 7, furnace; 8, quartz tube; 9, microbalance; 10, telemicroscope.

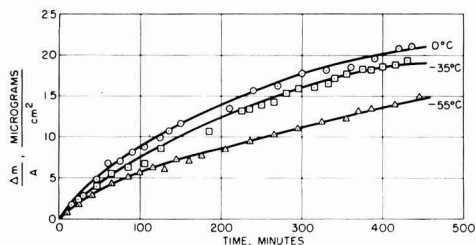


Fig. 2. Weight gain-time relations at several dewpoints for oxidation of 4.8% Al-Fe in hydrogen at 800°C.

weight gain vs. time curves are shown in Fig. 2. Two series of experiments were carried out with this technique; the first consisted of a series of runs at 800°C in which the  $H_2O/H_2$  ratio was varied by changing the hydrogen dewpoint from  $-55^\circ$  to  $0^\circ$  in several steps. The second series was carried out at constant hydrogen dewpoint ( $0^\circ$ ) at oxidizing temperatures of  $700^\circ$ ,  $800^\circ$ , and  $900^\circ$  C.

When the runs were finished, the furnace was lowered from the sample, and it was allowed to cool to  $100^\circ$  C before the quartz chamber was evacuated. Generally, the samples exhibited a pastel interference color when they were removed from the furnace. This color was very uniform over the entire sample surface, indicating a smooth surface film. The films were of the order of  $2000\text{\AA}$  thick. Electron diffraction patterns were taken by reflection from the oxidized surface. Finally, the samples were measured with a metric micrometer and their areas were computed to the nearest  $0.001\text{ cm}^2$ , with the assumption that the as-polished surface was perfectly plane.

### Results

The results of the weight gain-time studies fit an equation of the type

$$\left(\frac{\Delta M}{A}\right)^2 = k_p (t - t_0) \quad [2]$$

where  $\Delta M/A$  = weight gain per unit area;  $t$  = time;  $t_0$  = time constant; and  $k_p$  = parabolic rate constant.

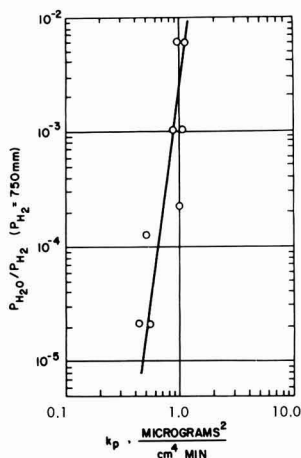


Fig. 3. Variation of parabolic rate constant with  $H_2O/H_2$  ratio at  $800^\circ$  C.

Table I. Electron diffraction data of surface oxide on 4.8% Al-Fe alloy

Typical unknowns*			Standards*	
Sample No. 11 d, Å	No. 14 d, Å	(hkl)	No. 1 d, Å	No. 2 d, Å
2.740		220	2.80	2.79 s
2.381		311	2.39 m	2.38 vs
		222	2.28	
1.946 m	1.987 m	400	1.98 m	1.97 s
			1.82	
			1.62	1.61
1.491		422	1.52 m	1.52 m
1.37 s†	1.410 s†	440	1.40 s	1.395 s
		533	1.24	
1.211		622	1.21	1.19
1.163	1.160 m	444	1.14	1.14
1.105		711		
1.060		642	1.06	
1.015	1.016	553, 731	1.03	1.03
0.971		800	0.991	0.988
	0.906	555, 751	0.916	0.912
0.897		840	0.885	0.886
			0.844	
	0.820	844		0.806
$a_0 = 7.79$	$a_0 = 7.95$		$a_0 = 7.93$	$a_0 = 7.88$

\* No. 11, 4.8% Al-Fe oxidized at  $800^\circ$  C, 20 hr,  $-55^\circ$  C dewpoint. No. 14, 4.8% Al-Fe oxidized at  $800^\circ$  C, 7 hr,  $0^\circ$  C dewpoint. No. 1, ASTM card No. 2-1420;  $\gamma$ - $Al_2O_3$ . No. 2, oxide on pure Al  $> 680^\circ$  C in air [see Ref. (4)]  $\gamma$ - $Al_2O_3$ .

† Heavily textured line.

Two preliminary runs showed that the parabolic behavior continued for at least 20 hr, but most of the runs were made only for 7 hr duration. The effect of various  $H_2O/H_2$  gas ratios on the parabolic rate constant at  $800^\circ$  C is shown in Fig. 3. Increased water content of the gas brings about an increase in the rate of oxidation, but the effect is small. The slope of the line in Fig. 3 shows that the parabolic rate constant is approximately proportional to the  $H_2O/H_2$  gas ratio to the  $+1/7$  power.

Table I compares typical electron diffraction data from samples No. 11 and No. 14 with standard x-ray powder patterns for  $\gamma$ - $Al_2O_3$ . The diffraction patterns for all samples indicated that the oxidation product was substantially the same at  $700^\circ$ ,  $800^\circ$ , and  $900^\circ$  C and at all the dewpoints studied. The patterns for the samples held at  $700^\circ$  and  $800^\circ$  C for 7 hr corresponded to sample No. 14, while the patterns for the samples at  $800^\circ$  C (20 hr) and  $900^\circ$  C resembled that of sample No. 11. Longer times at temperatures and increased temperatures of oxidation increased the number and sharpness of lines appearing in the diffraction patterns.

Table II gives a summary of all the experimental data including sample treatments; parabolic rate constant,  $k_p$ ; time constant,  $t_0$ ; and electron diffraction results. Several preliminary experiments on the determination of the oxide structure have not been included in this table. Those results did not differ from samples 9, 11, 14, and 15. In certain experiments using dewpoints of nominally  $-78^\circ$  and  $-196^\circ$  C, the sample gained more weight than the amount of oxygen available in these dry gases. The water content of the hydrogen could not be reduced to a dewpoint as low as  $-78^\circ$  C in the apparatus used.

Table II. Summary of experimental data

Sample	Treatment All runs at 800°C except where noted	$k_p$ $\frac{\mu\text{g}^2}{\text{cm}^2 \text{ min}}$	$t_o$ min- utes	Remarks (Electron diffraction)
4	As polished 2/0 paper, acetone- toluene rinse	—	—	No oxide present
11	-55° dewpoint H <sub>2</sub> 20 hr; 200 cc/min	—	—	$a_o = 7.79 \text{ \AA}$ Spinel
17	-55° dewpoint H <sub>2</sub> 6 hr; 200 cc/min	0.44	35	—
19	-55° dewpoint H <sub>2</sub> 6 hr; 200 cc/min	0.55	70	—
24	-40°C dewpoint H <sub>2</sub> 6½ hr; 200 cc/min	0.50	60	—
16	-35°C dewpoint H <sub>2</sub> 7 hr; 200 cc/min	1.0	50	—
627	-20°C dewpoint H <sub>2</sub> 8 hr; 200 cc/min	1.04	60	—
23	-20°C dewpoint H <sub>2</sub> 7½ hr; 200 cc/min	0.89	100	—
14	0°C dewpoint H <sub>2</sub> 7 hr; 200 cc/min	1.1	35	$a_o = 7.95 \text{ \AA}$ Spinel
20	0°C dewpoint H <sub>2</sub> 7½ hr; 200 cc/min	0.96	125	—
15	Furnace at 900°C -55°C dewpoint H <sub>2</sub> 5 hr; 125 cc/min	—	—	Spinel $a_o = 7.84 \text{ \AA}$
21	Furnace at 900°C 0°C dewpoint H <sub>2</sub> 4 hr; 200 cc/min	18.4	50	—
9	Furnace at 700°C 0°C dewpoint H <sub>2</sub> 5½ hr; 160 cc/min	—	—	Spinel $a_o = 7.98 \text{ \AA}$
22	Furnace at 700°C 0°C dewpoint H <sub>2</sub> 7½ hr; 200 cc/min	0.033	15	—

The temperature dependence of the parabolic rate constant with 0°C dewpoint hydrogen gas can be given by the equation

$$k_p = 4.0 \times 10^{11} \exp \left[ -\frac{72000}{RT} \right] \frac{\mu\text{g}^2}{\text{cm}^2 \text{ min}} \quad [3]$$

This equation was determined from the plot shown in Fig. 4, which shows the temperature dependence of  $k_p$  on a semilog plot. The error in the experimental activation energy is about  $\pm 2$  kcal/mole. Uhlig (8) has pointed out that activation energies may be higher above the Curie temperature in some alloys in which the rate-controlling oxidation step is a surface reaction at the metal/oxide interface. However, when diffusion through the oxide film is rate controlling, magnetic effects are not important.

### Discussion

The results of this study have several things in common with the oxidation of pure Al. Preston and Bircumshaw (4), Brouckère (5), Haas (6), and Keller and Edwards (7) report  $\gamma\text{-Al}_2\text{O}_3$  with spinel structures having a unit cell of about 7.9Å. Gulbransen and Wysong (3) have taken microbalance weighings at various temperatures and oxygen pressures and have found a slight increase in the parabolic rate constant with increasing oxygen pressure (0.76, 7.6 mm Hg), but their temperature coefficient was uncertain. Preston and Bircumshaw (4) report recrystallization of  $\gamma\text{-Al}_2\text{O}_3$  at temperatures in ex-

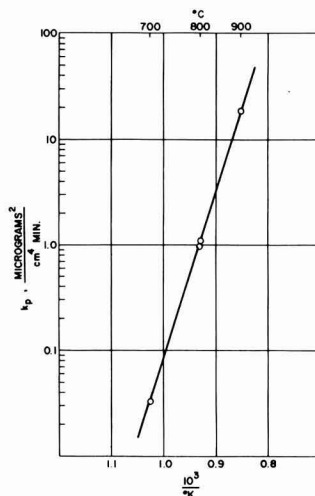
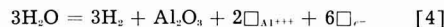


Fig. 4. Temperature dependence of the parabolic rate constant  $k_p$  (0°C dewpoint gas).

cess of 680°C, while Brouckère (5) reports an amorphous and crystalline mixture of  $\gamma\text{-Al}_2\text{O}_3$  with a tendency toward epitaxy, the cube faces being normal to the growth direction.

The results of this investigation show that the initial stage of oxidation is different from the parabolic rate which becomes operative after 1 or 2 hr of oxidation. This effect may be due to one or more of the following: solution of oxygen in the alloy, nucleation and growth of oxide patches before film coverage is complete, or growth of an amorphous oxide which becomes crystalline upon holding at the oxidation temperature. Because of the observed appearance of new lines and sharpening of the (400) and (440) lines upon holding at temperature, the latter explanation appears plausible.

Assuming that the stoichiometric oxide composition is nearly maintained, one can attempt to account for the observed pressure dependence of the oxidation rate by postulating fast surface equilibria at the oxide interfaces and that the film grows by diffusion processes within it. Several defect equations can be written for the oxide/gas interface. These are of the type given below:



or

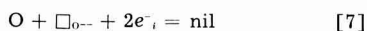


In Eq. [4] the concentration of aluminum ion vacancies varies with  $\text{H}_2\text{O}/\text{H}_2$  gas ratio to a positive fractional power,  $+3/8$ . This type of pressure dependence would correspond to a cation deficient p-type semiconductor. On the other hand, if  $\gamma\text{-Al}_2\text{O}_3$  is an n-type semiconductor having anion vacancies which permit anions to diffuse inward during oxide growth, possible equilibria at the gas/oxide interface can be written as follows:

\* Equations [5], [7], and [9] may be taken as representative of the fast equilibria at the alloy/oxide interface. In Eqs. [4]-[7] diffusion fluxes will be approximately dependent on the concentration differences of vacancies per unit volume at the inner and outer interfaces, divided by the instantaneous film thickness. In Eqs. [8] and [9] diffusion fluxes will be determined by concentration differences of interstitial metal ions.

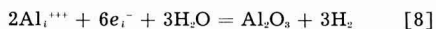


or

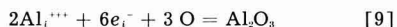


In Eq. [6] the concentration of anion vacancies varies with  $\text{H}_2\text{O}/\text{H}_2$  gas ratio to the  $-1/3$  power;  $e_i^-$  is an excess or defect electron.

If  $\gamma$ -alumina is an n-type semiconductor (9) with excess metal ions and electrons in interstitial positions, the following equilibria at the gas/oxide interface might apply



or



The concentration of excess metal ions in Eq. [8] would be dependent on the  $\text{H}_2\text{O}/\text{H}_2$  gas ratio to the  $-3/8$  power.

Because of the small positive pressure effect on the rate of formation of  $\gamma$ - $\text{Al}_2\text{O}_3$ , it is supposed that this structure has both cation and anion vacancies. Growth must proceed by countercurrent diffusion of cations outward and anions inward through the oxide film. This kind of a structure would correspond to a transition-type semiconductor with a probable excess of cation vacancies and electron defects. The measured pressure effect agrees generally with the small positive effect demonstrated by Gulbransen and Wysong (3).

The large value of the experimental heat of activation is in agreement with the above considerations. At least four distinct processes are involved in the growth of the oxide generation and diffusion of anion vacancies and of cation vacancies. If the nature of the oxidation product varied with temperature, one would not expect the linear relation in Fig. 4 to hold. That the electron diffraction patterns were identical for all temperatures is further

proof that the oxidation product in all experiments was essentially the same.

### Summary

1. Aluminum in solid solution in iron was oxidized selectively with damp hydrogen at  $700^\circ$ - $900^\circ\text{C}$ .
2. Microbalance weight gain data followed a parabolic time law after an initial time lag.
3. The surface oxidation product was identified by electron diffraction to be the crystalline spinel,  $\gamma$ - $\text{Al}_2\text{O}_3$ .
4. The parabolic rate constants varied approximately linearly with  $\text{H}_2\text{O}/\text{H}_2$  gas ratio to the  $+1/7$  power.
5. The experimental activation energy for the over-all oxidation reaction was 72 kcal/mole.

### Acknowledgments

The authors wish to thank Dr. W. F. Claussen for some stimulating discussions. The help of Eileen Alessandrini and Leo Butler is also appreciated.

Manuscript received Jan. 13, 1958. This paper was prepared for delivery before the Ottawa Meeting, Sept. 28-Oct. 2, 1958.

Any discussion of this paper will appear in a Discussion Section to be published in the June 1959 JOURNAL.

### REFERENCES

1. J. Moreau and J. Bénard, *J. Inst. Met.*, **83**, 87 (1954-55).
2. A. U. Seybolt and E. Alessandrini, Private communication.
3. E. A. Gulbransen and W. S. Wysong, *J. Phys. Chem.*, **51**, 1087 (1947).
4. G. D. Preston and L. L. Bircumshaw, *Phil. Mag.*, **22**, 654 (1936).
5. L. Brouckere, *J. Inst. Met.*, **71**, 131 (1945).
6. G. Haas, *Z. anorg. Chem.*, **254**, 96 (1947).
7. F. Keller and J. Edwards, *Int. Conf. Surf. React.*, 202 (1948).
8. H. H. Uhlig, *Acta Met.*, **4**, 541 (1956).
9. W. W. Smeltzer, *This Journal*, **103**, 209 (1956).

## Particle Size and Efficiency of Electroluminescent Zinc Sulfide Phosphors

W. Lehmann

Research Department, Westinghouse Electric Corporation, Bloomfield, New Jersey

### ABSTRACT

The brightness and the electric power absorption of an electroluminescent ZnS phosphor depend on the mean particle size of the phosphor. For constant amounts of phosphor by weight excited under identical conditions, decreasing particle size causes strongly decreased brightness at low voltages. However, at high voltages the brightness remains unchanged or tends to increase. At all voltages, the electric power absorption is proportional to the particle size. The efficiency, i.e., the ratio of brightness to power absorption, increases with decreasing particle size. With fine particles of a green emitting phosphor, a luminous efficiency of 14 lpw of a complete cell (corresponding to 18-19 lpw of the phosphor itself) could be measured.

Experimental data on the dependence of the emission intensity of electroluminescence on the mean particle size of zinc sulfide phosphors were presented recently by Goldberg (1). Similar experi-

ments have also been made in our laboratory including, however, in addition the dependence of the electric power absorption on the mean particle size. A standard, green-emitting ZnS:Cu,Cl phosphor

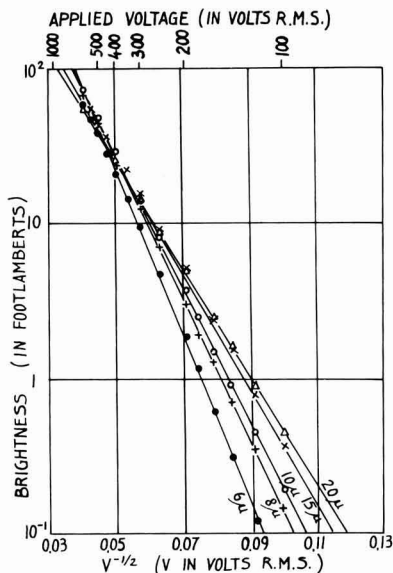


Fig. 1. Dependence of the electroluminescent brightness,  $L$ , on the exciting voltage,  $V$ , for several phosphor fractions of different mean particle diameter.

was separated by repeated sedimentation in alcohol into several fractions of different mean particle sizes. The distribution of the particle diameters of each fraction was determined microscopically. The resulting arithmetic means of the diameters and their standard deviations were:  $6 \pm 2\mu$ ;  $8 \pm 3\mu$ ;  $10 \pm 4\mu$ ;  $15 \pm 6\mu$ ;  $20 \pm 6\mu$ . These numbers indicate that the particle size distributions of the fractions overlap considerably. A sharper separation, i.e., smaller standard deviation, would, of course, be highly desirable but could not be obtained without losing too much phosphor. All fractions consisted mainly of separated, simple crystals and contained practically no agglomerates. The electroluminescence of these fractions was measured in the usual type of castor

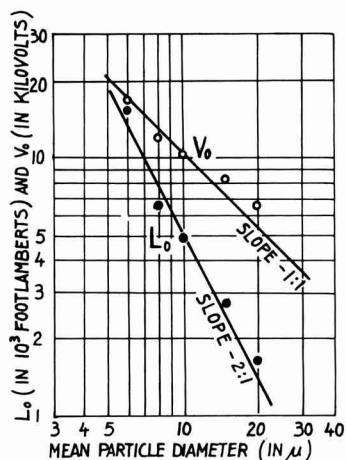


Fig. 2. Dependences of the two constants  $L_0$  and  $V_0$  in the equation  $L = L_0 \exp [-(V_0/V)^{1/2}]$  on the mean particle diameter.

oil cell, always employing the same cell geometry and the same amount of phosphor by weight in the cell. Precautions were taken to insure that the geometrical arrangement of the phosphor particles in the liquid dielectric of the cell, i.e., bridge formation (3), was stable and did not falsify the measurements.

Figure 1 shows the dependence of the emission intensity,  $L$ , of the complete cells on the applied voltage,  $V$ , plotted as  $\log L$  as a function of  $V^{-1/2}$ . This figure is quite in agreement with Goldberg's results. The straight lines in Fig. 1 approaching the experimental points represent the familiar expression (2)

$$L = L_0 \exp [-(V_0/V)^{1/2}] \quad [1]$$

where  $L_0$  and  $V_0$  are constants. Figure 2 shows the experimental dependence of  $L_0$  and  $V_0$  on the mean particle size,  $a$ , plotted on log-log scales. The points there seem to be grouped around the straight lines representing the relationships

$$L_0 = A/a^2 \quad [2a]$$

and

$$V_0 = B/a \quad [2b]$$

where  $A$  and  $B$  are two constants independent of the particle diameter. While Eq. [2b] is in agreement with Goldberg's results, he obtained an exponent of 3 for  $a$  in [2a]. The reason for this disagreement may be the finite particle size distributions of all fractions investigated so far.

The dependence of the electric power absorption,  $W$ , on the mean particle size was determined by measuring the capacitance,  $C$ , and the loss angle,  $\phi$ , of the complete cell and calculating

$$W = 2\pi f V^2 C \sin \phi \quad [3]$$

where  $f$  and  $V$  are the frequency and voltage, respectively. Details of this technique are described in an earlier publication (3). Control measurements of similar cells in two different ways, with an impedance bridge and with an electronic wattmeter, gave the same results as the measurements with the above loss angle method, so that it is believed that this method gives reliable results.

The experimentally determined dependencies of the capacitance,  $C$ , and the loss angle,  $\phi$ , are given in Fig. 3.  $C$  and  $\phi$  both increase with increasing particle size at finite exciting voltages,  $V$ . As  $V$  approaches zero,  $C$  approaches a constant value independent of the particle size, while  $\phi$  approaches values close to zero. The term  $C \sin \phi$  in Eq. [3] is that cell property which is responsible for the electric power absorption (the other two factors in [3],  $f$  and  $V^2$ , are not cell properties). It was found that the term  $C \sin \phi$  is almost proportional to the mean particle diameter,  $a$ . This is shown in Fig. 4 where the ratio  $C \sin \phi/a$  is plotted as a function of the exciting voltage,  $V$ . This result is somewhat peculiar since, in all cases, the same amount of phosphor was used in the cells. The cells containing the fine particles have a lower power consumption, although they contain many more particles than the cells containing the coarse particles.

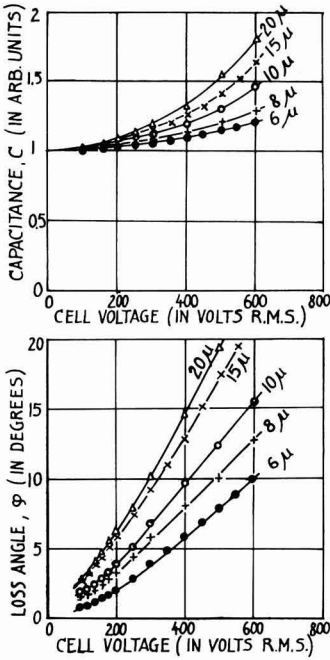


Fig. 3. Dependences of the cell capacitance, C, and the dielectric loss angle, φ, of the complete cell on the exciting voltage, for several phosphor fractions of different mean particle diameter.

The efficiency of electroluminescence is essentially the ratio of the emission intensity, L, to the electric power absorption, W. The emission intensity, L, is not very strongly dependent on the mean particle size in the region of moderate and higher exciting voltages (Fig. 1). The electric power absorption, however, decreases with decreasing mean particle diameter (Fig. 4). Consequently, the effi-

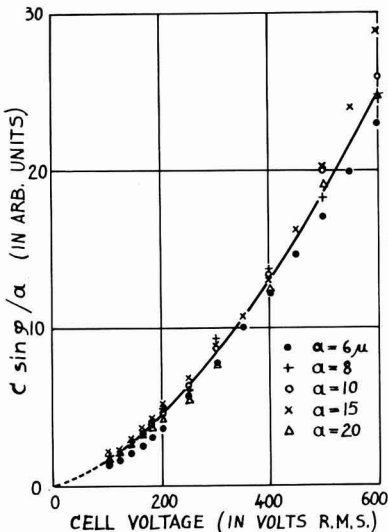


Fig. 4. Demonstration of the proportionality between C sin φ and the mean particle diameter, a.

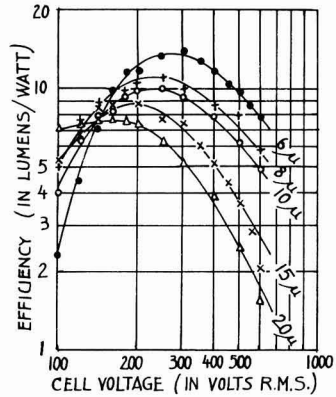


Fig. 5. Dependence of the luminous efficiency of electroluminescence on the exciting voltage for several phosphor fractions of different mean particle diameter.

ciency  $\eta = L/W$  increases with decreasing mean particle diameter. Experimental results are shown in Fig. 5. The highest luminous efficiency of electroluminescence observed so far in this way is 14 lpw. This is, however, the luminous efficiency of the complete cell. Estimating the energy and radiation losses in constructional parts of the cell (especially the reabsorption of light emitted from the phosphor in the cell electrodes), this value of 14 lpw corresponds to about 18 to 19 lpw for the efficiency of the phosphor itself. This is considerably above the theoretical maxima of 12 lpw predicted by Bowtell and Bate (4) and of 14 lpw calculated by Zalm (5). Furthermore, it is not believed that this value of 18 to 19 lpw is the upper limit of what is obtainable.

The peak efficiencies of Fig. 5 are replotted in Fig. 6 on a log-log basis. The experimental points are grouped around a straight line of slope  $-1/2$  corresponding to a dependence

$$\eta_{\max} = c/a^{1/2}$$

where c is a constant. Any quantitative foundation for this relationship is still missing.

Results essentially similar to those described here for a green-emitting ZnS:Cu,Cl phosphor have also been obtained for a yellow-emitting ZnS:Cu,Mn phosphor.

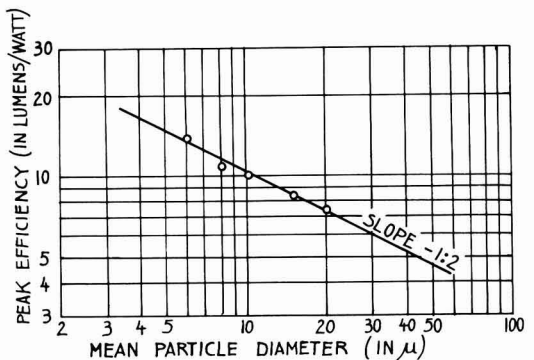


Fig. 6. Dependence of the peak electroluminescence efficiency on the mean particle diameter of the phosphor.

A qualitative explanation of all results might be possible with the familiar barrier model for electroluminescence, assuming that the excitation mechanism occurs primarily near the surface while the electric power absorption is mainly a bulk property of the phosphor particles. A decrease of the particle size increases the surface to volume ratio and hence should increase the efficiency. However, quantitative agreement of this model with the experimental data has not yet been obtained. More experiments should be made on phosphors having still more uniform particle sizes in order to obtain more information about these questions.

Manuscript received May 12, 1958. This paper was prepared for delivery before the New York Meeting, April 27-May 1, 1958.

Any discussion of this paper will appear in a Discussion Section to be published in the June 1959 JOURNAL.

#### REFERENCES

1. P. Goldberg, Paper presented at The Electrochemical Society Meeting, New York, April 29, 1958.
2. G. F. Alfrey and J. B. Taylor, *Proc. Phys. Soc.*, **B68**, 775 (1956).
3. W. Lehmann, *This Journal*, **103**, 24 (1956).
4. J. N. Bowtell and H. C. Bate, *Trans. Illum. Engng. Soc. (London)*, **20**, 3 (1955).
5. P. Zalm, *Philips Res. Repts.*, **11**, 438 (1956).

## Gold in Silicon

G. Bemski and J. D. Struthers

*Bell Telephone Laboratories, Incorporated, Murray Hill, New Jersey*

#### ABSTRACT

Heat treatment of silicon, both p-type and n-type, to temperatures in excess of 900°C frequently results in a decrease of lifetime and is sometimes accompanied by an increase in resistivity. In the present experiments, gold has been found to be introduced during such heat treatments in concentrations sufficient to account for the observed changes in the electrical characteristics. Gold has been observed on the surfaces of all the silicon samples examined so far. Heat treatments in the temperature range 1100°-1300°C result in a concentration of gold in the bulk material of about  $10^{14}$  at./cm<sup>3</sup>. A film of nickel or copper on the silicon surface during the heat treatment has a gettering action for gold. Heat treatment in vacuum can also be effective in the removal of gold.

Recently, the growth of silicon single crystals with a high minority carrier lifetime has become possible. However, in subsequent heat treatments to temperatures above 900°C, the lifetime is frequently degraded. At temperatures above 1100°C the degradation of lifetime is sometimes accompanied by the introduction of donor levels in p-type and acceptor levels in n-type Si, resulting in an increase of resistivity.

These effects could be due to either structural or chemical imperfections. It has been demonstrated that Si can be heated to high temperatures under proper conditions (in floating zone equipment), even followed by a fast cooling cycle, without significantly degrading the lifetime (1). This experiment is a strong indication that the drastic lifetime degradations normally encountered must be due to chemical impurities.

In the present experiments, neutron activation measurements were used in an attempt to correlate the electrical effects encountered in heat-treated Si with particular chemical impurities.

#### Experimental

The electrical effects in heat-treated Si, that is, the change in carrier density and the change in lifetime, were studied by standard techniques. The change in carrier density was obtained from Hall effect measurements and from resistivity measure-

ments as a function of temperature. The lifetime was measured by the injection-extraction method (2).

For the neutron activation analysis the samples were irradiated in the Brookhaven National Laboratory Reactor. Energies and decay rates were measured using a single channel scintillation spectrometer. Beta particle energies were measured by the aluminum absorber technique, and decay rates by conventional Geiger-Müller counting methods. In a few cases, radiochemical separations were made by adding inactive carriers to confirm the conclusions obtained on the basis of the measured half-life and energies of the observed radiations.

Heat treatments of the samples were performed in three different vacuum stations as well as in three different Sentry ovens in a He atmosphere. The different systems were used in order to minimize the possibility of introducing impurities due to a contamination of any one particular system. The results obtained, however, were independent of the system used.

#### Results

*Surface contamination of silicon.*—It has been observed that Si wafers cut from pulled crystals, after neutron irradiation, showed an induced radioactivity other than the Si activity, or an activity due to the donor or acceptor impurities. A typical autoradiograph is shown in Fig. 1. The spotty appearance of the radioactive centers on the surface is notice-

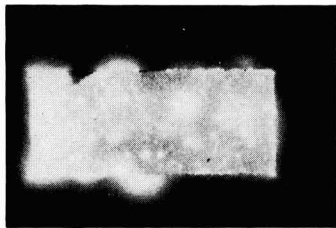


Fig. 1. Autoradiograph of an unheated Si sample (not etched after irradiation).

able in most samples. The activity is confined to the surface only; after a slight surface etch of the irradiated sample, the activity drops by orders of magnitude.

The unknown activity could be identified as  $\text{Au}^{198}$ , which is the isotope obtained on neutron activation from the stable isotope  $\text{Au}^{197}$ . This identification was obtained from the beta decay half-life of approximately 65 hr, the  $\beta$  energy of 0.9 m.e.v., and the  $\gamma$  energy of 0.4 m.e.v. A radiochemical separation confirmed this finding.

Several experiments have been performed in order to find a surface treatment not giving rise to Au contamination. Prior to irradiation, the following cleansing procedures have been used on the various wafers: (a) 48% HF (Baker) followed by a rinse in cold deionized water, (b) 70%  $\text{HNO}_3$  (Baker) followed by a rinse in cold deionized water, (c)  $\text{HNO}_3 + \text{HF}$ , (d) aqua regia, (e) boiled deionized water, (f) lapped and rinsed in cold deionized water, and (g) HF, dried by evaporation. After all these procedures, an average Au concentration of  $10^{12}$  to  $10^{13}$  Au at./ $\text{cm}^2$  was observed.

Even a crystal which has been pulled, then broken off at the seed, and handled with filter paper only showed Au contamination at the surface after irradiation. Polycrystalline Si material (du Pont), in the form of crystallites, has also been subjected to neutron irradiation and showed a Au concentration on the surface exceeding  $10^{13}$  Au at./ $\text{cm}^2$ . The Al foil, used for wrapping the Si samples, showed no Au activity on irradiation. This proves that the Au was not introduced during the handling procedures.

**Volume contamination.**—As mentioned above, the activity observed on the surface disappears after slight etching. From this, one can estimate that the Au concentration in the crystal, as grown, is less than  $10^{12}$  at./ $\text{cm}^3$ .

Gold is known to have a comparatively high-diffusion constant and a high-solid solubility in Si (3, 4); therefore, one expects a Au contamination on the surface to diffuse into the bulk of the material upon heating. Silicon wafers heated to temperatures above  $1100^\circ\text{C}$  have been analyzed by the neutron activation technique. After removing a surface layer to eliminate activity located at the surface, the sample still showed a  $\beta$  and  $\gamma$  activity uniform throughout the volume. Figure 2 shows an autoradiograph of a heated and etched sample. Figure 3 compares the  $\beta$  decay observed in a gold-doped crystal with the  $\beta$  decay observed in a heat-treated sample. One sees that the half-life in both samples is identical. The  $\beta$  and  $\gamma$  energies were also identical.

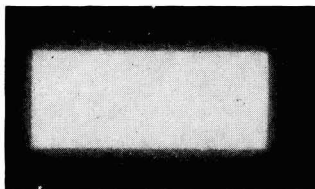


Fig. 2. Autoradiograph of a p-type Si sample heated to  $1300^\circ\text{C}$  (etched after irradiation).

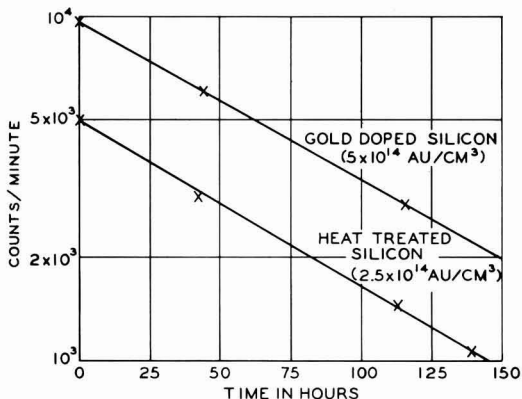


Fig. 3. Beta decay in a gold-doped Si crystal and in a heat-treated Si sample.

These findings confirm that Au had diffused into the sample during the heating cycle. The concentration of Au as found by this analysis is of the order of  $10^{14}$  at./ $\text{cm}^3$  and can be accounted for by the surface concentration of Au as measured prior to heating. Different samples gave similar results.

The hole concentration has been measured by the Hall effect on several p-type silicon samples of a resistivity of 20 ohm-cm or higher. Figure 4 shows the hole concentration thus found as a function of

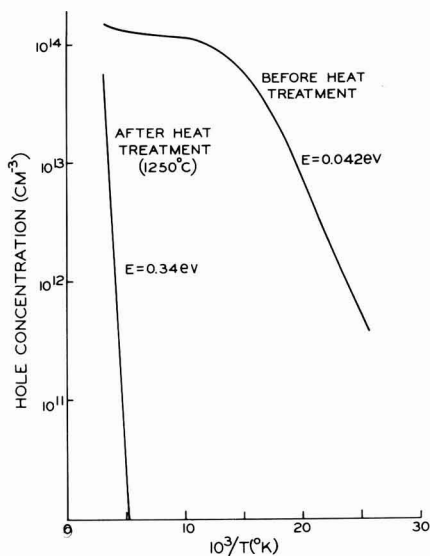


Fig. 4. Hole concentration vs.  $10^3/T$  in p-type Si before and after heating to  $1250^\circ\text{C}$  (Hall effect data).

temperature before and after heating. In this particular case the samples were heated for 1 hr at 1250°C. Results were similar in samples heated in air or in a vacuum of  $10^{-5}$  mm Hg. The data in Fig. 4 indicate an introduction of donors in a concentration of  $10^{14}$  at./cm<sup>3</sup> with an energy level at 0.34 eV from the valence band. This level can be observed only in fairly high resistivity Si in which the concentration of the added donor is larger than the original acceptor concentration. Among the known electrically active impurities in Si only Au, with a donor level at 0.35 eV from the valence band, comes within experimental error of the donor energy observed here.

As stated elsewhere (5), the room temperature capture cross section for minority carriers on Au levels in Si is of the order of  $10^{-15}$  cm<sup>2</sup>. This implies that a Au concentration of  $10^{14}$  at./cm<sup>3</sup> will result in a room temperature lifetime in p-type silicon up to resistivities of 100 ohm-cm of less than 1 μsec. A room temperature, low-injection lifetime of 0.2 μsec was observed in the sample shown in Fig. 4. If one attributes this lifetime to recombination by Au centers only, one also obtains a Au concentration of the order of  $10^{14}$  at./cm<sup>3</sup>.

The agreement in the concentrations obtained from the neutron activation analysis, the Hall effect, and the lifetime measurement indicates that Au is the major contaminant responsible for the electrical effects observed in these samples.

#### Techniques to avoid gold contamination in silicon.

—Two techniques have been reported previously which lead to an increase in lifetime during a heat treatment and in which one would suspect chemical impurities to play a role.

Baker and Bemski (6) found that vacuum heat treatment can partially restore the minority carrier lifetime in a degraded silicon sample. They suspected that chemical impurities diffused out of the bulk of the Si during such a treatment.

Silverman and Singleton (7) are reporting that the lifetime during heat treatment can be considerably increased by plating the surface of the Si with Ni, prior to the heating cycle. Nickel forms a liquid alloy on the surface of the Si at elevated temperatures. As has been shown previously for a similar system [Au-Ge liquidus on Ge (8)], such a liquidus can act as a getter for a third component if the distribution coefficient in the ternary alloy dilute in the third component is significantly less than unity. This is the case for a Ni- (or Cu-) Si alloy with Au as the dilute third component (9). Such getters can effectively prevent Au from entering the Si and they can remove Au previously introduced.

Gettering of Au by a liquidus layer has been observed whereby the Au was identified by the neutron activation analysis. Copper, as well as Ni, was used for the formation of the gettering liquidus layer. Two Si samples have been heated to 1250°C for 1 hr in an open tube furnace. One sample "A" had a Cu film on its surfaces while the other sample "B" had unprotected surfaces. After neutron activation and etching these samples gave autoradiographs as shown in Fig. 5. It is apparent that sample A shows essentially no Au concentration

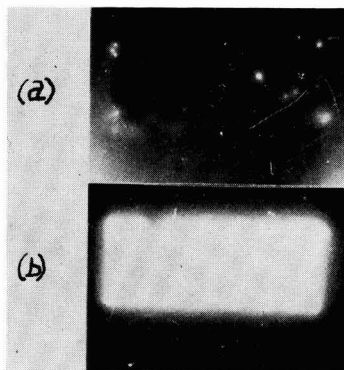


Fig. 5. Autoradiographs of Si samples heated to 1100°C. (a) in the presence of a Cu film on the surfaces; (b) without films on the surfaces. (Etched after irradiation.)

(less than  $10^{12}$  at./cm<sup>3</sup>), while sample B shows a strong Au concentration calculated to be  $5 \times 10^{14}$  at./cm<sup>3</sup>.

The results of a typical experiment, illustrating the removal of Au from the bulk, are shown in Fig. 6. Curve A shows the resistivity which has been measured as a function of temperature on samples from a gold-doped, p-type Si crystal with  $5 \times 10^{14}$  Au at./cm<sup>3</sup>. The 0.34 eV level is seen. Curve B was obtained on a sample which had been nickel plated and heated for 2 hr at 1100°C. These two curves indicate that the Au donor level had disappeared. Curve C was obtained on a sample after vacuum heat treatment and resembles curve B. An activation analysis showed approximately an 80% decrease in the Au concentration in the samples B and C as compared with A.

### Conclusions

The experiments so far indicate that Au is one of the major electrically active elements which are introduced in Si during heat treatment. Gold concentrations found in the material studied are sufficient to account for the changes of resistivity and lifetime. Gold contamination on the surface of the Si as well as Au in the bulk of the Si can be removed

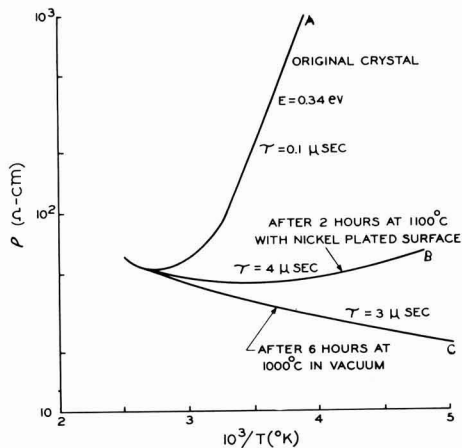


Fig. 6. Resistivity vs.  $10^3/T$  in gold-doped p-type Si

effectively, preferably by a Ni-Si liquidus on the surface of the samples or by a vacuum heat treatment. The crystals as grown show no Au in the bulk. This is easily understandable since the liquid Si must act as a strong getter (distribution coefficient for Au approximately  $10^{-3}$ ). The surface film of Au observed on the grown crystals must have been deposited after the material solidified. The Au observed on etched material must have its origin in the chemicals used. One can therefore conclude that special precautions will be necessary to reduce the Au contamination to levels below those encountered here, which correspond to approximately 0.001 of a monolayer.

#### Acknowledgments

The authors wish to thank Dr. F. M. Smits for helpful discussions, Miss K. Wolfstirn, Mr. F. Worthing, and Mr. R. M. Mikulyak for help in the measurements, and Mr. D. T. Lassota for growing the silicon crystals.

Manuscript received March 3, 1958. This paper was prepared for delivery before the Buffalo Meeting, Oct. 6-10, 1957.

Any discussion of this paper will appear in a Discussion Section to be published in the June 1959 JOURNAL.

#### REFERENCES

1. H. C. Theuerer, J. M. Whelan, H. E. Bridgers, and E. Buehler, *This Journal*, **104**, 721 (1957).
2. R. H. Kingston, *Proc. I.R.E.*, **42**, 849 (1954).
3. J. D. Struthers, *J. Appl. Phys.*, **27**, 1560 (1956).
4. C. B. Collins, R. O. Carlson, and C. J. Gallagher, *Phys. Rev.*, **105**, 1168 (1957).
5. G. Bemski, To be published.
6. A. N. Baker and G. Bemski, "Vacuum Heat Treatment of Silicon," presented at I.R.E.-A.I.E.E. Semiconductor Device Research Conference, Boulder, Colo., July 1957.
7. S. J. Silverman and J. B. Singleton, *This Journal*, **105**, 591 (1958).
8. C. D. Thurmond and R. A. Logan, *J. Phys. Chem.*, **60**, 591 (1956).
9. C. D. Thurmond, Private communication.

## Technique for Preserving Lifetime in Diffused Silicon

S. J. Silverman and J. B. Singleton

*Bell Telephone Laboratories, Incorporated, Allentown, Pennsylvania*

#### ABSTRACT

After a silicon crystal has been grown, contamination prior to and during the diffusion process is considered a significant cause of lifetime degradation. If, prior to diffusion, a suitable gettering agent is formed on the surface of a silicon slice, then the resultant average lifetime is approximately an order of magnitude greater than that in an untreated slice from the same crystal subjected to the same process. It is believed that a metal-silicon liquid phase established on the silicon surface getters recombination centers from within the bulk of the material, thereby preserving the lifetime. Nickel, silver, or bismuth has been independently applied with comparable results.

In the course of silicon device fabrication, an outstanding problem has been the maintenance of a minimum lifetime after the conventional high-temperature heat treatment, at 1000°C or above for an hour or more. If the minimum lifetime can be retained after processing, the lifetime-dependent electrical characteristics are assured. We have investigated this problem in connection with diffused, high-voltage, conductivity-modulated rectifiers. After processing the diodes, lifetimes equal to or greater than 1  $\mu$ sec have been obtained in 20-60 ohm-cm Si (n- or p-type) through the gettering action of a metal-silicon liquid phase on the surface of the material. Nickel, silver, or bismuth has been used with equal success. Without this technique, the lifetime is often degraded to less than a few tenths of a microsecond.

#### Experimental

The general characteristics desirable for this liquid phase metal-silicon gettering action may be postulated as follows.

- (a) The eutectic temperature should be low enough to form a liquid phase on the surface, permitting diffusion and segregation of the impurity.
- (b) The metal vapor pressure should be suffi-

ciently low at the diffusion temperature to assure establishment of a permanent liquid phase on the surface.

(c) The gettering process should have no discernible electrical effect on the device other than preserving the lifetime.

It has been found that the metal can be applied to the Si surface by any of the following methods: (a) electroless plating, (b) electroplating, (c) vacuum deposition, (d) bulk metal in intimate contact with surface, (e) mixing the metal powder with the "paint-on" diffusant, or (f) mixing a reducible metal compound with the paint-on diffusant.

The most convenient of the above methods was the mixing of a reducible metal compound with a paint-on diffusant. This procedure consisted of mixing 2 g of NiCO<sub>3</sub> in a solution of 5 g of P<sub>2</sub>O<sub>5</sub> and 100 cc of 2-methoxyethanol. This mixture was applied uniformly onto the Si surface with a clean camel's hair brush. The specimens, placed on a suitable quartz tray, were inserted into a resistance-heated furnace having a quartz tube open to the air and maintained at 1250°C for 16 hr. A cooling period followed at the rate of 10°C/min until 400°C, after which the specimens were removed from the

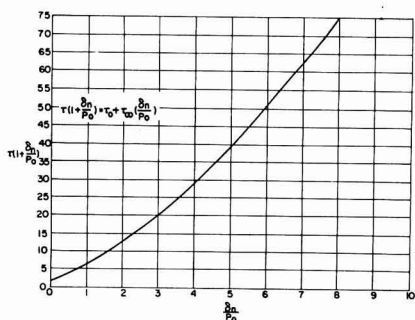


Fig. 1. Relative values of lifetime as a function of injection level.

furnace. (This slow cooling, originally considered beneficial to lifetime, will be shown unnecessary in a later section.) Under such conditions, a 1.5-mil diffusion depth of the phosphorus was obtained. The lifetime was then measured by the injection-extraction technique of Kingston (1).

It is important to stress the interpretation of lifetime values measured by this technique. One must be aware of the lifetime dependence on both (a) the injection level and (b) the composition of the material. Figure 1 is a plot of experimental data modified after the original equations proposed by Shockley and Read (2). Here, the equation is in terms of  $\tau_0$  (lifetime at zero injection level) and  $\tau_0$  (the slope in the linear portion of the curve). The relative values of  $\tau$  are plotted as function of  $\delta n/p_0$ , (injection level). It is noteworthy that all other observations for  $\tau$  were standardized at a forward current value such that  $\delta n/p_0$  was approximately 8, which is well beyond saturation. This curve does not include the correction arising from the ratio of the width of the conductivity modulated region to the diffusion length (3). Such a correction would increase the value of the true lifetime relative to the observed lifetime. Emphasis is, therefore, placed not so much on the absolute value of  $\tau$ , but rather on the relative values of the treated and the untreated specimens when measured at the same injection level for a particular base width.

Keeping these conditions in mind, it can be shown that within certain limitations the preservation of lifetime is independent of: (a) material preparation, (b) cooling cycle, (c) the use of protective covering on both surfaces, (d) the material used in

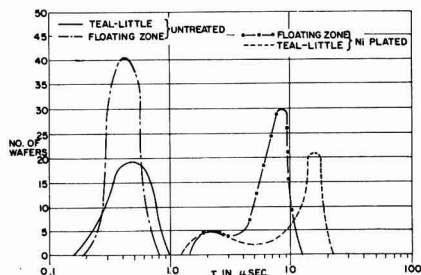


Fig. 2. Comparison of lifetime distributions between floating zone and pulled Si crystals.

the surface-gettering liquid phase (specifically: Ni, Ag, or Bi), and (e) the previous heat-treatment history before the final stage in which the liquid phase mechanism is used.

In the first experiment, two crystals were doped to the same resistivity range and conductivity type. The first was grown by the floating zone technique. The original lifetime was measured by the Haynes-Hornbeck technique at 500-300  $\mu$ sec. The second, grown from a quartz crucible by the Czochralski technique, gave a lifetime between 50 and 20  $\mu$ sec. The two crystal sections were cut along the growth axis. The first group of half-slices were nickel-plated and their adjacent half-slices were left as controls. All were subjected simultaneously to the previously described heat treatment. Figure 2 shows that the Ni was equally effective for both types of material, whereas the controls were equally degraded.

In the next experiment, slices from the same Czochralski crystal were cut in half. The first group of half-slices was treated with Ni; the second was used as controls. All specimens were subjected to the previously described treatment except that at the end of the heating interval, they were quenched from a temperature of 1250° to 60°C by dropping them into a silicone oil bath. This change of temperature was accomplished in approximately 5 sec. Figure 3 shows that the average lifetime of the nickel-plated specimens is a factor of 10 greater than that of the controls. As a result of this experiment, the previous lengthy cooling cycle has been considerably shortened without sacrificing any of the electrical requirements of the device.

These observations on quenching (Fig. 3) compared with slow cooling at 10°C/min (Fig. 2) indicate that a metal-silicon surface liquid phase completely obscures whatever beneficial effects the latter procedure may offer under these circumstances. No apparent advantage is gained by combining the slow cooling rate with the metal-silicon liquid phase.

The question has arisen concerning the necessity of masking the entire Si surface with Ni to prevent entry of contaminants. The next experiment indicates that this precaution is unwarranted. Only a single surface covered with the gettering agent is sufficient to preserve the lifetime. Figure 4 is a comparison of units selected and processed in the same manner as in the first experiment, but divided into three groups: nickel on one surface; nickel on two surfaces; and a control. These results are of practical importance when one is restricted to single-surface treatment by the nature of the fabrication procedure.

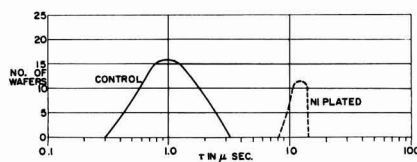


Fig. 3. Lifetimes after diffusion and quenching

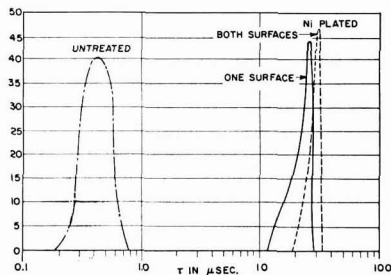


Fig. 4. Comparison of lifetimes for single and double surface treatments.

To show that Ni is not unique in this surface-gettering action, slices from the same crystal were treated independently with Ag or Bi. Silver was applied using an electroless chemiplating bath, consisting of 4 g  $\text{AgNO}_3$ , 0.4 cc HF, and 100 cc  $\text{H}_2\text{O}$ . Bismuth was introduced in the form of 2 g of  $\text{Bi}_2\text{O}_3$  mixed with the previously mentioned paint-on diffusant. Figure 5 indicates that all three metals, which conform to the previously described characteristics, give substantially the same distribution groups.

The last experiment was devised to show how the lifetime, when purposely degraded beforehand, can be recovered by subsequent Ni plating on the surface and reheating above the eutectic temperature. The results are seen in Fig. 6. A slice was divided into three sections. The first was given the previously described diffusion heat cycle, then nickel-plated and reheated for 2 hr at  $1250^\circ\text{C}$ . The second was subjected to the same conditions as the first, without any Ni. The third was used as a control after first diffusion only. This experiment demonstrates that, regardless of the previous history of heat treatment, lifetime can still be preserved if a metal-silicon liquid phase is established during or after the final heat treatment in which the tempera-

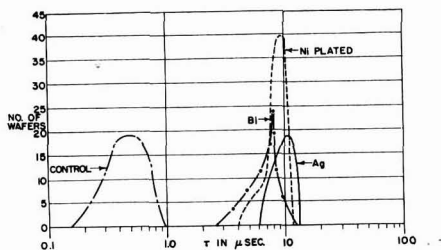


Fig. 5. Comparison of lifetimes preserved by various metals forming eutectic on Si surface.

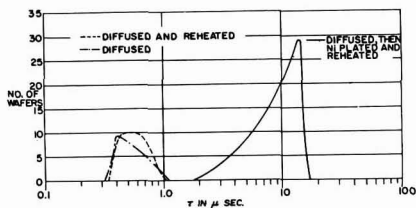


Fig. 6. Comparison of lifetimes on Si purposely degraded before final heat treatment.

ture at some time must be greater than the eutectic temperature. This period of heating has been as little as 1 hr.

### Discussion

The deterioration of lifetime as described in the previous experiments is attributed to surface contamination resulting from (a) the processing steps prior to heating and (b) the ensuing high-temperature cycle in the relatively unclean furnace environment. A significant experiment demonstrating the effect of these conditions has been successfully performed by Theuerer, *et al.* (4). A single crystal of silicon was grown by the floating zone process. The room temperature lifetime as measured by the Haynes-Hornbeck (5) technique was 500-300  $\mu\text{sec}$ . The surface was then etched with CP-8,<sup>1</sup> rinsed with deionized water, and dried. After reheating the sample at  $1100^\circ\text{C}$  for 1 hr in the floating zone apparatus, the lifetime was remeasured and found to be degraded to less than 3  $\mu\text{sec}$ . However, when the same heat treatment was performed without touching or treating the crystal in any manner, the original order of magnitude was retained. In an independent experiment, water ordinarily used to cool the floating zone envelope was eliminated; the interior surface of the quartz chamber was allowed to reach an elevated temperature during heat treatment, causing the same degree of degradation. In both cases the silicon surface was exposed to sufficient chemical contamination to deteriorate the lifetime. The known contaminants adversely affecting lifetime have been identified as Au, Fe, Cu, and Mn, as shown independently by Carlson (6) and others (7, 8).

Several techniques have been proposed previously to control the degradation of lifetime. They are: (a) slow cooling in a gaseous ambient, as originally proposed by Bemski (9); (b) heating and cooling under special conditions in vacuum, as suggested by Baker (10); and (c) the use of a surface-gettering liquid phase as discussed by Trousil (11) and by Logan and Schwartz (12).

There are two possible mechanisms associated with this last technique. Consider the case of Ni on the surface of Si. One possibility is that Ni, a fast diffuser, rapidly permeates the bulk of the material at the elevated diffusion temperature. Once within the lattice, the Ni neutralizes the recombination centers in such a manner as to reduce the capture cross section, subsequently improving the lifetime.

An attempt to verify this hypothesis experimentally was made by Buehler (13). A crystal as grown by the Czochralski technique (14) was started in the normal manner. After the first half had been solidified, Ni was added to the remainder of the melt, doping the second half of the crystal. The resistivities and lifetimes after growth did not change radically from the top to the bottom. After heat treatment, the lifetime was degraded to the same extent in both halves. The results, however, were inconclusive because of the uncertainty concerning the actual concentration of Ni successfully introduced into the lattice.

<sup>1</sup> 5  $\text{HNO}_3$ :3 HF.

To insure the maximum concentration of Ni in the material, a separate experiment was designed whereby a thin film of the metal was deposited on the surface and then diffused at  $T \sim 1200^\circ\text{C}$  for 1 hr. The layer containing the excess Ni was removed by lapping, etching, rinsing, and drying. The sample was then reheated to see if the lifetime could be preserved effectively by the Ni within the lattice. However, the lifetimes measured after this heat treatment were sufficiently degraded to show no beneficial effects from Ni employed in this manner.

Another possible role of Ni is that it forms a gettering liquid phase on the surface of the Si. This is analogous to the action of a thin film of Au on Ge, described by Logan and Schwartz (12). In the latter situation the recombination center (Cu) diffuses toward the Au-Ge liquid phase, depleting its concentration in the solid Ge and thereby improving lifetime. Logan and Thurmond (15) describe conditions under which the concentration of recombination centers can be controlled using this gettering technique. Similarly, the Ni-Si system is in a liquid state at the diffusion temperature. The equally fast-diffusing recombination centers migrate toward the liquid phase on the surface. If, as in the case of Au in Si, its effective segregation coefficient is small, this impurity becomes trapped in the liquid sink where it remains as the temperature is lowered. When the experiment was repeated at temperatures below the Ni-Si eutectic, the results were not successful. Another surface-gettering action involving diffusion and vaporization of the recombination center (Au) is described in the accompanying paper (16) by Bemski and Struthers.

### Conclusions

It is believed that the observations reported here give strong support to a surface-gettering mech-

anism whereby fast-diffusing recombination centers (i.e., Au, Cu, Fe, or Mn) may be effectively segregated from within the volume of Si. This action, it is felt, has been responsible for increasing lifetime by an order of magnitude or more under the previously described conditions of high-injection level in relatively high-resistivity silicon material.

Manuscript received March 3, 1958. This paper was prepared for delivery before the Buffalo Meeting, Oct. 6-10, 1957.

Any discussion of this paper will appear in a Discussion Section to be published in the June 1959 JOURNAL.

### REFERENCES

1. R. H. Kingston, *Proc. IRE*, **42**, 829 (1954).
2. W. Shockley and W. T. Read, *J. Phys. Rev.*, **87**, 835 (1952).
3. J. Madigan and M. Byczkowski, *J. Appl. Phys.*, **28**, 878 (1957).
4. H. C. Theuerer, H. E. Bridgers, E. Buehler, and J. Whelan, Paper presented at the Washington, D. C. Meeting of The Electrochemical Society, May 1957.
5. J. R. Haynes and J. A. Hornbeck, *Phys. Rev.*, **97**, 311 (1955).
6. R. O. Carlson, *ibid.*, **104**, 937 (1956).
7. C. B. Collins, R. O. Carlson, and C. J. Gallagher, *ibid.*, **105**, 1168 (1957).
8. G. Bemski and H. E. Bridgers, Paper presented at the Cleveland Meeting of The Electrochemical Society, October 1956.
9. G. Bemski, *Phys. Rev.*, **103**, 567 (1956).
10. A. Baker, Paper presented at IRE Semiconductor Devices Conference, Denver, Colo., Spring, 1957.
11. Z. Trousil, *Czechoslov. J. Phys.*, **4**, 251 (1954).
12. R. A. Logan and M. Schwartz, *J. Appl. Phys.*, **26**, 1287 (1955).
13. E. Buehler, Private communication.
14. J. Czochralski, *Z. physik Chem.*, **92**, 219 (1918).
15. R. A. Logan and D. C. Thurmond, *J. Phys. Chem.*, **60**, 591 (1956).
16. G. Bemski and J. D. Struthers, *This Journal*, **105**, 588 (1958).

## Bonding Materials for Making Contacts to p-Type Silicon

Donald R. Mason and John C. Sarace

*Department of Chemical and Metallurgical Engineering, University of Michigan, Ann Arbor, Michigan*

### ABSTRACT

Molybdenum clad on one side with aluminum, or aluminum-silicon eutectic, has been used to form structurally sound ohmic contacts to p-type silicon, although a flux was necessary when the Al-Si eutectic-clad material was used. The desired aluminum-silicon solid solution can be formed before a substantial amount of aluminum reacts with the molybdenum. The coefficients of thermal expansion are sufficiently well matched so that the silicon wafer does not crack during fabrication, and only minimal alloy penetration into the silicon is observed with the eutectic-clad material.

Nickel and iron-base metals were found to be unsatisfactory, and process troubles with indium ruled out its choice as a bonding agent. Materials produced by cladding with electroplating processes, vacuum evaporation, direct sintering, or dipping operations, either with or without a dipping flux, were unsatisfactory and only roll-clad products could be used successfully.

The necessity for making structurally sound non-rectifying contacts to the various regions of a semiconductor device is an ever recurring problem. The

chemically deposited or electroless nickel plate as described by Sullivan and Eigler (1) has been developed for making broad area contacts to lapped

silicon surfaces and can be adapted readily for use on etched n-type Si surfaces. However, many devices including transistors cannot be made without using one or more controlled area contacts, and at least one alloy or bonded contact has been necessary on all junction transistors.

Low-resistance structural bonds have been made to etched n-type Si using an Sb-doped Au bond, but the low distribution coefficients of acceptors into Si from Au solutions (2) produced a high-resistance layer.

Satisfactory nonstructural contacts have been made to etched Si surfaces by alloying with a fine wire (3) or a thin film of vacuum-evaporated Al (4). Thick Al sections induce cracking because of a mismatch in the thermal coefficient of linear expansion. Peterson and McConville (5) have used Mo wire on which a layer of Al has been electroplated for making alloy junctions to n-type Si, with the aid of a post-alloying etch. Henkels (6) used a Si-Al eutectic foil to dope the n-type Si in forming flat p-n junctions, and the foil is fused to a Mo or Ta backing plate during the alloying cycle. A post-alloying etch is used.

Although the objective of this research was limited to the formation of ohmic contacts on etched p-type Si, it was found that alloy junctions which were quite satisfactory as emitters could also be produced, even without a post-alloying etch. Similarly, there is no inherent reason which would prevent the formation of good contacts to lapped or sand-blasted silicon surfaces.

## Experimental

### Test Specimen

The test specimen which was used to evaluate the various base plate materials is shown schematically

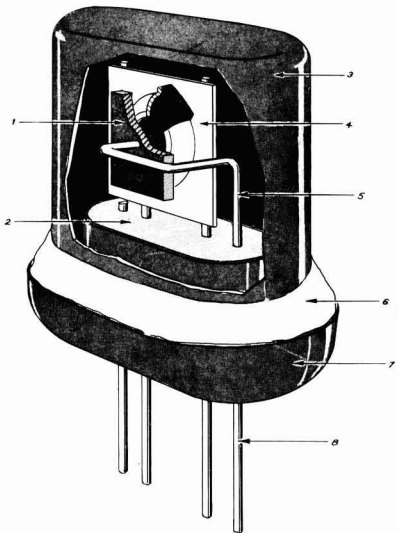


Fig. 1. Sealed diode test specimen used for evaluation of base plate materials: 1, Si wafer with diffused junction; 2, glass; 3, gold-plated can; 4, embossed alloy-clad base plate; 5, Au-Sb electroplate on this pin; 6, Sn-Ag eutectic solder; 7, Kovar eyelet; 8, Mo pins.

in Fig. 1. It comprised an n-type Si wafer having (111) major faces, into one face of which boron had been diffused to form a p'-n junction. The p-layer, having a thickness of about 0.001 in. and a surface concentration of about  $10^{20}$  boron atoms/cm<sup>2</sup>, was placed in contact with the alloy-clad base plate which in turn had been spot-welded onto the superstructure of a solder-type, symmetrical four-pin transistor header. One wire of the header which was electroplated with Au-Sb alloy was bent around to hold the Si wafer securely against the base plate, and a satisfactory ohmic contact to the n-type region was obtained during the alloying cycle. After the alloying cycle, the superstructure could be sealed to protect the surfaces from subsequent contaminating influences, if desired, by dropping a can into the solder trough of the header. With this structure, a unitized material was simpler to use in the fabrication procedure instead of a separate solder alloy and backing plate.

### Base Plate Material

A variety of base plate materials was obtained and evaluated.

The pertinent variables which characterize the base plate material can be classified into three categories; first, composition of the base metal; second, composition of the cladding material; and third, technique of applying the cladding material to the base metal.

Base metals of Fe, Ni, and Mo were investigated, using pure Al as the alloying film material. Aluminum-clad Fe and Ni were available from commercial sources; molybdenum samples were made to specification.

Whenever Fe was used, the reverse current of the diodes was intolerably high. A typical current-voltage characteristic is shown by diode A in Fig. 2. This result is consistent with observations by Bemski (7) that the minority carrier lifetime in Si is reduced when small traces of Fe are added to the system at high temperatures. The Fe could be acting as a recombination-generation center in the space charge region. Good uniform mechanical bonds were not formed, and other Fe-containing base metals such as Kovar were not considered.

The bonding to Si with Al-clad Ni was erratic. Good bonds were invariably accompanied by crack-

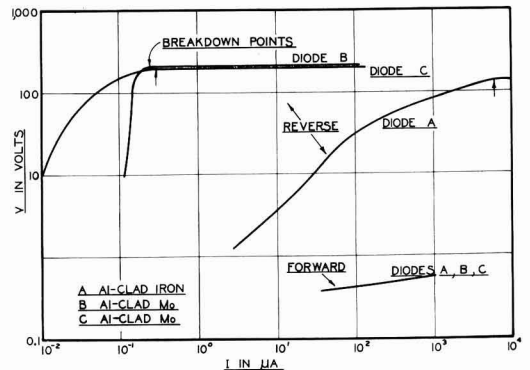


Fig. 2. Rectification characteristics of diodes made with Al-clad base plate materials.

ing of the Si wafers and hence poor electrical characteristics, because of the mismatch in the coefficients of thermal expansion. Nickel was also rejected.

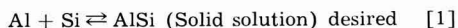
Occasionally, however, satisfactory bonds and electrical characteristics were obtained using early samples of Al-clad Mo, so Mo was chosen for further investigation. Other metals, such as tungsten, having coefficients of expansion relatively close to Si could just as well have been used. However, Mo is readily available and has sufficient ductility to permit forming and manipulation in the fabrication of piece-parts for semiconductor device structures.

#### Cladding Film Compositions

Since the cladding film must contain acceptors, the choice is almost automatically limited to Al or In in their pure forms, and Ga can be used only with a carrier alloy. In our experience Au is not a satisfactory carrier alloy because of the formation of the high-resistance film.<sup>1</sup>

Indium not only reacts with the molybdenum-tungsten welds which were used to fabricate the test specimen but also imposes a maximum operating temperature on the device of well below 150°C; consequently, it was not considered further.

Reactions between the Al and the transition metals were observed in the preliminary work. These elements all react chemically with Al below its melting point (660°C) to form complex chemical compounds which effectively precipitate the Al from the system so that it is not available to form a solid solution alloy with the silicon. In effect, the Al is in the center of a sandwich with Mo on one side and Si on the other side. Very stable compounds of the form  $Al_3M$  are known to exist, so that at equilibrium the Al may not be available to dope the Si. Perhaps as an oversimplification, it can be thought of as a reversible reaction on the Si side which is competing with an irreversible reaction on the Mo side for the utilization of the Al.



where M is Fe, Ni, Mo, or similar element.

Since it appeared that Al was necessary for good contacts, the precipitation or diffusion of the Al into the base plate had to be overcome to permit the formation of an alloy bond to Si before all the Al was precipitated. This could be done either by interposing a barrier between the Si and the base metal to retard the precipitation reaction or by adding another component to depress the melting temperature and/or lower the Al concentration. Silver was found to be satisfactory as a third component, but the over-all results were not as good as those that were obtained with the Al-clad combinations which will be discussed in detail.

#### Aluminum Cladding Processes

Most processes available for cladding Mo with Al also form a thin oxide film at the Al-Mo interface. Aluminum films, obtained by (a) electroplating

<sup>1</sup> In reviewing this manuscript, M. Tanenbaum reports that he has been able to make satisfactory contacts to p-type Si using Au doped with B or Ga.

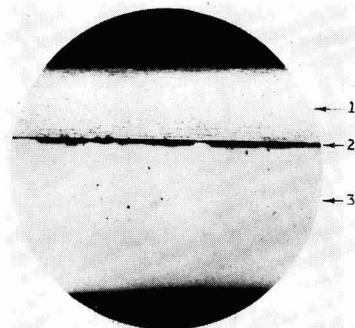


Fig. 3. Longitudinal cross section of attempted bond to Si using fluxed and Al-dipped Mo strip. 1, Mo sheet; 2, Al diffused away from here; 3, Si wafer. Magnification 200X before reduction for publication.

ing, (b) vacuum evaporation, (c) direct sintering, and (d) dipping into molten Al without a flux, were nonadherent and could be peeled off. Films applied by dipping Mo sheets into molten Al after treatment with a sodium potassium aluminum fluoride flux were nonreproducible, but very adherent; in fact, the intimacy of contact was so good that the Al apparently reacted with the Mo before the Al-Si bond could be formed. A cross section of an attempted bond to Si using this material is shown in Fig. 3. Portions of the Si surface definitely have been dissolved, but there is no trace of the Al. The thin film that is visible on the Mo surface is probably residual Si that has been deposited there as the Al diffused into the interior of the Mo.

#### Rolled-On Aluminum

Samples of Mo sheet having a pure Al film rolled onto one side were prepared to specifications<sup>2</sup> for evaluation. These comprised 0.005 in. Mo sheets having 0.0005 in. of pure Al rolled onto one side and were formed as the result of a substantial thickness reduction to promote the formation of atomic bonds between newly formed Al-Mo interfaces. Spectrochemical analyses showed the materials to be very pure.

<sup>2</sup> From Kassel Industries, Inc., P.O. Box 432, Englewood, N. J. (Aluminum film contains ½% silicon), and General Plate Division, Metals and Controls Corp., Attleboro, Mass.

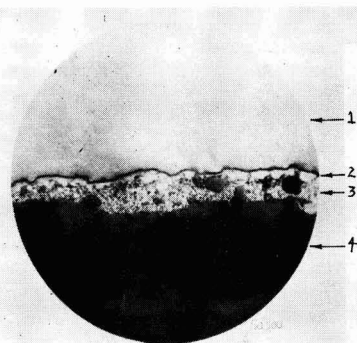


Fig. 4. Longitudinal cross section of bond to Si using Al-clad Mo. 1, Mo sheet; 2, unalloyed Al; 3, Al-Si eutectic; 4, Si wafer. Magnification 1500X before reduction for publication.

During alloying, the Al film dissolves enough of the Si wafer to form an Al-Si eutectic. A microscopic cross section of an alloyed structure is shown in Fig. 4.

Several distinct phases are distinguishable in the photomicrograph. The Si wafer has been dissolved at discrete regions over the surface, but the wetting and penetration are not uniform. During the solidification of the alloy, some of the Si redeposited on the Si surface, and some crystallites of Si remained suspended in the Al-rich phase. The grainy portion of the Al region is the Al-Si eutectic, and apparently the Al in the immediate vicinity of the Mo surface was not melted. At the same time the Al thickness is sufficiently thin to avoid cracking of the Si when alloying is carried out at temperatures around 580°-610°C. At lower temperatures no mechanical bonding occurs, while Al precipitation becomes a problem at higher temperatures.

Typical small area p-n junction characteristics are shown by diodes B and C in Fig. 2. The differences in reverse current around 0.1  $\mu$ a are thought to arise from varying degrees of background contamination from the process. Minority carrier lifetimes (8) measured on these diodes by a junction recovery method were found to be in the range of from 50 to 100 m $\mu$  sec.

#### Penetration Control:

##### Silicon-Aluminum-Clad Molybdenum

Although these results were quite satisfactory and reproducible, the penetration into the Si wafer might be undesirable for some applications. With a 0.0005 in. thick film of Al as the alloying agent, the depth of penetration into the Si at 600°C would be about 0.0001 in. This penetration could be reduced by using a Si-Al eutectic as the alloying medium. Accordingly, a composite structure was made to specification by the rolling-on process described previously.<sup>3</sup> It comprised a Mo sheet 0.008 in. thick onto one side of which an Al film 0.0005 in. thick containing nominally 12% Si had been applied. During rolling, the Mo developed a micallike striated structure, and separations were observed inside the Mo sheet. In all probability this rolling texture is not inherent in the material and could be eliminated, as it was not present on the pure Al-clad material.

The alloying characteristics of this material were found to be substantially different from the pure Al material. It was impossible to form an alloy bond between the Al-Si and the Si even by heating to temperatures in excess of 700°C. These observations were corroborated in the work with the Ag carrier alloy. When as little as 4% Si was added to a Ag-Al eutectic solution, the resulting alloy would not wet spontaneously to the Si wafers.

Experiments with Al-Si clad Mo were carried out in a different furnace using flat plates instead of the formed plates as shown in Fig. 1; however, the consistency of the results with the alloys containing Si seems to indicate that the test specimen configuration and alloying furnace are of secondary importance. Since the surface properties of the system are

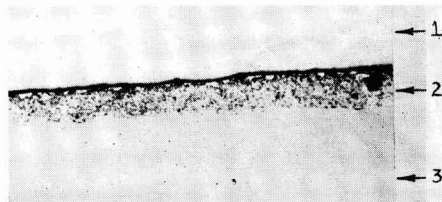


Fig. 5. Cross section of bond to Si using Mo sheet clad with Al-Si eutectic. 1, Mo sheet; 2, Al-Si eutectic; 3, Si wafer. Magnification 500X before reduction for publication.

such that wetting would not occur spontaneously, the use of a flux was indicated.

#### Wetting

By using various fluxes it was possible to obtain uniform wetting of the Al-Si-clad Mo to the Si slices with a minimum of penetration. In all cases the fluxes used were made from elements which either were acceptors in Si or were substantially inert, electronically, Lithium, for example, was avoided since it acts as a donor when introduced interstitially into Si (9). Although several fluxing agents were tried, the best results seemed to be obtained by painting the eutectic film with a dilute solution of boric acid in denatured alcohol immediately prior to assembling the wafer stack for alloying. Anhydrous ethyl sodamide was also used successfully, but its effectiveness decreased as the solution absorbed moisture from the atmosphere.

A photomicrograph of a boric acid-fluxed bond is shown in Fig. 5. The alloying was carried out at about 675°-700°C in an atmosphere of anhydrous, deoxidized N<sub>2</sub> for an alloying time of 5-10 min. At lower temperatures an apparent bond forms since the boric oxide acts as a glassy cement, but the bond can be ruptured by boiling in water for a few minutes. Bonds made in the alloying temperature range were mechanically sound, and on rupture, either the Mo was separated or the Si was pulled out of the Si wafer in the vicinity of the bond.

In making relatively large area contacts, it is desirable that the specimen should be cooled at a rate no greater than about 5°C/min. If substantially faster cooling rates are used, the differential thermal expansions of the system are sufficiently great to induce cracking in the Si wafers. Observations made at the corners of the specimens (silicon-eutectic-flux interfaces) indicate that the wetting angle has been reduced considerably in comparison with the Si-Al-gas interfaces.

These diodes did not have electrical characteristics quite as good as those shown in Fig. 1, presumably because it was not possible under the experimental conditions used to stabilize the ambient atmosphere around the junction with a hermetic seal subsequent to the time of alloying.

#### Conclusion

Wafers of p-type Si have been bonded successfully to alloy-clad Mo to form structurally sound ohmic contacts. Molybdenum has been used as the base plate material because its coefficient in linear expansion is reasonably well-matched to that of Si and introduces no deleterious elements into the p-n

<sup>3</sup> From Kassel Industries, Inc., P.O. Box 432, Englewood, N. J.

junction structure during processing. Bonding agents of pure Al or Al-Si eutectic were applied to the Mo sheet by rolling accompanied by a substantial thickness reduction to promote the formation of atomic bonds between newly formed Al-Mo interfaces. The Si bonding temperature cycle must be carried out in either an inert or reducing atmosphere. The maximum temperature is limited by the reaction of Al with the Mo, and the cooling rate is limited by the necessity for relieving stresses in the bimetallic structure without inducing fracture. When Si is added to the Al bonding material, considerably more stringent alloying conditions must be used to obtain a satisfactory bond.

#### Acknowledgments

It is a pleasure to acknowledge assistance from Mr. Carl Frosch for the diffused silicon wafers, Mr. F. G. Foster and Mr. V. K. Mehra for the photomicrographs, and Mr. D. L. Hilderley for laboratory assistance. This work was made possible in part by a grant from the Faculty Research Fund of the Horace H.

Rackham School of Graduate Studies at The University of Michigan. Another part of the work was carried out at the Bell Telephone Laboratories, Inc., Murray Hill, New Jersey.

Manuscript received Feb. 20, 1958. This paper was prepared for delivery before the Washington Meeting, May 13-16, 1957.

Any discussion of this paper will appear in a Discussion Section to be published in the June 1959 JOURNAL.

#### REFERENCES

1. M. V. Sullivan and J. H. Eigler, *This Journal*, **104**, 226 (1957).
2. D. K. Wilson, Private communication (see Footnote 1).
3. G. L. Pearson and B. Sawyer, *Proc. IRE*, **40**, 1348 (1952).
4. J. M. Goldey, Paper presented at the Washington Meeting of The Electrochem. Society, May 13-16, 1957.
5. Private communication.
6. H. W. Henkels, Private communication.
7. G. Bemski, Private communication.
8. G. Bemski, *Phys. Rev.*, **100**, 523 (1955).
9. C. S. Fuller and J. A. Ditzenberger, *ibid.*, **91**, 193 (1953).

## Electrolytic Reduction of Cyanamide

### II. The Nature of the Reduction of Cyanamide and Formamidine

Keijiro Odo, Eiichi Ichikawa, Katsujiro Shimogai, and Kiichiro Sugino

*Laboratory of Organic Electrochemistry, Department of Chemical Engineering,  
Tokyo Institute of Technology, Tokyo, Japan*

#### ABSTRACT

Two consecutive steps in the electrolytic reduction of cyanamide have different natures from the viewpoint of organic electrode process. The first step is catalytic and the second step is voltage-controlled. Therefore, the most active cathode for one step may not be the most effective for another. Tin was an effective cathode for the over-all reduction process.

In the course of the reduction of formamidine to methylamine and ammonia, the existence of methylenediamine as second intermediate was verified.

On the electrolytic reduction of cyanamide the isolation of formamidine as intermediate and the confirmation of methylamine and ammonia as final products was reported (1). In the present work, the effect of cathode materials and other electrolytic conditions on the yield of each product was studied. Also, the reduction of formamidine at various cathodes was investigated in order to clarify the over-all reduction mechanism. The results are reported here along with some unusual phenomena observed in the course of this study.

#### Experimental

The apparatus used was the same as that already described (1). However, the cell was covered in order to measure the H evolution.

Crystalline cyanamide was freshly prepared from commercial calcium cyanamide by an improved

procedure (2), and its purity was determined by the usual method (as silver cyanamide) before use.

Formamidine sulfate was prepared by the catalytic reduction of cyanamide with Pd catalyst (3), mp 156°-158°C.

*Separation of the reduction products of cyanamide.*—The separation of each product was carried out more rigidly than previously (1).

After reduction, the catholyte (about 110-120 cc) was neutralized with a small amount of H<sub>2</sub>SO<sub>4</sub> (or NH<sub>3</sub>) and diluted to 200 cc; 10 cc was used as the determination of unconverted cyanamide. The remaining part was evaporated to dryness at 50°-60°C under diminished pressure and the residue was dried for 24 hr in a vacuum-desiccator over P<sub>2</sub>O<sub>5</sub>. This was extracted twice with 50 cc isopropyl alcohol to remove unconverted cyanamide. The residue was again extracted twice with 50 cc absolute

methanol. The final residue was dried at 100°C and weighed (ammonium sulfate).

The methanol extract<sup>1</sup> was evaporated to dryness and the residue was dissolved in 100 cc water. Then, a suitable amount of picric acid (2% excess based on converted cyanamide) was added to it, the mixture was warmed to make a clear solution, and allowed to cool overnight. The precipitate was filtered off, washed with 50 cc water, and dried. Then it was purified by extraction with absolute ether to remove free picric acid, dried at 100°C, and weighed (formamidine picrate). Solubility correction was applied.

After removing the dissolved picric acid by acidification with HCl and extraction with ether, the filtrate was concentrated to 100 cc. The concentrate of isopropyl alcohol extract was added to it, and the mixture was poured into a Kjeldahl flask and heated with 20 g NaOH/50 cc water solution. Methylamine was distilled into N-HCl and the resulting solution (100 cc) was evaporated to dryness and allowed to stand in a vacuum desiccator over P<sub>2</sub>O<sub>5</sub> overnight. The residue was extracted twice with 50 cc butanol at 50°C. The butanol extract was concentrated to 10 cc and allowed to stand in an ice box. Methylamine hydrochloride crystals which separated out were filtered off, dried at 100°C, and weighed. Some methylamine hydrochloride was recovered from the mixture of the filtrate and the wash.

Determination was not carried out for nonnitrogenous hydrolytic products of intermediate compounds, such as formic acid and formaldehyde.

*Separation of the reduction products of formamidine.*—After reduction, the catholyte (110-120 cc) was neutralized with a small amount of H<sub>2</sub>SO<sub>4</sub> (or NH<sub>3</sub>), evaporated to dryness at 50°-60°C under diminished pressure, and the residue was dried for 24 hr in a vacuum desiccator over P<sub>2</sub>O<sub>5</sub>. This was refluxed twice with 50 cc absolute methanol, and the insoluble residue was filtered off from the hot solution. The residue was dried at 100°C and weighed (ammonium sulfate).

The methanol extract was worked up to separate unconverted formamidine as picrate and then to collect methylamine hydrochloride just as in the separation of the reduction products of cyanamide. However, in the case, 25 g picric acid was added with 50 cc water to 100 cc aqueous solution made from the evaporation residue of the methanol extract for the separation of unconverted formamidine.

As for nonnitrogenous hydrolytic products of starting material and the intermediate product, the determination of formaldehyde with formic acid was carried out in some cases as described later.

## Results and Discussion

### Reduction of Cyanamide

The yield of each reduction product at various cathode materials is shown in Table I.

<sup>1</sup> In the case of the reduction at Pd, the methanol extract was concentrated and allowed to cool to give formamidine sulfate. After separating these crystals, the filtrate was diluted to 100 cc with water and worked up by the same procedure.

Table I

Run No.	Cathode	Cyanamide converted		Yield				
		g	%	Formamidine picrate	%	Methylamine HCl	%	(NH <sub>4</sub> ) <sub>2</sub> SO <sub>4</sub> g
1	Sn	5.1	53	4.1	13	0.7	9	2.7
2	Pb	1.9	20	nearly zero	—	0.2	7	0.9
3	Hg	2.8	30	nearly zero	—	nearly zero	—	1.0
4	Cu	3.1	32	0.30	1.5	0	—	0.8
5	Pd black on Pd.	8.7	90	sulfate* 8.3	52	0	—	3.7
				+picrate 7.0				

\* Of the total yield of formamidine, 8.3 g was obtained as sulfate and 7.0 g was obtained as picrate.

The reduction of cyanamide occurred at all cathodes used (1). It was confirmed that Sn was an effective cathode material for over-all reduction process. Pb and Hg, which have a high H overvoltage, were not so effective in this reduction. Especially at Hg, methylamine was scarcely obtained and ammonia was the only nitrogenous product. It was noticed that formamidine was not obtained at these two cathodes. This is due to the effectiveness of these cathodes on the reduction of formamidine as described below. Cu, a low H overvoltage metal, was also an active cathode leaving a small amount of formamidine as product. Pd black cathode was seen to be very effective for the formation of formamidine. However, at Pd, methylamine could not be obtained at all.

*Current efficiency at various cathodes.*—Since several products were obtained in the reduction of cyanamide, H evolution at the cathodes was measured to observe the differences in current efficiency of the cathodes (except Hg<sup>2</sup>). The measurement was carried out at intervals of several minutes till the theoretical amount of current (6 faradays/mole) was passed. Results are shown in Fig. 1.

Palladium was the most effective from the viewpoint of current efficiency. However, even at Pd, the efficiency decreased markedly with time.<sup>3</sup> At Sn, the efficiency was not so high at the beginning, but it was maintained at about the same level. At Pb, the efficiency once reached to the same level as at Sn but it decreased greatly after 2 hr<sup>4</sup> and came down to zero after 6 hr. At Cu, the efficiency was very low and it reached to zero at the end. These observations coincided well with the results in Table I.

*Influence of pH and current density on current efficiency at tin cathode.*—The influence of pH and current density on current efficiency was then examined at the Sn cathode for a typical run. Results are shown in Fig. 2.

<sup>2</sup> At Hg, accurate measurement was difficult due to the formation of ammonium amalgam.

<sup>3</sup> This might be due to poisonous action of cyanamide on the catalytic activity of Pd.

<sup>4</sup> It may be possible that this is due to the formation of an insoluble film on the cathode surface, resulting from the action of cyanamide with lead.

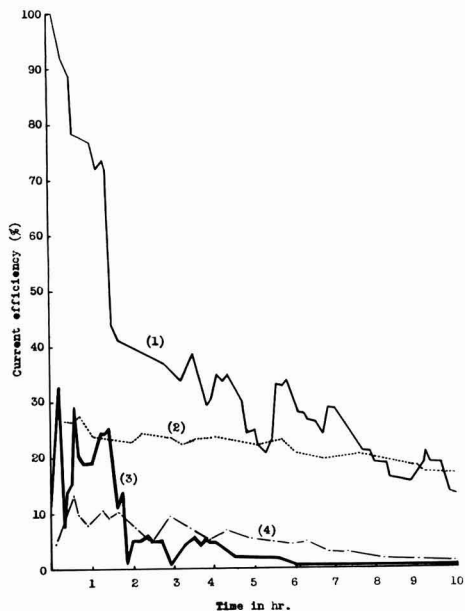


Fig. 1. Current efficiency at various cathodes (reduction of cyanamide): 1, Pd; 2, Sn; 3, Pb; 4, Cu; conditions: same as in Table I.

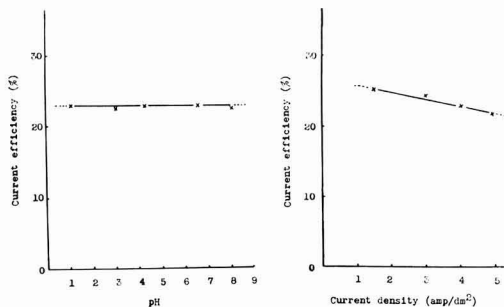


Fig. 2. Effect of pH and current density on current efficiency at Sn (reduction of cyanamide); conditions: same as in Table I.

The change of pH from 1 to 8 had no effect on the current efficiency. As for the influence of current density, the efficiency had a tendency to decrease slightly with increasing current density from 1 to 5 amp/dm<sup>2</sup>.

#### Reduction of Formamidine

The yield of each reduction product at various cathode materials is shown in Table II.

Contrary to cyanamide, the reduction of formamidine was found to occur only at cathodes having a high H overvoltage such as Sn, Pb, or Hg. The yield of methylamine based on formamidine converted was the highest at Sn, although it was relatively small. A large amount of ammonia was formed at every cathode. Especially at Hg, the largest amount of ammonia was obtained with a very small amount of methylamine. It was interesting to note that a fairly large amount (40%) of

Table II

Run No.	Cathode	Amount of current amp-hr	Formamidine unconverted %	Yield			Remarks
				Methylamine g	HCl %	(NH <sub>4</sub> ) <sub>2</sub> SO <sub>4</sub> g	
1	Sn	57.5	43	0.8	18	6.2	
2	Pb	57.5†	0	1.1	15	9.0	
3	Hg	17.3	0	0.1	2	11.0	Urotropine obtained
4	Cu	11.5	65	0	—	3.6	
5	Pd	11.5	76	0	—	1.4	

\* It is well known that formamidine is hydrolyzed very easily to give ammonia and formic acid, especially in alkaline medium.

† In the case of Pb, this amount was more than enough to convert all of the formamidine.

hexamethylenetetramine was found in the product at Hg.<sup>5</sup> This is a characteristic of a mercury cathode and led us to suppose that methylenediamine was formed in the course of this reduction.

At Pd, which has the greatest activity toward the reduction of cyanamide to formamidine, no reduction products were obtained which showed its inactivity toward formamidine. At Cu, no reduction products were also obtained as well as at Pd, but the amount of ammonia formed by hydrolysis was somewhat larger than that at Pd.

*Current efficiency at various cathodes.*—Hydrogen evolution at the cathodes (except Hg)<sup>6</sup> was measured to observe the differences in current efficiency of the cathodes on the reduction of formamidine. The variation of pH of the catholyte was measured by pH test paper at the same time because it had a great influence on current efficiency. The measurement was carried out at intervals of several minutes till the theoretical amount of current (4 frs/mole) was passed. Results are shown in Fig. 3.

Lead showed a high current efficiency at the start, but it decreased with time and reached a small value at the end.<sup>7</sup> On the other hand, at Sn, a moderate efficiency was maintained, as in the reduction of cyanamide. At Pd, at which the efficiency was the highest in the reduction of cyanamide, a definite H absorption due to the reduction was not observed. At Cu, practically zero efficiency was recorded after 1 hr. These observations coincided well with the results in Table II.

*Influence of pH on current efficiency.*<sup>8</sup>—Using a tin cathode, the influence of pH on current efficiency was studied when 17 amp-hr had passed (Fig. 4).

It was found that the current efficiency greatly decreased below pH 2. This was also observed at

<sup>5</sup> The electrolyte close to the cathode might be ammoniacal after ammonia had been formed by reduction or by hydrolysis.

<sup>6</sup> At Hg, accurate measurement was impossible due to the formation of ammonium amalgam, but H evolution could scarcely be observed during the reduction.

<sup>7</sup> This may be due to the disappearance of formamidine. It may be possible that the decomposition of formamidine is affected by current through its discharge.

<sup>8</sup> The influence of current density could not be measured due to the variation of pH with the variation of current density.

<sup>9</sup> At about this time, the variation of pH with current was relatively small.

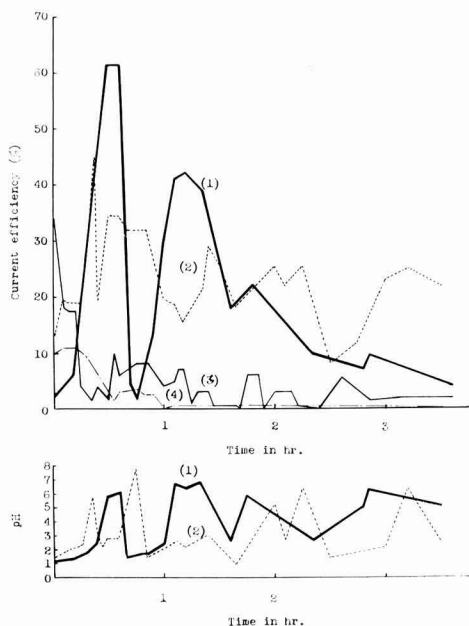


Fig. 3. Current efficiency at various cathodes (reduction of formamidine): 1, Pb; 2, Sn; 3, Pd; 4, Cu; conditions: same as in Table II.

active cathodes other than Sn, as shown in Fig. 3, and was a characteristic of formamidine reduction. This is the reason of great irregularities in current efficiency-time curves in Fig. 3.

#### Formation of Formaldehyde by Reduction of Formamidine; Indirect Confirmation of Methylene-diamine as the Intermediate

In the preceding paper, it was pointed out that in the course of the reduction of cyanamide at Sn, formamidine—the intermediate—was not only reduced to methylamine and ammonia, but hydrolyzed to ammonia and formic acid. In that case, the formation of formaldehyde was very small and barely confirmed. However, as described above, the reduction of formamidine at Hg gave a large amount of hexamethylenetetramine as follows.

Ten grams of formamidine sulfate was reduced at Hg under the same conditions as in Table II. After 13.8 amp-hr passed, the catholyte was worked up according to the procedure described above to the methanol extraction; 8.8 g ammonium sulfate was obtained. The methanol extract<sup>10</sup> was then concentrated to 30 cc under diminished pressure and allowed to stand until it reached to room temperature. Some crystals were separated (0.40 g). The filtrate was again evaporated to dryness to give further crops of the same crystals. The combined crystals were purified from methanol by dilution of a methanolic solution with ether, yield 1.0 g. The characteristic  $\text{HgCl}_2$  compound was then prepared, mp  $225^\circ\text{--}230^\circ\text{C}$  dec.

<sup>10</sup> When the methanol extract was allowed to cool, a small amount of brilliant crystals were separated. This was filtered off, washed with methanol, and dried in a desiccator. Yield 0.02 g, mp  $215^\circ\text{C}$ , plicaric mp  $185^\circ\text{--}186^\circ\text{C}$ . The identification of this compound has not yet been carried out.

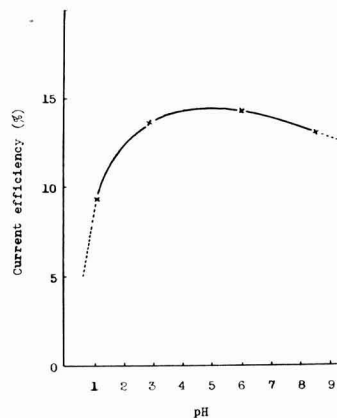


Fig. 4. Effect of pH on current efficiency at Sn (reduction of formamidine); conditions: Same as in Table II.

The isolation of hexamethylenetetramine suggested the formation of formaldehyde in the catholyte. Moreover, a small amount of formaldehyde was also recovered with formic acid from the reduction product at Pb. This may be due either (a) to the hydrolysis of methylenediamine which may be the intermediate from formamidine to methylamine and ammonia or (b) to the reduction of formic acid formed by the hydrolysis of formamidine itself. The reduction of formic acid [catholyte: 6.8 g ammonium formate in 100 cc 5%  $(\text{NH}_4)_2\text{SO}_4$ ; other conditions: the same as in Table II] was then carried out at pH 2-7 at Sn and at Hg. Hydrogen was evolved quantitatively and no products were obtained after 11.6 amp-hr of current was passed.

It may be seen, therefore, that formaldehyde was formed by the hydrolysis of methylenediamine. To confirm it, methylenediamine was prepared by the procedure of Knudsen (4) and the hydrolysis and the reduction of it were carried out.

#### Methylenediamine $2\text{HCl}$ , needle crystal

Anal. Calc'd for  $\text{CH}_6\text{N}_2\text{Cl}_2$ : N, 23.9; Cl, 59.6

Found: N, 24.0; Cl, 60.9

2.3081 g sample in 100 cc water acidified with 2 cc HCl was subjected to distillation. 0.567 g, 98% formaldehyde<sup>11</sup> was found in the distillate (50 cc) by the  $\text{Na}_2\text{SO}_3$  method. 0.648 g, 98%  $\text{NH}_3$  was recovered from the residue as usual.

This indicated the quantitative formation of formaldehyde and ammonia by hydrolysis as well as the authenticity of the sample.

Then the electrolytic reduction of methylenediamine was carried out at Sn to confirm the formation of methylamine.

After reduction, the catholyte (140 cc) was acidified with HCl and subjected to distillation to give 120 cc distillate. Further distillation of the residue with 30 cc water and 3 cc HCl gave 30 cc second distillate. Formaldehyde in the combined distillate was determined by  $\text{Na}_2\text{SO}_3$  method. The distillation residue was diluted with water and evaporated to

<sup>11</sup> Identified as dimedon derivative, mp  $187^\circ\text{--}188^\circ\text{C}$ .

Table III

Anode: Pt
Anolyte: 60 cc 5% H <sub>2</sub> SO <sub>4</sub>
Catholyte: 5.95 g methylenediamine 2HCl, 8.0 g NH <sub>4</sub> Cl, 80 cc CH <sub>3</sub> OH, 50 cc H <sub>2</sub> O (initial pH 1.2). pH* adjusted at 1-7 by adding a small amount of HCl.
Temp: 6°-8°C
Current density: 3 amp/dm <sup>2</sup>
Amount of current: 7 amp-hr†
Results: Pure methylamine HCl obtained: 0.56 g, 18% (based on methylenediamine used) mp 210°C, picrate mp 200°C; methylguanidine picrate was then prepared, mp 198°C. Formaldehyde (resulted from unconverted methylenediamine and its hydrolytic product): 0.84 g, 56%.

\* In the reduction of methylenediamine, keeping pH in a desirable range was very easy as compared with that in cyanamide or formamidinium reduction.

† The electrolysis was conducted until hydrogen began to evolve quantitatively.

dryness. The solid, after drying overnight in a vacuum-desiccator over P<sub>2</sub>O<sub>5</sub>, was extracted with 50 cc hot butanol. From the extract, methylamine hydrochloride was collected by working up as described above and weighed.

Results are shown in Table III.

5.95 g methylenediamine 2HCl was also reduced at Hg and at Pb under conditions similar to those in Table III. Although the efficiency was smaller than that at Sn, the reduction occurred to give 0.1 g and 0.15 g methylamine hydrochloride after 6.12 amp-hr and 2.68 amp-hr of current was passed, respectively.<sup>12</sup>

These results might be proofs for existing methylenediamine as the intermediate of the reduction of formamidinium.

### Polarographic Measurement<sup>13</sup>

Polarographic measurement was carried out for cyanamide and formamidinium in order to explain the results obtained by macroelectrolysis more clearly.

<sup>12</sup> In these cases, formaldehyde could not be obtained from the product. At present, this is a problem we still can not understand.

<sup>13</sup> This was carried out by T. Sekine in our laboratory.

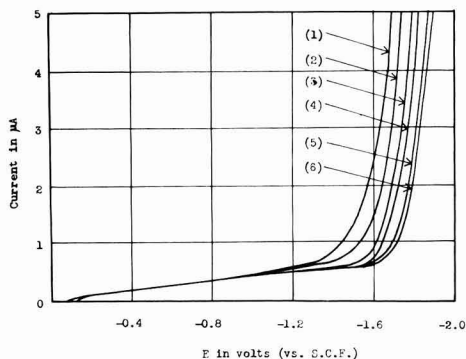


Fig. 5. Polarograms of cyanamide. Concentration of cyanamide: 1, 1.2 mole/l; 2,  $2.4 \times 10^{-1}$  mole/l; 3,  $4.8 \times 10^{-2}$  mole/l; 4,  $9.5 \times 10^{-3}$  mole/l; 5,  $1.9 \times 10^{-3}$  mole/l; 6, 0 (supporting electrolyte). Supporting electrolyte: 7.456 g KCl/1 Sorensen's phosphate buffer solution (pH 6.75); sensitivity of galvanometer:  $6.58 \times 10^{-8}$  amp/mm; dropping mercury electrode:  $m = 1.67$  mg/sec,  $t = 2.55$  sec ( $m^{2/3} t^{1/6} = 1.65$ ),  $h = 72$  cm.

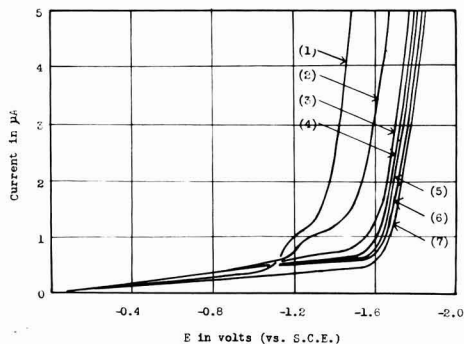


Fig. 6. Polarograms of formamidinium sulfate. Concentration of formamidinium: 1, 3.5 mole/l; 2, 1.2 mole/l; 3,  $2.4 \times 10^{-1}$  mole/l; 4,  $4.8 \times 10^{-2}$  mole/l; 5,  $9.5 \times 10^{-3}$  mole/l; 6,  $1.9 \times 10^{-3}$  mole/l; 7, 0 (supporting electrolyte). Supporting electrolyte: 7.456 g KCl/1 Sorensen's phosphate buffer solution (pH 6.75); sensitivity of galvanometer:  $6.58 \times 10^{-8}$  amp/mm; dropping mercury electrode:  $m = 1.67$  mg/sec,  $t = 2.55$  sec ( $m^{2/3} t^{1/6} = 1.65$ ),  $h = 72$  cm.

Polarograms for cyanamide and formamidinium sulfate are shown in Fig. 5 and Fig. 6.

Cyanamide: No distinct wave was detected prior to hydrogen discharge wave. The shift of H wave to a more positive potential with increasing concentration of cyanamide was observed.

Formamidinium sulfate: No wave was detected up to the concentration of  $10^{-2}$  M in Sorensen buffer (pH 6.75). However, in 1M solution, a wave appeared at  $E^{1/2}$ ,  $-1.20$  v (vs. S.C.E.). This is probably due to the reduction of undissociated molecule of formamidinium, because this wave disappeared at pH 2.2 even in 1M solutions.<sup>11</sup> The shift of H wave to a more positive potential with increasing concentration of formamidinium was also observed.

### Nature of Two Successive Reductions of Cyanamide

By combining the results of these studies, it is seen that two successive reductions of cyanamide have different natures from the viewpoint of electrochemical reduction. That is, the first step reduction is an exceptionally slow process and affected by the use of cathode material having catalytic action. On the other hand, the second step reduction may be a voltage-controlled one and affected by the use of cathode material having a high H overvoltage. Thus the most active cathode for one step may not be the most effective for another. For the over-all reduction process, Sn was the only effective cathode material among the cathodes used. This may be a problem in electro-organic reduction.

Moreover, the second step reduction was greatly influenced by pH. This is the reason for the necessity of adjusting the pH between 2-7 in order to carry out the reduction of cyanamide to the final state.

These gained support from the results of polarographic measurement.

### Conclusions

1. The reduction of cyanamide occurred at Pd smoothly to give formamidinium in a fair yield. Tin

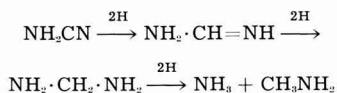
<sup>11</sup> This accounted for no occurrence of macroreduction below pH 2.

seems to have a mediocre activity toward this reduction, but the reduction could proceed beyond the formamidine level to methylamine and ammonia. Lead and mercury were not so effective for this reduction.

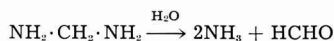
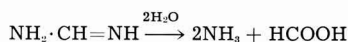
2. The reduction of formamidine, on the other hand, was effected by the use of cathodes having a high H overvoltage, such as Sn, Pb, Hg.

3. For the over-all reduction process, Sn was the only effective cathode material among the cathodes used in this study.

4. The formation of a large amount of formaldehyde at Hg suggested the existence of methylenediamine as second intermediate. This was further supported by the fact that methylenediamine gave methylamine by the reduction at Sn and other cathodes. The complete mechanism is as follows.



Main side reactions are



Low yield of the final products was seen to be due to the hydrolysis of two intermediate compounds.

Manuscript received Oct. 24, 1957. This paper was prepared for delivery before the Buffalo Meeting, Oct. 6-10, 1957.

Any discussion of this paper will appear in a Discussion Section to be published in the June 1959 JOURNAL.

#### REFERENCES

1. K. Odo and K. Sugino, *This Journal*, **104**, 160 (1957).
2. K. Odo and E. Ichikawa, "A New Method for the Preparation of Cyanamide" given at the 9th meeting of the Chemical Society of Japan (1956).
3. K. Odo, E. Ichikawa, K. Shirai, and K. Sugino, *J. Org. Chem.*, **22**, 1715 (1957).
4. P. Knudsen, *Ber.*, **47**, 2698 (1914).

## The Measurement of Magnetic Fields in Aluminum Reduction Furnaces

J. H. Kent

*Research Department, British Aluminium Company Limited, Kinlochleven,  
Argyll, Scotland*

#### ABSTRACT

The efficient operation of aluminum reduction furnaces of capacities greater than about 50 KA is affected by electromagnetic forces acting in the molten bath. Measurement of the magnetic fields which give rise to these forces is made difficult because of the high temperature and corrosive nature of the molten bath. A technique is described which overcomes these difficulties. Results are given of measurements made in the baths of furnaces operating at 100 KA with different conductor layouts. It is shown how conductor layout design affects the magnetic characteristics of the furnace.

Electromagnetic forces acting in the molten bath, i.e., both metal and electrolyte, of an aluminum reduction furnace are known to affect the performance of the furnace and reduce its current efficiency (1, 2). Particularly is this so in large furnaces operating at currents above 50 KA. Briefly, their effect is to set the bath in motion and displace the molten metal layer, thus upsetting those stable conditions which are known to be essential for efficient operation. The forces can be divided into two main categories: those that arise from the interaction between the vertical component of the current and the horizontal component of the magnetic fields in the bath, and those that arise from the interaction between the horizontal component of the current in the molten metal and the vertical and horizontal components of the magnetic fields. To reduce the effect of electromagnetic forces it is necessary to reduce as much as possible and make suitably symmetrical the magnetic fields in the bath and to re-

duce the horizontal component of the current in the metal layer. The magnetic fields can be reduced and made suitably symmetrical by various arrangements of busbars and by magnetic shielding, such as the methods devised by Elektrokemisk (3, 4). Similarly, the horizontal component of the current in the molten metal layer can be reduced by various designs of current feed and collection such as, for instance, the methods of current collection devised by Thayer (5) or Elektrokemisk (6).

An exact calculation of the magnetic fields in the bath of a furnace is made extremely difficult by saturation and temperature effects in the steel parts of a furnace and steel structures close to it. For this reason, a design based on calculations alone may fall far short of achieving minimum magnetic fields in the bath. The use of scale models such as described by Böckman (7) overcomes many of the difficulties. However having laid down an experimental furnace in the furnaceroom to a design

based on calculation, perhaps aided by measurements on a model, a knowledge of the extent to which a reduction in the magnetic fields in the bath has been achieved can be gained only by measurement. At this stage, measurements of the fields in the bath will point the way to modifications that can be tried out on an experimental scale before standardizing the design. Such measurements present formidable difficulties owing to the extremely corrosive nature of the electrolyte and the temperature of the bath which approaches  $1000^{\circ}\text{C}$ .

#### Method of Measurement

The difficulties of measuring field strength in a highly corrosive fluid at a high temperature can be overcome by using a suitably protected search coil. However, the necessary determination of field direction by the same means is far from straightforward. It was decided, therefore, to use an entirely different method to measure this quantity. A means was sought of introducing into the molten bath a soft iron needle that would first of all be free to align itself with the field direction and then set in that direction so that on removal from the bath it indicated the field direction, with respect to predetermined axes of reference, at the point at which it was placed in the bath. To achieve this, a small soft iron rod was suspended at its center in an aluminum cylinder attached to an aluminum rod (Fig. 1). The cylinder contained a synthetic resin in the liquid state. This was placed at the bottom of a graphite tube sealed at the bottom end, and alumina was packed round it to act as thermal insulation. The end of the tube containing the cylinder was then inserted under the anode of a working furnace so that the soft iron rod was freely suspended at the point at which the measurement was required and could take up the direction of the field at that point. After a predetermined time and at a predetermined temperature, the resin set hard, fixing in space the soft iron rod. The cylinder containing the rod was then removed and the field direction ob-

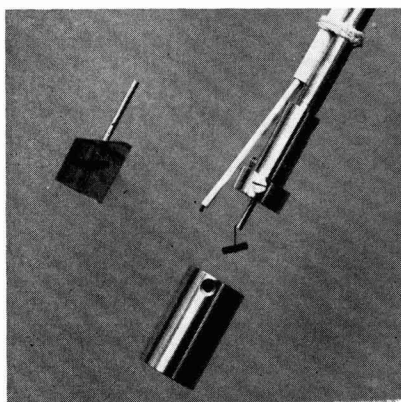


Fig. 1. Apparatus for measuring magnetic field directions in furnace baths. The suspension of the soft iron rod, its aluminum cylinder, and the rod set in the solid resin after removal from a furnace bath are shown. The thermocouple which serves to control the time of immersion in the bath is also shown.

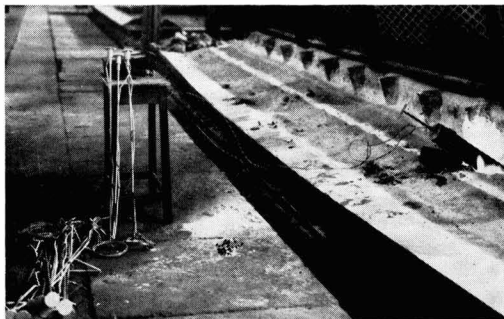


Fig. 2. Apparatus for measuring magnetic field directions in furnace baths set up beside a 100 KA furnace. To the base of the aluminum cylinders are attached asbestos disks to keep the cylinders central in the graphite tube which is shown inserted under the anode. A protected search coil is inserted into the tube to measure field strength.

tained by measuring the direction of the rod embedded in solid resin. The axis of the cylinder was used as a reference, its direction with respect to the furnace having been noted when the cylinder was in position in the furnace. Figure 1 shows the aluminum cylinder, the suspended soft iron rod and thermocouple for measuring the temperature rise. To the left is a soft iron rod set in the solid resin. Figure 2 shows the apparatus inserted under the anode of a working furnace.

The aluminum cylinder used to contain the resin is approximately 2.5 cm diameter by 4 cm deep and is bored out with a slight taper to facilitate the removal of the solid resin shape. Into the top of the lid of the cylinder is screwed an aluminum rod which protrudes from the top of the graphite tube when the cylinder is in position (Fig. 2). It has a pointer attached to it which is aligned with a mark on the cylinder. The lower end of the graphite tube is shown in Fig. 3. The rod is held centrally in the tube by a slotted Sindanyo cap fitting into the top of the tube. The resin chosen was the type that requires a catalyst and accelerator to set it. The catalyst was added some hours before the resin was required; the accelerator was stirred into the resin in the cylinder before assembling the apparatus to make a measurement. While placing the graphite tube in position in the furnace, care was taken to be sure that the tube was not making contact with the anode. When the cylinder reached the temperature at which it was known the resin would be set hard, about 3 min after insertion, the cylinder was removed and immediately placed against a current carrying busbar so that the soft iron rod would be obviously dislodged if the resin had failed to set.

Field strengths were measured in the bath with thermally insulated search coils used with a flux meter which had a full scale deflection of  $7 \times 10^5$  line turns. Two coil sizes have been found necessary to measure sufficiently accurately the range of field strengths found in the baths of furnaces ranging from about 40 KA to 100 KA. Both coils measured approximately 8 cm x 1 cm x 1 cm. One carried 350 turns and the other 200 turns of fine enamelled copper wire. Figure 3 shows the details of construction

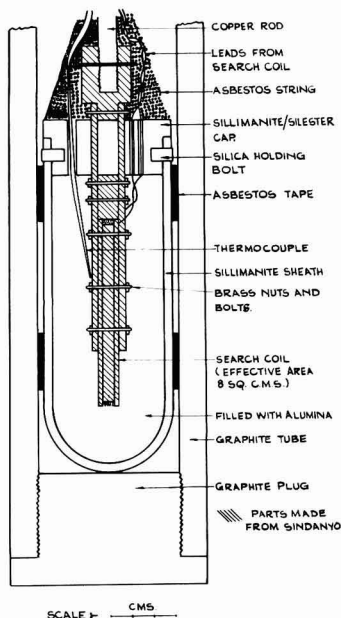


Fig. 3. Details of construction of a protected search coil

of the coils. The coil former and attachments are made of Sindanyo. A copper rod is screwed into the top of the coil assembly. The whole assembly is mounted in a ceramic cylindrical sheath packed with alumina. On rotating the copper rod about its axis the coil and its protective sheath rotate together. The sheath was made slightly smaller than the graphite tube used for holding the field direction measuring apparatus. The copper rod protrudes from the end of the graphite tube when the sheath is resting on the closed end of the tube. To make a measurement of the field strength in the bath of a furnace, the graphite tube is placed in the furnace so that the center of the coil coincides with a point at which the field direction has been measured. The coil is then rotated through  $180^\circ$  by twisting the copper rod. For the sake of accuracy it is best to find, by rapid trial and error, before making a measurement, that position of the coil with respect to its axis of rotation which gives a maximum deflection on the flux meter. This position must be noted so that the direction of the component of the field measured is known. Thus, knowing the total field direction, the total field strength can be calculated. To make rotation of the coil a simple and accurate operation, a circular scale was fitted to the copper rod. This scale fitted into the top of the graphite tube which had cut into it reference marks. The scale also served to keep the copper rod central in the graphite tube. A handle was fitted to the end of the rod protruding from the graphite tube.

The thermal insulation of the search coils described was sufficient to permit measurements to be made at several points in a furnace before having to cool the coils. For this reason, although the insulation could be improved upon, it was not found

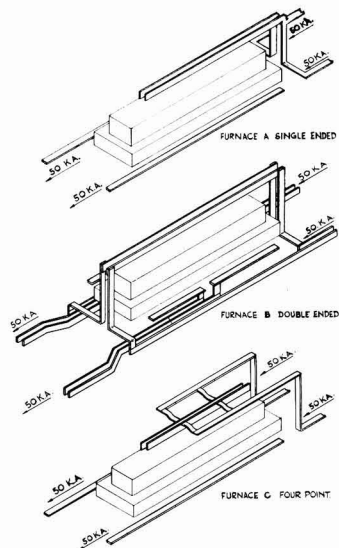


Fig. 4. Diagram of the three kinds of conductor layout of furnaces measured.

necessary to do so. The thermocouple shown in Fig. 3 was used to determine when the coil was getting too hot. A temperature of  $250^\circ\text{C}$  was found to be a suitable limit to work to. The increase in resistance of the coils did not appreciably increase the drift rate of the flux meter used.

The methods described above refer to measurements at points in the molten bath which can be reached by inserting a graphite tube under the anode. Measurements can be made on furnaces with prebaked anodes by inserting the tube from above between the anode blocks. Alternatively, in the case of Soderberg anodes, the tube can be passed down through holes in the anode. These can be made by baking in a steel tube fed from above into the soft paste so that it is gradually taken down to the working face as the anode is consumed.

#### Results Obtained on 100 KA Furnaces

The field strengths and directions have been measured in the molten baths of several designs of furnaces. Figure 5 shows some results obtained on three 100 KA furnaces with different conductor layouts. Figure 4 indicates in principle the three kinds of conductor layouts chosen. Furnace A has the current fed to the anode at one end and collected from the cathode to busbars on either side of the furnace. These busbars therefore carry tapering currents building up to 50 KA each at the end opposite to that at which the current is fed to the anode. This arrangement has been termed "single-ended." In furnace B the current is divided equally, 50 KA being fed to each end of the anode. The current is collected half way down each side of the cathode so that there is a busbar extending half way down each side of the cathode carrying 50 KA. This arrangement has been termed "double-ended." Furnace C has the same cathode arrangement as furnace A but the current is fed in equal amounts to

four points of the twin anode busbar from busbars fed from one end, positioned on either side of the anode some distance above it. The points at which the anode is fed divide the anode at the quarter and three-quarter points along its length. This arrangement has been termed "four-point."

The double-ended arrangement, with various proportions of current fed to each end, is a simple and well-known means of reducing the fields at one end of the furnace and making the fields in the bath more symmetrical. It also helps to reduce horizontal currents in the metal. The four-point arrangement was designed to improve further the symmetry of the fields in the bath and at the same time to reduce the fields at the ends of the bath which were known to be responsible for unstable working conditions. It was also designed to reduce the vertical components of the field in the bath. This latter component interacts with horizontal currents in the metal which can have a very high current density, particularly when the distribution of current in the cathode or anode is temporarily upset. By reducing the vertical component of the field, those bath conditions essential to efficient operation are less easily disturbed by temporary upsets in current distribution.

The thick arrows in Fig. 5 show the direction of field in the horizontal plane. The thin arrows are vectors representing those electromagnetic forces acting at the points of measurement which are due to the interaction between the horizontal component of the magnetic field and the vertical current. It has been assumed, when calculating these vectors, that the current distribution in the cathode and anode

is everywhere uniform and that the current is everywhere vertical. It will be appreciated that the vector picture so presented gives a general idea of the disposition of those forces due to the horizontal field and the vertical current acting in the metal layer of a furnace in good condition. This picture will be altered whenever the current distribution in the anode or cathode becomes uneven, to an extent dependent upon the degree of upset of current distribution.

It can be seen from Fig. 5 that the forces associated with the double-ended arrangement are more suitably symmetrical than those associated with the single-ended arrangement, in that they act more toward the center of the furnace, tending to confine the metal layer within the shadow of the anode. This is achieved to a slightly better degree by the four-point arrangement. The figures shown opposite to the arrows in Fig. 5 give the strength in gauss of the vertical component of the field at the points. The forces arising from the interaction between the vertical component of the magnetic field and horizontal currents cannot, of course, be calculated without a knowledge of the horizontal currents. It should be stressed that these latter forces will only seriously upset furnace conditions and hence affect performance when there are large horizontal currents in the metal due to uneven current distribution in the anode or cathode. Such cur-

Table I\*

Busbar arrangement	Point of measurement	H (gauss)	F (gauss)	$\theta^\circ$
Single-ended	a	178 (101)	186	17
	b	166 (101)	166	0
	c	58 (86)	64	24
	d	73 (70)	78	20
	e	54 (58)	54	5
	f	42 (37)	44	17
	g	63 (37)	63	0
	h	69 (58)	74	22
	i	64 (70)	81	38
	j	49 (86)	66	42
Double-ended	a	106 (65)	115	22
	b	98 (65)	99	10
	c	69 (60)	76	25
	d	68 (56)	69	6
	e	79 (60)	79	3
	f	107 (65)	124	30
	g	113 (65)	113	0
	h	96 (60)	96	0
	i	92 (56)	97	17
	j	67 (60)	73	27
Four-point	a	74	74	0
	b	67	67	8
	c	85	85	6
	d	96	96	0
	e	94	94	2
	f	51	51	4
	g	56	58	16
	h	69	70	10
	i	76	81	20
	j	62	62	10

\* Field strengths are given to the nearest whole number and therefore in some cases small values of  $\theta$  do not show a difference between the horizontal (H) and total (F) field but the corresponding vertical component is given in Fig. 5. The numbers in parenthesis are calculated horizontal field strengths.

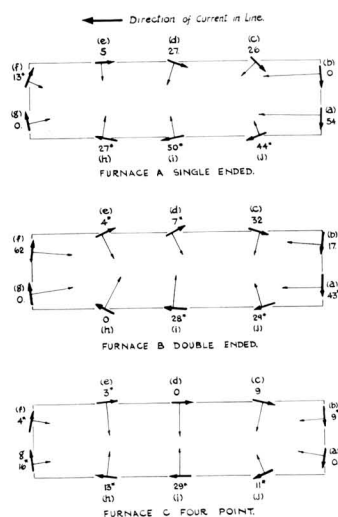


Fig. 5. Magnetic field measurements made beneath the edge of the anode in the molten metal layers of the three kinds of 100 KA furnaces shown in Fig. 4. The numbers represent the vertical components of the field in gauss. Where there is a \* the conventional direction of this component is out of the paper (or upward in the furnace). Heavy arrows represent field direction in the horizontal plane; thin arrows are vectors representing those electromagnetic forces acting horizontally in the molten metal, which are due to the interaction between the horizontal field and the vertical current.

rents are not predictable and therefore a general pattern of the forces cannot be obtained. However, it can be seen that it is of great importance to reduce as much as possible the vertical component of the magnetic fields. It will be noticed that the four-point arrangement achieves a reduction in this component.

Table I completes the information by giving the strength in gauss of the total field  $F$  and the horizontal component  $H$  measured at the points indicated in Fig. 5. The angle  $\theta$  that the field makes with the horizontal at these points is also given. All the points of measurement shown are in the molten metal layer just inside the edge of the anode. For comparison, the calculated horizontal components of the magnetic field at the points of measurement are given for the single-ended and double-ended furnaces. These values are shown in parentheses next to the measured values. The calculations were made by the usual method for fields due to finite conductors, taking into account tapering currents where applicable. Allowance was made in the calculations for the screening effect of the furnace box based on measurements made on empty furnace sites with and without the furnace box in position.

A lack of symmetry of the measured fields about the longitudinal axis will be noticed in each furnace. This is due to adjacent lines of furnaces and to the disposition of nearby steel structures. This asymmetry emphasizes the need for measurements of fields made in the baths of furnaces that have been designed to achieve certain reductions and modifications of the magnetic field characteristics in

the bath. The results for the four-point arrangement, for example, point the way to further improvements in design which it would have been impossible to foresee by calculation and the need for which arises out of local conditions peculiar to the particular layout of the furnaceroom. It is of interest to note that the four-point arrangement did in fact show the expected improvement in the stability of operating conditions.

#### Acknowledgments

The author gratefully acknowledges the cooperation of colleagues in the research laboratories and factories of The British Aluminium Co. Ltd.

Manuscript received March 17, 1958. This paper was prepared for delivery before the New York Meeting, April 27-May 1, 1958.

Any discussion of this paper will appear in a Discussion Section to be published in the June 1959 JOURNAL.

#### REFERENCES

1. R. Jötten, *Aluminio*, **22**, 751 (1953).
2. J. Wleügel, *ibid.*, **22**, 759 (1953).
3. Elektrokemisk A/S, British Pat. 740,025 Nov. 9, 1955.
4. Elektrokemisk A/S, British Pat. 754,697 Aug. 8, 1956.
5. C. S. Thayer (To Aluminum Company of America), Canadian Pat. 517,514 Oct. 18, 1955.
6. Elektrokemisk A/S, British Pat. 740,063 Nov. 9, 1955.
7. O. C. Böckman, "The Use of Scale Models for Investigating the Effect of Steel Parts on Magnetic Fields in Large Aluminium Furnaces," *Rapports presentes au Congres International de l'Aluminium Paris 1954*, p. 151 (La Societe Chimique de France et de l'Aluminium Francais).

## Destruction of Cyanide Wastes by Electrolytic Chlorination

J. T. Byrne, W. S. Turnley, and A. K. Williams

*The Dow Chemical Company, Rocky Flats Plant, Denver, Colorado*

#### ABSTRACT

By combining the principles of the well-known processes of alkaline chlorination and electrolytic oxidation it has been demonstrated that it is possible to obtain more effective treatment of concentrated cyanide wastes. Rock salt is added to the waste solution and hypochlorite is produced by electrolysis in the solution. Complete destruction of cyanide and destruction of most of the cyanate formed results at the rate of about 0.1 lb cyanide/kwhr. Plating metals can be recovered by cathodic deposition. During the course of the electrolysis, the discharge of cadmium ions at the cathode results in a lowering of the pH until the optimum value for cyanate oxidation is reached. Safety hazards are minimized since there is never more than a slight excess of chlorine present. A graphite anode can be used with no overvoltage problems and with a long life expectancy.

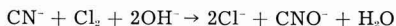
A number of methods for treating cyanide wastes from metal finishing operations have been described (1, 2). When the water supply is not adequate for dilution and ventilation limitations do not permit volatilization of hydrogen cyanide, the most widely used methods appear to be chlorination and electrolytic oxidation.

Chlorination is accomplished (3) either by the addition of chlorine gas or of hypochlorites to the

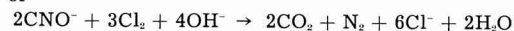
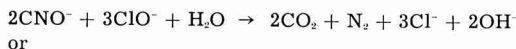
waste stream. The first stage of the destruction proceeds rapidly by the reaction



or



The second stage involving the oxidation of cyanate to carbon dioxide and nitrogen is considerably slower



The stoichiometric reagent requirements are 2.73 parts of chlorine and 3.08 parts of sodium hydroxide per part of cyanide for the first stage and an additional 4.09 parts of chlorine and 3.08 parts of sodium hydroxide per part of cyanide for the second stage. In practice, at least 10% excess reagents are added to speed the reactions.

Either sodium hypochlorite or calcium hypochlorite could be used instead of chlorine gas for this process, but these must be added as solutions. An excessive sludge of calcium hydroxide forms when solid calcium hypochlorite is used. In cadmium cyanide solutions, the cadmium is precipitated as a carbonate sludge if either sodium or calcium hypochlorite solution is used. The alkaline chlorination process is rapid and it successfully reduces the cyanide concentration to below 1 ppm.

Electrolytic oxidation of cyanide has been attributed (4) principally to oxidation by the oxygen liberated at the anode. The method produces no sludge and plating metals can be recovered on the cathode. Available operating data are meager, but it appears that the oxidation of cyanide to cyanate takes place at the rate of about 0.3 lb/kwhr using carbon steel electrodes (5). Selection of the anode presents a problem since steel and nickel are attacked by cyanide, and graphite has a high overvoltage for oxygen evolution. The method suffers the additional disadvantage (6) that it does not result in complete destruction of the cyanide and apparently does not destroy cyanate at all.

Despite the wide use of alkaline chlorination and of electrolytic oxidation, no mention has been made of the combination of the principles of these two methods to produce a treatment combining the advantages of each.

### Experimental

**Apparatus.**—The laboratory experiments were carried out using a battery charger for the source and powerstat for control of the applied voltage. In the plant experiments (runs 4 and 5, Table I) a 150-amp full wave rectifier was used.

A graphite anode rod and a graphite, cadmium, or iron cathode rod were spaced about  $\frac{1}{4}$  in. apart. The Pyrex electrolysis beaker was equipped with a peripheral cooling coil which maintained the temperature of the solution at 40°–50°C during most of the electrolysis. All runs were stirred thoroughly during electrolysis. The plant experiments (runs 4 and 5) were run without cooling, and the temperature reached about 80°C.

**Procedure.**—Prior to electrolysis, each solution was analyzed for cyanide with a p-dimethylaminobenzalrhodanine indicator (7), and for cadmium using a polarographic method. The solutions were saturated with sodium chloride by adding rock salt, and the electrolyses were carried out at the specified voltage and current. During the electrolyses, samples were taken for cadmium, cyanide, and cyanate analyses. The cyanate analyses were performed (8) by decomposing the cyanate into am-

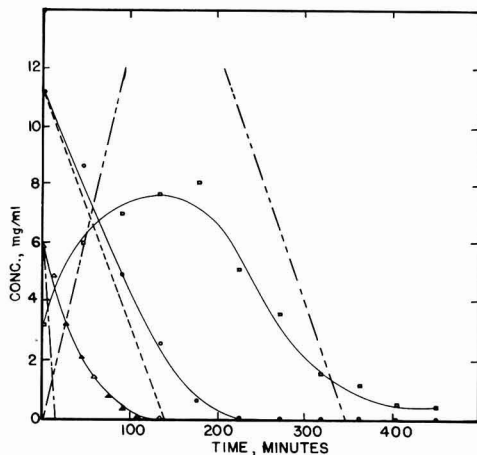


Fig. 1. Removal of cyanide, cyanate, and cadmium from plating solution during electrolytic generation of hypochlorite at 4 amp, 4.25 v, Run No. 9. O mg  $\text{CN}^-/\text{ml}$  (exp); □ mg  $\text{CNO}^-/\text{ml}$  (exp); Δ mg  $\text{Cd}^{++}/\text{ml}$  (exp); - - - - - mg  $\text{CN}^-/\text{ml}$  (theor. at 100% current eff.); - - - - - mg  $\text{CNO}^-/\text{ml}$  (theor. at 100% current eff.); - - - - - mg  $\text{Cd}^{++}/\text{ml}$  (theor. at 100% current eff.).

monia during a Kjeldahl digestion, distilling the ammonia, and developing color with Nessler's reagent.

**Results.**—The results of all electrolyses for which data are available are shown in Table I. Detailed studies of runs 9 and 10 were made by sampling the solution at 45-min intervals and analyzing for cyanide, cyanate, and cadmium. Results are plotted in Fig. 1. These curves show the ultimate removal of the cyanide, cyanate, and cadmium from the solution.

Cadmium proved to be the most satisfactory cathode material. When graphite was used (run No. 1), the cadmium deposit did not adhere to the cathode. When iron was used, the solution became contaminated with ferrocyanide which interfered with the cyanide analysis. Uniform and adherent deposits of cadmium were obtained in runs 4 to 11.

Current densities ranged from 72 to 470 amp/ft<sup>2</sup> as shown by the areas and currents listed in Table I.

Measurements of pH during run 9 showed a decrease from 10.9 at the start to 9.1 after 3.5 hr. The pH remained between 8.9 and 9.1 for the remaining 4 hr. The initial decrease is due to the consumption of two equivalents of hydroxyl ion per mole of chlorine in the oxidation of an equivalent of cyanide to cyanate. This is only partially compensated by the production of hydroxyl ions at the cathode, since one-third of an equivalent of cadmium is reduced per equivalent of cyanide. Qualitative confirmation of this explanation was obtained from a titration curve of the plating solution which showed a pH of 8.8 in a buffer region after sulfuric acid, in an amount equivalent to the cadmium, had been added.

During the oxidation of one equivalent of cyanate to carbon dioxide and nitrogen, 4/3 equivalents of hydroxyl ion are required per mole of chlorine. This would tend to lower the pH further if the cyanate oxidation were not so slow that an appreciable ex-

Table I. Effect of cell conditions on electrolytic chlorination of cyanide

Run No.	Volume (ml)	Initial CN- (ppm)	Final CN- (ppm)	Time (hr)	Electrode area (in. <sup>2</sup> )	Cathode	Amp	Volt
1	300	1800	10	1.5	2	Graphite	1	—
2	300	1800	12	0.75	2	Iron	4	—
3	300	1800	16	0.25	2	Iron	5	—
4	2000	55,000	254	7	44	Cadmium	140	9-10
5a	8000	55,000	8000	2	44	Cadmium	80-150	10-11
b	8000	55,000	4200	5	44	Cadmium	80-150	10-11
6	35	55,000	17	3	2	Cadmium	4	4-4.5
7	35	55,000	38	2	3	Cadmium	4	4-4.5
8	35	55,000	32	3	6	Cadmium	4	4-4.5
9	400	11,050	<5	8	3	Cadmium	4	4-4.5
10	400	8690	<5	7.5	3	Cadmium	4	4-4.5

cess of chlorine (and hydroxyl) is produced at the electrode. These pH changes keep the system close to the recommended ranges of 10-12.5 for the oxidation of cyanide and 7.5-9 for the oxidation of cyanate (3).

### Discussion

*Power.*—Commercial hypochlorite cells produce about 0.34 lb (3 eq.) of ClO<sup>-</sup>/kwhr, while commercial chlorine cells achieve a production of about 0.8 lb (5 eq.) of Cl<sub>2</sub>/kwhr (8). In the chlorine cell the product is continuously taken off as gaseous chlorine, but in the hypochlorite cell the product is held in the form of soluble hypochlorite and the yield is diminished by side reactions.

The oxidation of 1 lb of cyanide to cyanate requires 2.73 lb of chlorine, and the oxidation of the cyanate formed requires an additional 4.09 lb of chlorine. Therefore, if all the chlorine produced in a chlorine cell were used for reaction with cyanide, it would be possible to convert 0.29 lb of cyanide to cyanate per kwhr and to completely destroy 0.12 lb/kwhr.

Within the uncertainty of the current measurement, both runs 9 and 10 proceeded at the rate of 0.08-0.10 lb of cyanide destroyed per kwhr for the first 5 hr. The last stages of cyanate decomposition proceeded much more slowly. The toxicity of cyanate is reported (2) to be some 1000 times less than that of cyanide and so, in most cases, essentially complete destruction of cyanide and 90%, or less, destruction of cyanate would be sufficient.

*Cell design.*—As in the commercial production of hypochlorite and chlorine, the most satisfactory anode material is graphite. If a plating metal is to be recovered on the cathode, any material that accepts a good plate of the plating metal can be used for a cathode.

The electrodes should be arranged to give a minimum anode-cathode spacing, e.g., 1/4 to 1/2 in. is de-

sirable. With this spacing it should be possible to produce 1000-2000 amp by applying 3.5 to 4.5 v/cell with a current density of 100-500 amp/ft<sup>2</sup>. The current density must be selected to produce an adherent cathode deposit of recoverable metal.

Each cell requires stirring and an operating temperature between 40° and 50°C. Higher temperatures favor the formation of chlorate rather than hypochlorite.

Ventilation is necessary to prevent the accumulation of hydrogen and to remove small amounts of toxic gases such as chlorine, cyanogen chloride, and hydrogen cyanide.

### Acknowledgment

The authors wish to thank L. C. Farrell and R. W. Hawley for their continued interest and encouragement.

This work was done under AEC Contract No. AT(29-1)-1106.

Manuscript received Sept. 27, 1957.

Any discussion of this paper will appear in a Discussion Section to be published in the June 1959 JOURNAL.

### REFERENCES

- Ohio River Valley Water Sanitation Committee, "Methods for Treating Metal-Finishing Wastes," January 1953.
- B. F. Dodge and D. C. Reams, American Electroplaters Society Research Report Serial No. 14 (1949).
- B. F. Dodge and W. Zabban, American Electroplaters Society Research Report Serial No. 22 (1952).
- G. H. Clevenger and M. L. Hall, *Trans. Am. Electrochem. Soc.*, **24**, 271 (1913).
- L. B. Sperry and M. N. Caldwell, *Plating*, **36**, 343, 412 (1949).
- R. W. Oyler, *ibid.*, **36**, 341 (1949).
- B. F. Dodge, W. Zabban, E. J. Serfass, and R. B. Freeman, American Electroplaters Society Research Report Serial No. 19 (1952).
- H. J. Creighton and W. A. Koehler, "Principles and Applications of Electrochemistry, Vol. II, Applications," 2nd ed., p. 275, John Wiley & Sons, Inc., New York (1944).



## Reaction of Hydrogen with Uranium

W. M. Albrecht and M. W. Mallett

*Ferrous Metallurgy Division, Battelle Memorial Institute, Columbus, Ohio*

In our paper, "Reaction of Hydrogen with Uranium," published in the July 1956 JOURNAL, pp. 404-409, certain apparent anomalies exist in the kinetics data. The following discussion may be considered an addendum to that paper. It will be noted in Fig. 6 of our paper that for each nominal pressure series the total system pressure actually was increased experimentally for runs above 250°C. In spite of this, the reaction rates decreased with increasing temperature.

It is stated in the paper that the significance of the pressure dependency of the reaction is not known. Also, it is implied that consideration of the dissociation pressure of the hydride product is important to the interpretation of the rate data. Further work with other metal-hydride systems has emphasized the great need for interpretive studies of reactions where the reaction rates are a function of both pressure and product composition. In view of this, the basic premises of kinetic studies were reviewed.

In the simplest and most often encountered case of the oxidation of metals, the kinetics of formation of a saturated phase on the metal surface is determined. Characteristic of this phase is its very low dissociation pressure, often  $<10^{-6}$  mm Hg. In manometric systems where the limit of measurement is of the order of 0.1 mm Hg, such pressures are undetectable. Under these circumstances, the composition of the reaction product (if only one is formed) is constant under all experimental conditions of pressure.

In contrast with this, we have the metal hydrides which have comparatively high dissociation pressures of several millimeters of Hg or several atmospheres, depending on the hydride and the temperature. Thus, unless the system pressure equals or exceeds the dissociation pressure, the desired (saturated) reaction product is not formed. An additional complication is that many of the metal-hydride systems show wide solid-solubility regions of metal dissolved in a terminal hydride phase. In such systems, reactions carried out at constant system pressures yield products which vary in composition with temperature. Therefore, the kinetic data obtained in this manner show no recognizable relationship. However, orderly data should result if, first, the composition of the surface product (solid solution) is fixed. Then, the experiments are carried out at

system pressures corresponding to the dissociation pressures of the selected product at the experimental temperatures. If experiments are carried out in this manner for several product compositions, the effect of the composition variable may be evaluated.

In the study of hydrogen and uranium, the effect of pressure on the reaction was investigated but no attempt was made to determine the effect of the composition variable on the reaction. In the range 100° to about 250°C, the reaction rate depended on  $(p_{H_2})^{3/4}$ . This experimental value agrees fairly well with the theoretical value of  $(p_{H_2})^{2/3}$  for the dissociation of  $UH_3$ . Using these data and extrapolated equilibria data from the study of Gibb, *et al.* (1), calculations have been made to determine the variation of the reaction rates with temperature of certain compositions of uranium hydride. Constants for interpolated pressure equations are given in Table V.

The isopleths described by the values in Table V are plotted in Fig. 9 with the experimental rate data. An activation energy of 8600 cal/mole was obtained for the formation of  $UH_{2.900}$ . A similar energy was obtained for  $UH_{2.901}$ . Fortunately, in all cases, two or three rate values were obtained at temperature and pressure values close to those specified by an isopleth equation. The isopleths are divergent in

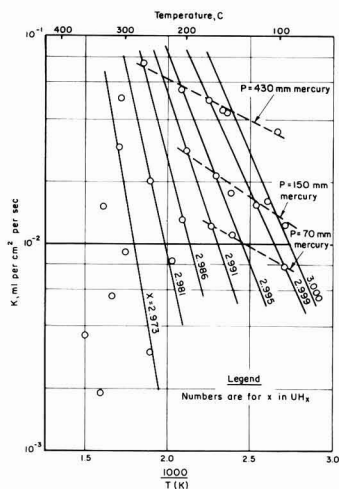


Fig. 9. Kinetics of reaction to produce constant compositions of  $UH_x$ .

Table V. Pressure equations for  $\text{UH}_{2.97}$  to  $\text{UH}_{3.0}$ 

Values of A and B for equation, $\log_{10}P_{\text{atm}} = (-A/T) + B$		
x in $\text{UH}_x$	A	B
2.973	3710	6.11
2.981	3340	5.70
2.986	3030	5.36
2.991	2660	4.96
2.995	2310	4.56
2.999	1860	4.02
3.000	1730	3.90

agreement with the data of Gibb. It is recognized that the long extrapolation from the high-pressure

data of Gibb may introduce some error to this treatment. However, there appears to be no mistaking the indication that the planning and interpretation of kinetic studies of reactions producing solid solutions should be based on exact knowledge of the temperature-pressure-composition equilibria of the product involved.

Manuscript received June 16, 1958.

Any discussion of this paper will appear in a Discussion Section to be published in the June 1959 JOURNAL.

#### REFERENCE

1. T. R. P. Gibb, J. J. McSharry, and H. W. Kruschwitz, Jr., *J. Am. Chem. Soc.*, **74**, 6203 (1952).

### June 1959 Discussion Section

A Discussion Section, covering papers published in the July-December 1958 JOURNALS, is scheduled for publication in the June 1959 issue. Any discussion which did not reach the Editor in time for inclusion in the December 1958 Discussion Section will be included in the June 1959 issue.

Those who plan to contribute remarks for this Discussion Section should submit their comments or questions in triplicate to the Managing Editor of the JOURNAL, 1860 Broadway, New York 23, N. Y., *not later than March 2, 1959*. All discussion will be forwarded to the author, or authors, for reply before being printed in the JOURNAL.

# FUTURE MEETINGS OF The Electrochemical Society



**Philadelphia, Pa., May 3, 4, 5, 6, and 7, 1959**

**Headquarters at the Sheraton Hotel**

Sessions probably will be scheduled on

**Electric Insulation, Electronics (including Luminescence  
and Semiconductors), Electrothermics and Metallurgy**

(including a Projected Symposium on "Mechanical Properties of Intermetallic Compounds"),

**Industrial Electrolytics, and Theoretical Electrochemistry**

★ ★ ★

**Columbus, Ohio, October 18, 19, 20, 21, and 22, 1959**

**Headquarters at the Deshler-Hilton Hotel**

★ ★ ★

**Chicago, Ill., May 1, 2, 3, 4, and 5, 1960**

**Headquarters at the Lasalle Hotel**

★ ★ ★

**Houston, Texas, October 9, 10, 11, 12, and 13, 1960**

**Headquarters at the Shamrock Hotel**

★ ★ ★

Papers are now being solicited for the meeting to be held in Philadelphia, Pa., May 3-7, 1959. Triplicate copies of each abstract (*not exceeding 75 words in length*) are due at Society Headquarters, 1860 Broadway, New York 23, N. Y., *not later than January 2, 1959* in order to be included in the program. *Please indicate on abstract for which Division's symposium the paper is to be scheduled, and underline the name of the author who will present the paper.* Complete manuscripts should be sent in triplicate to the Managing Editor of the JOURNAL at 1860 Broadway, New York 23, N. Y.



## Report on the Second Congress of the European Corrosion Federation, Frankfurt, June 5-8, 1958

R. Bakish

Ciba Limited, Basle, Switzerland

The second European Corrosion Congress held in Frankfurt from the 5th to the 8th of June 1958 was part of the European Chemical Engineering Congress, which takes place every three years. The theme of the Congress was "Corrosion and Chemistry."

The European Corrosion Federation consists of 51 member professional organizations. While all these organizations contributed to the conference, the Deutsche Bunsengesellschaft für Physikalische Chemie and the Gesellschaft für Deutsche Chemiker, both situated in Frankfurt a. Main, carried out all preparations and conducted the various meetings.

Participation in the conference included people from all over the world, including almost all European countries, the Soviet satellites and a fairly large Soviet delegation, and the U. S.

The conference consisted of six plenary lectures, which were read with simultaneous translations in English, German, and French, and a long list of discussion lectures, presented in either English, German, or French without translation. There were no papers presented from the Soviet Union. The conference was held in a spirit of a United Europe and in the program itself the speaker was identified only with his city of origin with no mention of the State from which he came. After the formal opening of the conference by Professor H. Fischer from Karlsruhe, the first plenary lecture was presented by Dr. G. H. Cartledge of Oak Ridge.

All papers presented at these meetings will eventually be published in the German publication *Werkstoffe und Korrosion* or possibly in the form of a monograph.

For additional information on the papers, one should write to either Deutsche Bunsengesellschaft für Physikalische Chemie or to Gesellschaft für Deutsche Chemiker, both in Frankfurt a. Main, stating the exact matter of interest.

### Papers, Authors, and Abstracts

#### Chemical and Electrochemical Aspects of Reactor Corrosion

G. H. Cartledge, Oak Ridge

A brief review of the complex reactor technology corrosion problems was followed by an analysis of variables in reactor problems. Next, a detailed analysis of the corrosion problem in the heavy water uranyl sulfate reactor was presented.

#### The Importance of the Physical Properties of the Soil in Connection with the Reaction Mechanism of Corrosion of Iron in It

T. Marcovic, Zagreb

A detailed analysis of the reaction system iron-soil was presented. The role of the physical variables of the soil, as well as chemical changes which take place in the course of the corrosion process, were analyzed. Experi-

ments using glass balls of various sizes to represent soil particles were also reported and it was demonstrated that these particles determine the distribution of anodic and cathodic areas.

#### Discussion Lectures on Corrosion Types and Causes

##### A Discussion on the Question of the Kinetics of Metal Corrosion

I. Sekerka, Prague

Corrosion experiments showing the dependence of corrosion or solution of metals on the concentration of corrosion agent, temperature of exposure, and time of exposure were presented. Results from experiments conducted on Cu, Fe, Al, and Zn in HNO<sub>3</sub>, H<sub>2</sub>SO<sub>4</sub>, and NH<sub>4</sub>OH (1N, 0.5, 0.05, 0.01 solutions) at 30°, 40°, 60°, and 80°C were reported.

##### The Electrochemical Behavior of Electrodes and the Interpretation of Polarization Curves in the Study of the Corrosion of Metals

G. Bianchi, Modena

Experiments demonstrating the use of balancing external currents to determine strength, origin, and growth of corrosion currents were reported.

##### Nature of the Thinnest Oxide Layers on Metals

L. Vlasakova, Prague

Data on the thickness of naturally formed oxide layers, as well as bonding strengths with the parent metal obtained by optical methods, were presented.

##### The Cause of Stress Corrosion Susceptibility in Nonferrous Metals and Steels

L. Graf, Stuttgart

Experimental as well as theoretical bases for a new approach to the stress corrosion cracking problem, which interprets the stress cracking behavior of ferrous alloys on the basis of active and passive cells and that of nonferrous alloys on the basis of a new so-called solid solution effect, were presented.

##### Studies of Corrosion Products and Protective Layers by Electrophoresis

J. H. Frasch, Paris

A new approach utilizing electrophoretic processes for measuring and following corrosion processes was presented. Visual observation is sufficient to follow corrosion processes when colored corrosion products are present, but suitable reagents which can develop colors are needed for studies where the corrosion products are colorless.

##### Contact Corrosion between Different Structural Materials

F. Podbrenznik, Belgrade

A study of contact corrosion investigating interface effects between wood/metal, paper/metal and glass/metal plastic was presented.

##### Investigation of the Problem of Pitting Corrosion in High-Alloy Austenitic Chromium Nickel Steels

G. Pier, Duisburg

Results of an investigation of 18/8 Ti stabilized; 18/10; 18/10 + 2 Mo and 18/10 + 2 M<sub>2</sub> Ti stabilized were reported. Polarization curves, potential measurements, pitting tests with K<sub>4</sub>[F(CN<sub>6</sub>)]<sup>-</sup> were used to demonstrate

the connection between active and passive cells and the need of a certain  $\text{Cl}^-$  concentration as reason for pitting corrosion.

*Discussion Section on Corrosion of Chemical Processing Equipment*

**The Corrosion of Titanium**

W. Fischer, Essen

A survey of the reactions of Ti under different conditions was presented.

**Cast Iron in the Construction of Equipment for the Chemical Industry**  
P. van de Forst, Duisburg

Properties of unalloyed and alloyed cast irons protected and unprotected by enameling and new applications of gray cast iron were presented.

**Steels for Containing Hydrogen and Synthetic Hydrocarbons**

V. Cihal, Prague

Data on low alloy steels resistant to hydrogen embrittlement up to 1000 atm pressure and 590°C were presented.

**The Corrosion of Mild Steel in Gas Streams**

A. J. Macnab, Manchester

Data on behavior of mild steel subjected to corrosion under wet and dry conditions in gases containing  $\text{SO}_2$  at different temperatures and for different duration were presented.

**The Corrosion Behavior of Pipelines Carrying High-Sulfur Crude Oils in Refinery Installations**

P. Csokan, Budapest

Steel pipelines for sulfur-rich crude oils show appreciable corrosion which can be interpreted by means of diffusion effects.

**High-Temperature Corrosion by Sulfur Compounds in Petroleum Processing**

W. G. Richards, Sunbury on Thames

A report of investigation of the intercrystalline corrosion caused by  $\text{H}_2\text{S}$  containing gases in 18/8 and the possibilities of the occurrence of stress corrosion cracking under these conditions were presented.

**Tubes from Duroplast**

G. Lorentz, Frankfurt a. Main

A comparative study of behavior of duroplast tubes, as well as tubes made of thermoplastic materials, earthenware, and impregnated graphite, was reported.

**Stress Corrosion Cracking of Metals and Alloys**

T. P. Hoar, Cambridge

After a historical review of the problem, recent experimental work on 18/8 at Cambridge was described. Corrosive medium used was 42%  $\text{MgCl}_2$ , and testing temperature, 150°C. Electrochemical measurements including polarization data were presented and the role of stress and crack formation studied. A 1-5 mm/hr crack propagation speed was established. On the assumption of a dimension at a crack tip of 10-1000 Å, current densities of  $10^{-2}$ - $10^{-1}$  amp/cm<sup>2</sup> at the sides of the crack and 1 amp/cm<sup>2</sup> at the tip of the crack were derived. The efficiency of cathodic protection was demonstrated and suitable potentials stated.

**Corrosion and Passivity**

U. Frank, Darmstadt

Reviewed existing theories and historical developments in the field. Discussed the passivation potential and showed the independence of passivation emf on the nature of the corrosive substance at a given pH. Passivity is limited to metals containing electron-conducting surface layers.

*Discussion Section on Inhibitors, Passivators, and Surface Films*

**New Researches on the Adsorption of Hydrogen in the Process of Dissolution of Iron**

L. Cavallaro, G. P. Bolognesi, and L. Felloni, Ferrara

The relation between adsorption and dissolution of Armco steels in 1N HCl was investigated. The transition of a proton to molecular hydrogen and the role of inhibitors in the process were also discussed.

**Electrochemical Investigations in the Mechanism of Inhibition with Organic Reagents**

H. Fischer, Karlsruhe

The determination of the primary and secondary inhibition effect in the different current density ranges of the polarization curves of an iron cathode in HCl was reported.

**Electrochemical Measurements on Inhibition of the Corrosion of Iron in Water Solutions**

H. Kaeche, Berlin-Schönberg

The determination of the speed of corrosion of Fe as it depends on the phenylthiocarbamide concentration through the extrapolation of the partial current potential curves to the steady-state potential was discussed.

**Developments in Cooling Tower System Treatments—Polyvalent Ion Phosphate Inhibitors**

M. Maraghini, Rome

Polyphosphates with small additions of ferrocyanide and other iron salts were shown to have increased inhibition effect on corrosion reactions.

**New Researches in the Field of Vapor Phase Corrosion Inhibitors**

L. Cavallaro and G. Mantovani, Ferrara

It was shown that vapor-phase inhibitors for cast iron must come in contact with the metal surface and also be in sufficient quantities. Good results are obtained when the vapor-saturated layer is in contact with surfaces.

**The Passivation of Zinc in 1,1 Dimethylethanolchromate in the Gas-Phase**

L. Cervený, Prague

It was shown that Zn handled with this material has a better corrosion resistance than Zn handled with chromates. The partial pressure of the chromate determines the passivating velocity.

*Plastics, Lacquers, and Paints*

**Protection Properties of Polyamide Coatings in Acid and Alkali Environments**

B. Dolezel, Prague

It was shown that, due to hydrolysis and permeability to acids, polyamide coatings are unsuitable for protection from acids but good for alkali.

**Contributions of Neoprene Foils for the Protection of Apparatus for the Chemical Industry**

H. Tixier, Dublin

Results from application of vulcanized neoprene layers for corrosion protection were given. Different examples of utilization were stated.

**Corrosion Protection of Metals through Coatings Applied by Immersion in Fluidized Beds and Flame Spraying**

E. Gemmer, Frankfurt a. Main

**Ion Transfer through Paint Films**

K. Barton, E. Beranek, and D. Cermakova, Prague

Donnan-equilibrium values and membrane potentials were measured for painted films. The interdependence between permeability and adherence of these films was discussed.

**Practical Results from Corrosion Protection of Zinc-Containing Paints**

H. Sagel, Hilden

Results of tests with various zinc powder paints were presented.

**New Silicate Protective Layers on Metal Surfaces**

O. Loebich, Hanau

The layers are produced by surface chemistry reactions between carbonate-free  $\text{SiO}_2$  glass containing heavy metals and the underlying metal.

**Electropolishing of Steel**

S. Aćimović, Belgrade

The optimum conditions for electrolytic polishing with sulfuric-chromic and phosphoric-acid containing electrolytes were presented.

### The Protection of Steel by Means of Sprayed Coatings of Zinc or Aluminum

T. K. Ross, E. L. Smith, and R. E. Mansford, Manchester

Practical results obtained as a consequence of application of sprayed Al and Zn coatings on steel and the actual processes of application of these coatings were discussed.

### Dip Zinc Coating

P. Debouté, Paris

Experiments show that a 2-3 dip in molten Zn at 450°C following a thorough cleaning of the surface will produce through a FeZn alloy formation a Zn layer of 800 g/m<sup>2</sup>.

### The Corrosion Protection of Underwater Structures of Steel by Flame-Sprayed Zinc

Z. Kowalski, Warsaw

The technique of flame spraying, grinding and polishing, the corrosion progress, and the life of these Zn layers were discussed.

### Dense and Bright Rhodium Plating

R. Lévy, Paris

It was shown that through addition of ionic and non-ionic wetting agents one can obtain a nonporous bright Rh deposit of greater density and resistance up to 10 $\mu$  thick.

### Comparative Field Studies on the Corrosion Resistance of Zinc Protected through Various Methods of Passivation

T. Biestek, Warsaw

This study shows that there exists only a loose connection between results obtained in the field and laboratory test methods. It also shows that passivation by different chemical processes considerably improved the corrosion resistance.

### On the Electrolytic Plating of Titanium from Water Solutions of Potassium-Titanium Fluoride

W. Machu, Cairo

The plating on Sb and Al is successful in the vicinity of a pH of 1.8. Ti can also be plated on Zn with H<sub>2</sub>O<sub>2</sub> and citric acid additions.

### On a Study of Corrosion of Pressure Conduits and the Means of Protection Which Have Been Devised

Ch. Tschäppät, Lausanne

The great complexity of the problem was presented and the difficulty of evaluating exactly the different variables was discussed. Experimental results from laboratory testing as well as results of many years of field studies were presented and discussed. Various means of protection were presented and their virtues discussed.

### The Corrosion of Tin Cans in the Canning Industry

H. Cheftel, Boulogne-Billancourt

A comprehensive survey of the problem was presented; a detailed discussion of types and nature of the variables involved, followed by the description of the types of corrosion taking place. The corrosion problem is in essence ascribed to the iron-tin couple.

### Corrosion and Testing Methods

#### A Comparison between the Results of Natural Exposure in Industrial Air and Short Time Testing in Sulfur Dioxide Atmosphere

A. Kutzelnigg, Erlangen

Experience of corrosion behavior of protective coatings with a Testor instrument and natural exposure was discussed.

#### On the Diagnosis of Corrosion Causes from Corrosion Products

G. Schikorr, Stuttgart

It was demonstrated with examples how the analysis of the corrosion product can provide clues for the corrosion causes.

#### On a Completely Automatic Working Apparatus for the Testing of Corrosive Effect of Solutions

G. Wilbrett, Weihenstephan

One apparatus capable of simultaneously treating 6 samples on a rotating arm with 5 stations for cleaning, dipping in solution, and drying was described. Results

obtained with it and those under best alternative conditions were presented and the great improvement of reproducibility shown.

#### Methods of Controlling Corrosion in Clean Oil Tankers

R. H. Maas, Linden, N. J.

A report on promising investigations for undermining the corrosion in tankers was presented.

#### On the Application of Polarization Curves for the Investigation of Local Corrosion in Stainless Steels

J. M. Defranoux, Ugene

A discussion of the determination of the limiting corrosion current and the cathode and anode areas resulting from differential aeration such as occurs in pitting corrosion.

#### Electrochemical Measurements for Clarification of Case Corrosion Damage

H. Schmeken, Dortmund-Aplerbeek

Polarization curves of corroded materials are used for determinations of corrosion currents under actual conditions.

#### Measurements of Inter-crystalline Corrosion by Resonance Frequency Method

K. Smrcek, Prague

A modified resonance frequency method for the determination of inter-crystalline damage in stainless steel.

#### Investigation of the Inter-crystalline Corrosion Susceptibility of Passive Chrome Nickel Steels by Application of Potentiostatic Technique

M. Prazák, Prague

Sensitive indications of the susceptibility to inter-crystalline corrosion through etching at a potential just above the passivation potential of the austenitic lattice.

#### Electrochemical Measurements at Temperatures up to 300°C and the Corresponding Equivalent Pressure

M. Prazák, Prague

A AgCl electrode for potential measurements above 1000°C was described.

#### Galvanic Series of the Metals in Practical Corrosion Media

J. Elze, Berlin-Dahlem

It was pointed out that the current-potential relationship of the metal in the vicinity of the equilibrium potential, rather than the equilibrium potential, is the factor which allows us to deduce corrosion behavior of metal combinations.

#### Coatings and Planning

##### Ceramic Coatings as High-Temperature Protection for Metals

A. Petzold, Freiburg/Sa

Radiation resistance, corrosion resistance, and fatigue of ceramic coated metals from the point of view of applications in gas turbines and reactors.

##### New Refractory Constructions

W. Füller, Frankfurt a. Main

Walling up with refractory cements and bricks and construction of refractories for furnaces with external heating.

##### Documentation of the Field of Corrosion

W. Wiederholt, Berlin-Dahlem

A new classification system for the corrosion literature which can be handled by semi- or fully-mechanized means.

##### A Program for New Field Studies for the Investigation of the Variables of a Painted Steel Surface

K. F. Trägårdh, Stockholm

Cost as a function of the quality of surface preparation prior to painting, thickness of paint, mode of application, etc., was discussed.

##### Corrosion Protection Looked at from a Different Viewpoint

K. Thalhofer, Essen-Rell

Ways and possibilities for determining the causes of corrosion, from the raw material through the production process until the final placing of the finished product in service, were discussed.

## Section News

### Speakers Needed

Local Sections, and particularly those in out-of-the-way locations, sometimes find it difficult to secure speakers due to financial limitations.

It is requested that potential speakers, Patron or Sustaining Members sending possible speakers into the Section area, offer services where possible. This could be done with the Local Section officer directly, or perhaps through Society Headquarters.

### India Section

*India Section Publication, "Symposium on Electrodeposition and Metal Finishing."*—The India Section is publishing a Special Number of the *Bulletin*, expected to be available this month, covering the 35 papers presented at the Symposium on Electrodeposition and Metal Finishing held at Karaikudi in December 1957. The subjects include electroplating, electrorefining, electrowinning, metal powders, anode phenomena, electroplating, anodizing, and protective coatings. The price per copy of the Special Number outside India is Rs.15.00, payable to "India Section, The Electrochemical Society," Indian Institute of Science, Bangalore 3, India, in *Indian Rupees only*. Special trade terms can be obtained on request.

*Electroplating Course in India.*—A three-month course of technical training in electroplating was organized by the CECRI, Karaikudi, in April 1958 for the purpose of training technical personnel engaged in the plating industry in modern developments in theory and practice.

*Symposium on Ferroalloy Industry in India.*—A Symposium on Ferroalloy Industry in India will be held in Delhi during December 1958 con-

current with the 12th annual technical meeting of the Indian Institute of Metals.

T. L. Rama Char  
*Regional Editor, India*

### Mohawk-Hudson Section

At the spring meeting of the Mohawk-Hudson Section of the Society, the following officers were elected for the 1958-1959 term:

*Chairman*—W. E. Tragert, Research Labs., General Electric Co., P.O. Box 1088, Schenectady, N. Y.

*Vice-Chairman*—R. A. Osteryoung, Dept. of Chemistry, Rensselaer Polytechnic Institute, Troy, N. Y.

*Secretary-Treasurer*—W. H. Smith, Research Labs., General Electric Co., P.O. Box 1088, Schenectady, N. Y.

*Local Section Councilor*—D. A. Vermilyea.

W. H. Smith, *Secretary-Treasurer*

### Midland Section

At the May 15, 1958 business meeting of the Midland Section, the following officers were elected for 1958-1959:

*Chairman*—P. F. George, 2905 Manor Drive, Midland, Mich.

*Vice-Chairman*—R. S. Karpiuk, 4608 Bristol Court, Midland, Mich.

*Secretary-Treasurer*—M. R. Bothwell, 13 Erie Court, Midland, Mich.

R. S. Karpiuk  
*Past Secretary-Treasurer*

### Pittsburgh Section

Newly elected officers of the Pittsburgh Section for 1958-1959 are:

*Chairman*—Ling Yang, Carnegie Institute of Technology, Schenley Park, Pittsburgh, Pa.

*Vice-Chairman*—E. H. Phelps, Applied Research Lab., U. S. Steel Corp., Pittsburgh, Pa.

*Secretary-Treasurer*—J. W. Faust, Jr., Research Lab., Westinghouse Electric Corp., Pittsburgh, Pa.

*Local Section Councilors*—J. J. Stokes, Jr., and A. J. Cornish.

E. H. Phelps  
*Past Secretary-Treasurer*

### Washington-Baltimore Section

The sixth regular meeting of the 1957-1958 year was held on March 6, 1958 at the National Bureau of Standards. The speaker was Dr. Norman Hackerman. He discussed the affairs of the Society and then proceeded to summarize some of the recent work and theories on the passivity of metals.

The seventh regular meeting of the 1957-1958 year was held on April 3, 1958 at the National Bureau of Standards. The speaker was Dr. Ralph Roberts of the Office of Naval Research and his topic was "A Program of Basic Research in Electrochemistry." The talk described the research program in electrochemistry that is being sponsored by the Office of Naval Research. This program has been in operation for 12 years and includes contracts between the Navy on one hand, and the various universities, government laboratories, industrial laboratories, and nonprofit research organizations on the other. Electrochemistry is only one of the fields in which research is supported by the Office of Naval Research.

ONR supports research in both theoretical and applied electrochemistry. In theoretical electrochemistry, the research contracts fall into two general groups, namely: 1. nature of electrolytes; 2. electrode reactions and electrode kinetics. The program for applied electrochemistry includes such topics as ion exchange, bimetallic corrosion, corrosion fundamentals, passivity, etc. This program has caused a substantial increase in the amount of basic research in electrochemistry in progress in this country.

David Schlain  
*Secretary 1957-1958*

## Manuscripts and Abstracts for Spring 1959 Meeting

Papers are now being solicited for the Spring Meeting of the Society, to be held at the Sheraton Hotel in Philadelphia, Pa., May 3, 4, 5, 6, and 7, 1959. Technical sessions probably will be scheduled on Electric Insulation, Electronics (including Luminescence and Semiconductors), Electrothermics and Metallurgy (including a Projected Symposium on "Mechanical Properties of Intermetallic Compounds"), Industrial Electrolytics, and Theoretical Electrochemistry.

To be considered for this meeting, triplicate copies of abstracts (*not to exceed 75 words in length*) must be received at Society Headquarters, 1860 Broadway, New York 23, N. Y., *not later than January 2, 1959. Please indicate on abstract for which Division's symposium the paper is to be scheduled, and underline the name of the author who will present the paper.* Complete manuscripts should be sent in triplicate to the Managing Editor of the JOURNAL at the same address.

★ ★ ★

The Fall 1959 Meeting will be held in Columbus, Ohio, October 18, 19, 20, 21, and 22, 1959, at the Deshler-Hilton Hotel. Sessions will be announced in a later issue.

### Washington-Baltimore Section

The annual joint meeting of the American Electroplaters' Society, National Association of Corrosion Engineers, and The Electrochemical Society, Inc., was held at Marty's Park Plaza in Baltimore, Md., on March 12, 1958. Clarence H. Sample addressed the joint meeting, describing the work of ASTM Committee B-8 and of the International Nickel Co., Inc., on the corrosion behavior of zinc, cadmium, and lead electrodeposited coatings as well as the properties of copper-nickel-chromium and nickel-chromium decorative coatings in marine, industrial, and urban atmospheres.

During the years when zinc was scarce, cadmium and lead electrodeposited coatings were investigated as substitutes for zinc. In this country, cadmium coatings were preferred to lead although lead coatings are used successfully in other countries. The Standard Salt Spray Test proved to be unsatisfactory in the evaluation of the corrosion resistance of the various coatings. While cadmium coatings are superior to zinc coatings in the Salt Spray test, they are inferior in corrosion resistance to zinc coatings in some atmospheres.

Decorative chromium coatings with an underlay of buffed Watts nickel maintained an acceptable appearance in various atmospheres longer than an equal thickness of copper-nickel-chromium coatings. The thickness of the nickel in the copper-nickel-chromium coating is the primary factor in determining the life of the coating. The life of the coating decreases as the ratio of copper to nickel increases. The Standard Salt Spray Test did not reveal the differences in the protective values of nickel-chromium and copper-nickel-chromium coatings on steel that appear in other atmospheric exposures.

Ralph Brodd

## Division News

### E & M Symposium on Mechanical Properties of Intermetallic Compounds

The Electrothermics and Metallurgy Division announces a Projected Symposium on "Mechanical Properties of Intermetallic Compounds" to be held during the 115th Meeting of The Electrochemical Society in Philadelphia, Pa., May 3-7, 1959.

For the purposes of this Symposium, intermetallic compounds will be held to comprise all intermediate phases in binary or higher order systems of true metals, including superlattices. Interstitial compounds of metals and nonmetals, such as the carbides, nitrides, borides, etc., will not be considered.

It is hoped to include papers covering the following topics:

#### Mechanical Properties of Intermetallic Compounds

Fundamental Behaviors: Deformation Modes; Initiation and Propagation of Fracture; Effects of Crystal Structure; Dislocations in Intermetallic Compounds; Influence of Point Defects; Radiation Damage.

Phenomenology: Effects of Processing Variables; Temperature Dependence of Mechanical Properties; Effects of Impurities; Effects of Alloying; Effects of Stress State and Strain Rate.

Experimental Techniques: Testing Techniques Applicable to Brittle Compounds; Preparation of Intermetallic Compounds with Reference to Mechanical Property Studies, e.g., Single Crystal, and High-Purity Samples.

Titles and authors of proposed papers should be sent immediately, and triplicate copies of 75-word abstracts by January 2, 1959, to the Secretary-Treasurer of the Electrothermics and Metallurgy Division (please underline the name of the author who will present the paper):

Dr. J. H. Westbrook  
Research Lab.  
General Electric Co.  
P.O. Box 1088  
Schenectady, N. Y.

Arrangements can be made for authors residing outside the United States who wish to have papers presented *in absentia*.

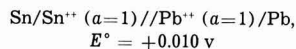
#### Notice to Members

By now you have received your official voting ballot from Society Headquarters. If you have not already done so, please return the ballot by December 15 so that your vote can be included in the final election count.

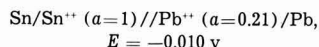
## Letter to the Editor

Dear Sir:

Recently, two notes in the JOURNAL have suggested that a "sign convention for the electromotive force of a voltaic cell, as formulated, . . . serves no purpose," [*This Journal*, **104**, 692 (1957)] and that "the left-right convention tends to confuse the issue" [*This Journal*, **105**, 359 (1958)]. Those who share this point of view should compare the two cells



and



The cells both have a voltage of 10 mv, yet they are by no means equivalent. The first cell does useful work through the consumption of tin and the plating-out of lead which becomes the + terminal. The second cell does useful work through the consumption of lead and the plating-out of tin which now becomes the + terminal. This example illustrates the justification for an algebraic sign, and for a left-right convention, in dealing with the electromotive forces of voltaic cells.

The whole-cell convention of G. N. Lewis, internationally accepted by the I.U.P.A.C. at Stockholm in 1953, is the one that should be recommended. This Lewis-Stockholm convention makes the whole-cell emf a positive quantity when the + terminal of the cell, as observed, occurs on the right-hand end of the cell-diagram, as written down. There can be no objections to this simple convention which has been in use in America for decades and has been accepted since 1953 by our friends in Europe. In terms of the sign-invariant Gibbs-Stockholm electrode potential [i.e., the zinc minus, copper plus, potential, *This Journal*, **102**, 288C (1955); *J. Chem. Educ.*, **34**, 433 (1957)] recommended by The Electrochemical Society, the Lewis-Stockholm whole-cell emf is simply  $E(\text{cell}) = V(\text{right}) - V(\text{left})$ , where the  $V$ 's denote, in the words of J. Willard Gibbs, "the electrical potentials in pieces of the same kind of metal connected with" the two electrodes.

Andre J. deBethune  
Dept. of Chemistry  
Boston College  
Chestnut Hill, Mass.

# Committees of The Electrochemical Society, Inc., 1958-1959

## Admissions Committee

Louis Weisberg, Chairman	<i>Term Expires</i> Spring 1961
L. I. Gilbertson	Spring 1962
M. F. Quaely	Spring 1963

## F. M. Becket Memorial Award Committee

	<i>Term Expires</i>
A. T. Hinkley	1958
A. C. Haskell	1959
G. M. Butler, Chairman	1960

## Committee for the Administration of the

### Corrosion Handbook Fund

Norman Hackerman—Board representative  
R. M. Burns—Representative of Editorial Advisory Board of Handbook  
C. V. King, Chairman—Corrosion Division Chairman  
H. H. Uhlig—Editor of Handbook

## Finance Committee

L. I. Gilbertson, Chairman	
H. B. Linford	R. A. Schaefer
W. C. Gardiner	Hans Neumark

## Honors and Awards Committee

	<i>Term Expires</i>
M. J. Udy	Nov. 1959
H. M. Scholberg, Chairman	Nov. 1959
R. M. Hunter	Nov. 1960
E. M. Sherwood	Nov. 1960
J. R. Musgrave	Nov. 1961
Abner Brenner	Nov. 1961
H. C. Froelich	Nov. 1962
W. J. Hamer	Nov. 1962

## Investment Advisory Panel

	<i>Term Expires</i>
G. W. Heise	Spring 1959
A. K. Graham, Chairman	Spring 1960
M. J. Udy	Spring 1961
Hans Thurnauer	Spring 1962
B. E. Field	Spring 1963

## Membership Committee (Contributing)

Hans Thurnauer, Chairman

## Membership Committee (Personal)

F. W. Koerker, Chairman

### Divisions—Representatives and Alternates

Battery—C. H. Clark, Rep.; R. C. Shair, Alt.  
Corrosion—H. R. Copson, Rep.  
Electric Insulation—A. Gunzenhauser, Rep.;  
A. J. Sherburne, Alt.  
Electrodeposition—R. A. Woofter, Rep.;  
Fielding Ogburn, Alt.  
Electronics—H. M. Pollock, Rep. (Semiconductor);  
C. W. Jerome (Luminescence)  
Electrothermics & Metallurgy—Morris Steinberg, Rep.  
Industrial Electrolytic—W. J. Sakowski, Rep.  
Theoretical Electrochemistry—S. Schuldiner, Rep.

### Sections—Representatives and Alternates

Boston—P. L. Raymond, Rep.; R. A. Peak, Alt.  
Detroit—A. E. Remick, Rep.  
Midland—J. L. Robinson, Rep.  
Philadelphia—F. X. McGarvey, Rep.; C. L. Scheer, Alt.  
Ontario-Quebec—L. G. Henry, Rep.  
San Francisco—H. P. Silverman, Rep.

## Nominating Committee

R. M. Hunter, Chairman	
T. P. May	M. F. Quaely
Hans Neumark	R. A. Schaefer

## Palladium Medal Award Committee

	<i>Term Expires</i>
H. A. Laitinen, Chairman	Jan. 1960
T. P. May	Jan. 1960
E. B. Yeager	Jan. 1960
H. A. Liebhafsky	Jan. 1962
A. L. Ferguson	Jan. 1962

## Perkin Medal Award Committee

S. Swann, Jr., Chairman Alternates: L. I. Gilbertson  
Norman Hackerman C. V. King

## Publication Committee

R. J. McKay, Chairman  
C. V. King H. B. Linford

## Resolutions Committee

H. B. Linford William Blum  
H. R. Copson

## Ways and Means Committee

R. A. Schaefer, Chairman  
W. C. Gardiner M. F. Quaely  
C. L. Faust A. C. Haskell  
Norman Hackerman H. B. Linford

## Council of Local Sections

M. F. Quaely, Chairman  
K. S. Willson, Vice-Chairman  
A. J. Cornish, Secretary  
Representatives on Board: C. A. Hampel and L. O. Case

<i>Section</i>	<i>Councilor</i>
Boston	L. B. Rogers F. C. Benner H. T. Francis C. A. Hampel N. C. Cahoon K. S. Willson A. C. Tripler W. M. Albrecht Frank Passal Lee O. Case
Chicago	—
Cleveland	—
Columbus	—
Detroit	—
India	—
Indianapolis	F. C. Mathers J. M. Booe R. C. Kirk F. W. Koerker D. A. Vermilyea A. C. Loonam M. F. Quaely R. Stambaugh J. Sullivan E. A. Hollingshead L. G. Henry G. H. Kissin J. F. Gall J. F. Hazel J. J. Stokes, Jr. A. J. Cornish R. F. Bechtold C. W. Tobias
Midland	—
Mohawk-Hudson	—
New York Metropolitan	—
Niagara Falls	—
Ontario-Quebec	—
Pacific Northwest	—
Philadelphia	—
Pittsburgh	—
San Francisco	—
Southern California-Nevada	—
Washington-Baltimore	M. E. Carlisle Fielding Ogburn J. C. White

## Representatives of ECS to Other Societies

*American Association for the Advancement of Science*  
George Heise—Term expires spring 1960  
Harry Alsentzer—Term expires spring 1961

### *American Standards Association*

Sectional Committee C-18—J. M. Booe  
Y-10 and Y-32—W. J. Hamer  
C-40—Eugene Willihnganz  
C-42—W. C. Vosburgh  
C-67—Guy Fetterley  
C-34.1—W. E. Gutzwiller

### *Inter-Society Corrosion Committee*

Paul Delahay K. G. Compton

*National Academy of Sciences—National Research Council Advisory Board for the Office of Critical Tables*

E. B. Yeager—Term expires June 30, 1961

*National Research Council—Division of Chemistry and Chemical Technology*

Norman Hackerman—Term expires June 30, 1961  
*Research Council on the Causes and Methods of Prevention of Internal Corrosion of Water Pipes*  
F. L. LaQue

**Personals**

**Thomas A. Henrie**, formerly with the Metals Research Labs., Electro Metallurgical Co., Niagara Falls, N. Y., has joined the staff of the Electrometallurgical Div. of the U. S. Bureau of Mines in Boulder City, Nev.

**W. G. Renshaw** and R. A. Lula of the Research and Development Lab. of Allegheny Ludlum Steel Corp., Pittsburgh, Pa., are the joint winners of the American Society for Testing Materials' Sam Tour Award, established in 1947 "for the purpose of stimulating papers on corrosion testing." A cash prize and certificates were presented to them for their prize-winning paper, "Corrosion Properties of the Chromium-Nickel-Manganese Austenitic Stainless Steel," at the annual meeting of the ASTM in Boston, June 25. Mr. Renshaw, research supervisor, Corrosion Section, has been with Allegheny Ludlum since 1940.

**E. Keith McMahon** recently was appointed chemical sales division manager of Tennessee Products & Chemical Corp., Nashville, Tenn.

**T. L. Rama Char** has been appointed a member of the Board of Technical Advisers of M/S. Grauer and Weil (India) Private Ltd., Bombay.

**A. N. Kappanna** has been named director of the Hindustan Salt Co. (P), Jaipur.

**S. Ramaswamy** and **K. S. G. Doss** visited Japan as members of a delegation to tour chlor-alkali plants.

**Dana J. Demorest**

Dana James Demorest, Emeritus Professor, Dept. of Metallurgy, Ohio State University, Columbus, died on June 30, 1958 at the age of 75.

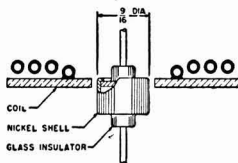
Professor Demorest graduated from the Ohio State University with the degree Bachelor of Chemical Engineering in 1907. Immediately after graduation, he joined the university's Dept. of Metallurgy as an instructor and, in 1918, became Chairman of the department, which office he held until 1948. He retired from teaching in 1952 at which time he was made Emeritus Professor.

Since 1921, he was Section Editor for *Chemical Abstracts* in charge of editing the Metallurgy and Mineralogy Sections. He revised the book  
(Continued on page 216C)



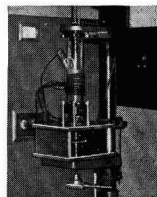
**TYPICAL INDUCTION HEATING APPLICATIONS IN THE MANUFACTURE OF TRANSISTORS**

**SOLDERING TRANSISTOR ASSEMBLIES BY INDUCTION HEATING**



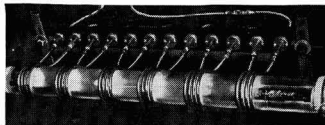
Concentrator-type coil creates high intensity, restricted heating at joint of nickel shell and tinned glass, thus causing solder to flow for permanent seal.

**SINGLE CRYSTAL PULLER**



General arrangement for pulling single crystals. Induction heating coil is shown surrounding quartz tube containing crucible with molten germanium in suitable atmosphere.

**MULTIPLE ZONE REFINING**



Induction heating apparatus used in zone refining. The six coils shown provide simultaneous molten zones in the ingot as it passes through the tube containing the protective atmosphere.

Electronic Tube Generators from 1 kw. to 100 kw.  
Spark Gap Converters from 2 kw. to 30 kw.

WRITE FOR THE NEW LEPEL CATALOG . . . 36 illustrated pages packed with valuable information.



All Lepel equipment is certified to comply with the requirements of the Federal Communications Commission.

**LEPEL HIGH FREQUENCY LABORATORIES, INC.**  
55th STREET and 37th AVENUE, WOODSIDE 77, NEW YORK CITY, N. Y.

on "Metallurgical Analysis" by the late Professor N. W. Lord in 1916 and again in 1924. It was published under the joint authorship of Lord and Demorest.

During World War I, Professor Demorest served as a Major in the Chemical Warfare Service, heading the production of toxic gases at the Edgewood Arsenal.

He organized, and for many years was President of, the Utah Alloys Corp., a mining organization that produces vanadium and uranium.

He was active in many charitable enterprises and professional societies. He was an Emeritus Member of The Electrochemical Society, which he joined in 1916. He also held active memberships in the American Society for Metals, of which he was the first Life Member; the American Institute of Mining Engineers; the American Chemical Society; and the American Society for Testing Materials.

Several years before his death, the alumni of the Dept. of Metallurgy at Ohio State established a scholarship in his name. It is now known as the Dana J. Demorest Scholarship.

His loss is deeply felt by all who knew him.

---

## News Items

---

### "Technology of Columbium (Niobium)" Now Available

The Electrochemical Society is pleased to announce the availability of the latest volume in the ECS Series, sponsored by the Society, and published by John Wiley & Sons, Inc.

"Technology of Columbium (Niobium)," published August 1958, is a compilation which includes most of the papers presented at the Symposium on Columbium (Niobium) of the Electrothermics and Metallurgy Division of The Electrochemical Society in Washington, D. C., May 15 and 16, 1958. It provides vital information on niobium, discussed by 25 authorities active in the field of high-temperature technology.

The 120-page book, listed at \$7.00, is available to ECS members at the 33 1/3% member discount. To obtain the discount, orders must be sent to Society Headquarters, 1860 Broadway, New York 23, N. Y. The Society will forward orders to Wiley who will ship the volume with the invoice. Nonmembers, including subscribers, should send their orders directly to John Wiley & Sons, Inc., 440 Fourth Ave., New York 16, N. Y.

### AIME Conference on Physical Metallurgy of Stress-Corrosion Fracture

In furtherance of the cooperative effort of concerned professional bodies in the development of information on corrosion-resistant metals, the American Institute of Mining, Metallurgical, and Petroleum Engineers (AIME) has announced that a Conference on the Physical Metallurgy of Stress-Corrosion Fracture will be held April 2-3, 1959, at the Mellon Institute, Pittsburgh.

The meeting will be sponsored by the Corrosion-Resistant Metals Committee of the Institute of Metals Division of The Metallurgical Society, a constituent organization of AIME, and the Pittsburgh Section of AIME. Cooperating with The Metallurgical

Society of AIME in the technical program will be The Electrochemical Society, The National Association of Corrosion Engineers, and the American Society for Testing Materials.

The program is intended to provide a broad basis for presentation and discussion of recent fundamental advances in stress-corrosion cracking. The sessions will center around these general subjects: theoretical aspects of stress corrosion and fracture; new experimental advance in stress corrosion and fracture; mechanisms of stress-corrosion cracking, including environmental and metallurgical aspects and the behavior of specific materials. Emphasis will be placed on the physical metallurgical, surface-chemical, and solid-state physics aspects of the phenomena.

# Shape of things to Come—in Copper

Plated Moulds, Inc., finds even heavy, intricate molds are plated faster—deposits are smoother, denser, more uniform—with "Plus-4" (Phosphorized Copper) Anodes

"Plus-4"® Copper Anodes have helped Plated Moulds, Inc., Yonkers, N. Y., open up new areas of business in electroformed copper molds for the mass production of intricately shaped products in vinyl plastisols.

A leader in the production of copper molds for dolls and toys, Plated Moulds also pioneered in making the molds for plastic footwear. About three years ago, the company tried "Plus-4" Anodes in its tanks with these results:

1. Deposits were uniform, with excellent density. They had experienced some porosity with ordinary anodes.
2. There were far fewer nodules. This was particularly important in building up shells as thick as 1/4".
3. They could plate faster, using higher current densities.

4. Efficiency in copper use was higher because the anodes corroded more uniformly.

5. Tank maintenance was reduced. There was less sulfate—no sludge.

These advantages made it practical and economical to try larger, heavier molds. The hobbyhorse mold illustrated is one result. And Plated Moulds is moving out into the commercial and industrial fields with molds for motorcycle and bicycle seats, automotive assemblies, display models.

**Write for information** on how you can obtain a test quantity to supply one tank. Address: The American Brass Company, Waterbury 20, Connecticut. In Canada: Anaconda American Brass Ltd., New Toronto, Ont.

58134

## ANACONDA®

### "PLUS-4" ANODES Phosphorized Copper

Made by The American Brass Company

On April 2, the sessions, as planned at present, will take up:

*Introduction and Background:* 1. significance of the stress-corrosion problem; 2. characteristics of stress-corrosion cracking.

*Theoretical Aspects of Stress, Corrosion, and Fracture:* 1. relationship of microstress to fracture (at or near solid-fuel interfaces); 2. thermodynamic relationship between stress and chemical potential; relationship of surface topology and structure to environment.

*Experimental Aspects of Stress, Corrosion, and Fracture:* 1. role of the corrosion product; 2. stress and microtopology; stress; and 3. electrode potential.

On April 3, the subject, *Mechanisms of Stress-Corrosion Cracking*,

will include: 1. environmental aspects; 2. metallurgical aspects; and 3. behavior of specific materials.

The sessions will be of the discussion type. Speakers will present summaries of their papers, which are to be preprinted and circulated in advance, thus providing that most of the time of the Conference may be devoted to discussion and exchange of scientific information.

#### Conference on Silicon Carbide

A conference on silicon carbide, the new semiconductor, is scheduled at Boston, April 2-3, 1959, under the auspices of the Air Force Cambridge Research Center. A twofold objective characterizes the arrangements for this meeting: 1. to consider the preparation, properties, and applica-

tions of the new material; 2. to consolidate efforts on its research and development.

The program includes several invited papers from this country and abroad, submitted comprehensive papers (30 minutes), and brief reports on recent developments. Four technical sessions are tentatively outlined as follows: 1. the growing of single crystals of silicon carbide by sublimation and from melts, together with the physicochemical aspects of these processes; 2. the physical properties of silicon carbide as a solid, with particular emphasis on stacking faults and dislocations; 3. the measurement of electronic and optical properties, such as resistivity, carrier mobility, photoconductivity, etc.; 4. the application of silicon carbide for active devices, diodes, luminescent sources, thermoelements, etc.

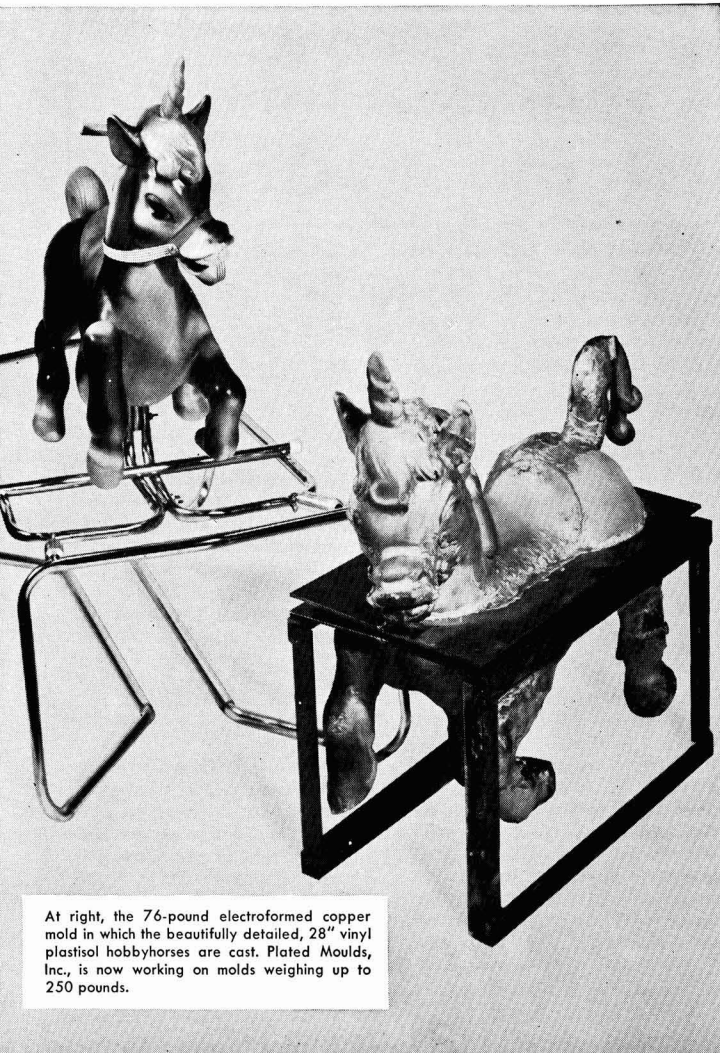
Scheduled in conjunction with the March meeting of the American Physical Society at the Massachusetts Institute of Technology, Cambridge, Mass., the conference has designated December 1, 1958 as the limiting date for the filing of applications. Abstracts (200 words or less) for submitted papers should also be filed by this date. Types of papers under the "recent news" classification will be most welcomed. A title and abstract for the latter group should be submitted by March 1, 1959.

For further information, or a copy of the program soon to be available, forward request to: J. R. O'Connor, Electronic Material Sciences Lab., Air Force Cambridge Research Center, L. G. Hanscom Field, Bedford, Mass.

#### Literature from Industry

**Titanium Tubing and Pipe.** Physical and mechanical properties, fabrication characteristics, and corrosion resistance of titanium tubing and pipe are described in a new bulletin. Data include working instructions for machining, forming, welding, heat treating, and cleaning. Resistance of commercially pure titanium to 80 corrodents is shown. Typical applications for use in the aircraft, chemical, and marine fields are also cited. Available from: *Alloy Tube Div., Carpenter Steel Co., Union, N. J.*

**"Allegheny Stainless in Chemical Processing."** A completely revised 40-page booklet on the use of stain-



At right, the 76-pound electroformed copper mold in which the beautifully detailed, 28" vinyl plastisol hobbyhorses are cast. Plated Moulds, Inc., is now working on molds weighing up to 250 pounds.



The Semiconductor-Components Division of

TEXAS INSTRUMENTS

*Invites*

SENIOR SCIENTISTS

... to participate in the creation of new semiconductor devices and improved materials.

Some of the specific device techniques currently being applied are... solid state diffusion... alloying of metals and semiconductors... vacuum deposition of metals... semiconductor surface chemistry... and solid-state physical measurements. Materials development embraces chemical processing equipment for preparing semiconductors and for controlling crystalline structures.

Senior scientists with experience in physical chemistry, inorganic chemistry, metallurgy, solid-state physics, semiconductor electronics or other related fields are invited to discuss their future at the world's largest semiconductor facility with...

Dr. Willis A. Adcock  
Manager of Development

**TEXAS INSTRUMENTS**

INCORPORATED

P. O. BOX 312 E • DALLAS, TEXAS

less steel in the chemical industry is being distributed. It includes special sections on the process industries, the plastics industry, petrochemical industry, detergents manufacturing, the nuclear power industry, and others. Simple, easy-to-follow diagrams and photographs are included. A special comparative table on stainless steels and a table on the corrosion resistance of Allegheny Ludlum stainless steels to various media are included also. Available from: *Advertising Dept., Allegheny Ludlum Steel Corp., Oliver Bldg., Pittsburgh 22, Pa.*

**Information on Cobalt.** The following publications are available from the Cobalt Information Center: "Metallographic Etching Reagents for Cobalt and Cobalt-Containing Alloys"; "Electrolytic Polishing of

Cobalt"; "Cobalt and its Alloys"; "Bibliography on Electroplating Cobalt and Cobalt Alloys"; "Corrosion Bibliography on Cobalt and Cobalt Alloys." They may be obtained by addressing requests on company letterhead to: *Cobalt Information Center, c/o Battelle Memorial Institute, 505 King Ave., Columbus 1, Ohio.*

**New Metal Charts.** Two new charts have been published by Fansteel Metallurgical Corp. as a service to industry. One chart shows the melting points of the metals, both in Fahrenheit and Centigrade scales, ranging from tungsten which melts at 3400°C (6152°F) to mercury which melts at -38.8°C (-38°F). The other chart shows the densities of metals, grouped into heavy, medium, and light classifications, ranging from the heaviest metal, osmium, whose density is 22.48 g/cc, to the lightest metal, lithium, whose density is 0.53, less than that of water. Charts are available without cost to readers who request them on company letterheads. Requests should be addressed to: *E. R. Jenstrom, Metals and Fabrication Div., Fansteel Metallurgical Corp., North Chicago, Ill.*

**Technical Manual on Stationary Storage Batteries.** A detailed technical manual on use of stationary

storage batteries has been published by Exide Industrial Div., Electric Storage Battery Co. The 24-page manual, Bulletin 210, has the first reports on recent engineering studies of the effect of temperature on battery capacity and, in addition, provides tabulated data and general information necessary for: selection of batteries and charging equipment; proper battery and charger maintenance, selection of battery racks; determination of battery discharge ratings. Available from: *Exide Industrial Div., Electric Storage Battery Co., Box 8109, Philadelphia 1, Pa.*

#### 1959 Bound Volume

Members and subscribers who wish to receive bound copies of Vol. 106 (for 1959) can receive the volume for the low, pre-publication price of \$6.00 if their orders are received at Society Headquarters, 1860 Broadway, New York 23, N. Y., by December 1, 1958. After that date, members will be charged \$12.00, and nonmembers, including subscribers, \$18.00.

Bound volumes are *not* offered independently of JOURNAL subscription.

#### JOURNAL ELECTROCHEMICAL SOCIETY

Wanted to Buy.

Back sets, volumes, and issues of this JOURNAL and TRANSACTIONS.

Especially volumes 1, 3 and from volume 60 to date.

We pay good prices.

Buy also Technical and Scientific Periodicals.

E. O. ASHLEY, 27 E. 21 St., New York 10, N. Y.

## ELECTROCHEMISTS SOLID STATE CHEMISTS

■ Ph.D. or equivalent experience for work on long-range problems in energy sources, fuel cells, dynamic reserve batteries, and solid state devices. Positions are in fundamental research and development at our laboratories in Palo Alto, near Stanford University.

For information regarding these and other related positions, please write Research and Development Staff, Lockheed Missile Systems Division, Sunnyvale 35, Calif.

# Lockheed

## MISSILE SYSTEMS DIVISION

SUNNYVALE, PALO ALTO, VAN NUYS, SANTA CRUZ,  
VANDENBERG AFB, CALIFORNIA · CAPE CANAVERAL, FLORIDA  
ALAMOGORDO, NEW MEXICO

### Announcements from Publishers

"A Selected Bibliography of Research and Development and Its Impact on the Economy." Published by National Science Foundation, Washington, D. C., May 1958. NSF-58-18; 21 pages.

This bibliography covers the following topics: General Background; Philosophy and History of Science; Public Policy; Socio-Economic Impact and Environment; Economic Growth and Stability; Technology—Invention—Patents; Administration and Management of Industrial Research; Funds and Manpower Statistics; Other Bibliographies.

"Study of Corrosion Inhibitors and Antioxidants for Glycol-Ethers," C. B. Jordon, Aberdeen Proving Ground, U. S. Army Ordnance Corps, May 1957. Report PB 131398,\* 29 pages; 75 cents.

"Thorium—A Literature Search." Atomic Energy Commission (AEC) report NLCO-727,\* March 1958. 19 pages; 75 cents.

\* Order from Office of Technical Services, U. S. Dept. of Commerce, Washington 25, D. C.

"A Combined Distillation-Electrochemical Method for Recovery of Hydrofluoric Acid." AEC Report ORNL-2038,\* June 1956. 14 pages; 30 cents.

"Test Methods for Magnesium Surface Treatments," F. W. Pfohl and H. T. Francis, Armour Research Foundation, for Wright Air Development Center, U. S. Air Force, Nov. 1957. Report PB 131600,\* 62 pages; \$1.75.

"A Basic Study of Corrosion of Magnesium," R. R. Addiss and others, Cornell University, for Wright Air Development Center, U. S. Air Force, Dec. 1957. Report PB 131662,\* 57 pages; \$1.50.

"Electrochemical Mechanisms of Noble-Metal/Hydrogen Systems: Part 1—Platinum," S. Schuldiner, Naval Research Lab., March 1958. Report PB 131526,\* 36 pages; \$1.00.

"Development of Oxidation and Liquid Sodium Resistant Brazing Alloys," D. A. Canonico and H. Schwartzbart, Armour Research Foundation, for Wright Air Development Center, U. S. Air Force, March 1958. Report PB 131745,\* 44 pages; \$1.25.

### Advertiser's Index

American Brass Company	216C-217C
E. I. du Pont de Nemours & Company, Inc.	208C
Enthone, Incorporated	Cover 4
Grace Electronic Chemicals, Inc.	204C
Great Lakes Carbon Corporation	Cover 2
Lepel High Frequency Laboratories, Inc.	215C
Lockheed Missile Systems Division	219C
E. H. Sargent & Company	207C
Texas Instruments Incorporated	218C
John Wiley & Sons, Inc.	205C

### Employment Situation

Please address replies to box shown, c/o The Electrochemical Society, Inc., 1860 Broadway, New York 23, N. Y.

#### Position Wanted

**Physical Chemist, Ph.D. 1958,** desires research position in electrochemistry and/or solid state. Strong instrumentation background; research experience; publications; honor societies. Will consider position in New York City or Metropolitan New Jersey area only. *Reply to Box 365.*

### Notice to Subscribers

Your subscription to the JOURNAL of The Electrochemical Society will expire on *December 31, 1958.* Avoid missing any issue. Send us your remittance now in the amount of \$18.00 for your 1959 subscription. (Subscribers located outside the United States must add \$1.00 to the subscription price for postage, and payment must be made by Money Order or New York draft, not local check.) An expiration notice has been mailed to all subscribers.

A bound volume of the 1959 JOURNALS can be obtained at the prepublication price of \$6.00 by adding this amount to your remittance. However, no orders will be accepted at this rate after *December 1, 1958,* when the price will be increased to \$18.00 subject to prior acceptance. Bound volumes are *not* offered independently of your JOURNAL subscription.



# The Electrochemical Society

## INSTRUCTIONS TO AUTHORS OF PAPERS

Address all correspondence to the Editor,  
JOURNAL OF THE ELECTROCHEMICAL SOCIETY,  
1860 BROADWAY, NEW YORK 23, N. Y.

FORM

**Manuscripts** submitted for publication should be in triplicate to expedite review. They should be typewritten, double-spaced, with 2½-4 cm (1-1½ in.) margins.

**Title** should be brief, followed by the author's name and his business or university connection.

**Abstract** of about 100 words should state the scope of the paper and give a brief summary of results.

ILLUSTRATIONS

**Drawings** will be reduced to column width, 8.3 cm (3¼ in.), after reduction should have lettering at least 0.15 cm (1/16 in.) high. Original drawings in India ink on tracing cloth or white paper are preferred. Curves may be drawn on coordinate paper only if the paper is ruled in blue. All lettering must be of lettering-guide quality. See sample drawing on reverse page.

**Photographs** must be glossy prints and mounted flat.

**Captions** for all figures must be included on a separate sheet. Captions and figure numbers should not appear in the body of the figure.

**General**—Figures should be used only when necessary. Omit drawings or photographs of familiar equipment. Figures from other publications are to be used only when the publication is not readily available, and should always be accompanied with written permission for reprinting.

SYMBOLS

If more than a few symbols are used, these should be defined in a list at the end of the paper, for example:

$a, b \dots$  = empirical constants of Brown equation  
 $f_i$  = fugacity of pure  $i$ th component, atm  
 $D_i$  = bulk diffusion coefficient,  $\text{cm}^2/\text{sec}$

REFERENCES

Literature and patent references should be listed at the end of the paper on a separate sheet, in the order in which they are cited. They should be given in the style adopted by *Chemical Abstracts*. For example:

R. Freas, *Trans. Electrochem. Soc.*, **40**, 109 (1921).

H. T. S. Britton, "Hydrogen Ions," Vol 1, p. 309, D. Van Nostrand Co., New York (1943).

H. F. Weiss (To Wood Conversion Co.), U. S. Pat. 1,695,445, Dec. 18, 1928.

UNITS OF MEASUREMENT

Metric units should be used throughout but, where desirable, English units may be given in parentheses.

Corrosion rates in the metric system should preferably be expressed as milligrams per square decimeter per day (mdd), and in the English system as inches penetration per year (ipy).

In reporting electrode potentials, the sign of the standard  $\text{Zn}/\text{Zn}^{++}$  electrode potential should be taken as negative;  $\text{Cu}/\text{Cu}^{++}$  as positive.

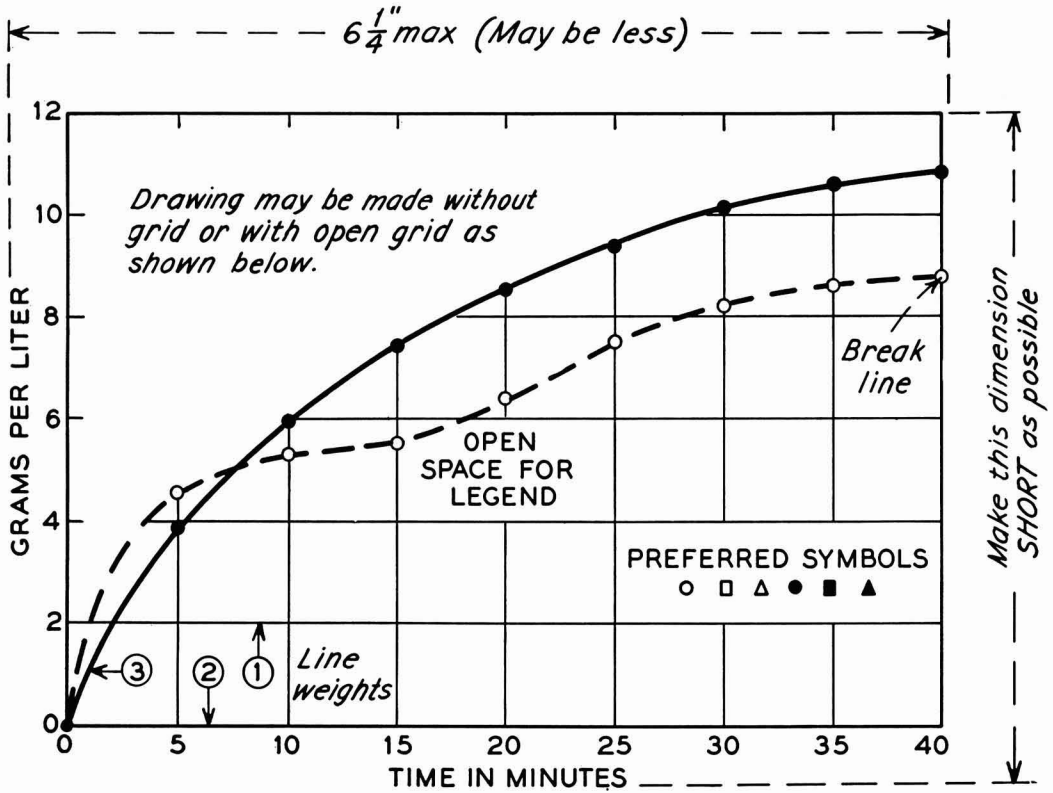
# ABBREVIATIONS

Abbreviations should conform with the American Standards Association's list of "Abbreviations for Scientific and Engineering Terms."

# GENERAL

Authors should be as brief as is consistent with clarity, and must omit all material which can be regarded as familiar to specialists in the particular field.

The use of proprietary names, trade-marks, and trade names should be avoided if possible. If used, these should be capitalized so that the owner's legal rights are not jeopardized.



Remarks: Line weight 2 is used for borders and zero lines. When several curves are shown, each may be numbered and described in the caption. Lettering shown is approximately 1/8 in. In plotting current or potential as ordinate, increasing negative values should go down.

SAMPLE CURVE DRAWING FOR REDUCTION TO 1/2 SIZE

# The Electrochemical Society

## Patron Members

Aluminum Company of Canada, Ltd.,  
Montreal, Que., Canada  
International Nickel Company, Inc.,  
New York, N. Y.  
Olin Mathieson Chemical Corporation,  
Niagara Falls, N. Y.  
Industrial Chemicals Division, Research  
and Development Department  
Union Carbide Corporation  
Divisions:  
Electro Metallurgical Company,  
New York, N. Y.  
National Carbon Company,  
New York, N. Y.  
Westinghouse Electric Corporation,  
Pittsburgh, Pa.

## Sustaining Members

Air Reduction Company, Inc.,  
New York, N. Y.  
Ajax Electro Metallurgical Corporation,  
Philadelphia, Pa.  
Allied Chemical & Dye Corporation  
General Chemical Division,  
Morristown, N. J.  
Solvay Process Division,  
Syracuse, N. Y. (3 memberships)  
Alloy Steel Products Company, Inc.,  
Linden, N. J.  
Aluminum Company of America,  
New Kensington, Pa.  
American Machine & Foundry Company,  
Raleigh, N. C.  
American Metal Company, Ltd.,  
New York, N. Y.  
American Platinum Works, Newark, N. J.  
(2 memberships)  
American Potash & Chemical Corporation,  
Los Angeles, Calif. (2 memberships)  
American Zinc Company of Illinois,  
East St. Louis, Ill.  
American Zinc, Lead & Smelting Company,  
St. Louis, Mo.  
American Zinc Oxide Company,  
Columbus, Ohio  
M. Ames Chemical Works, Inc.,  
Glens Falls, N. Y.  
Auto City Plating Company Foundation,  
Detroit, Mich.  
Bart Manufacturing Company, Bellville, N. J.  
Bell Telephone Laboratories, Inc.,  
New York, N. Y. (2 memberships)  
Bethlehem Steel Company,  
Bethlehem, Pa. (2 memberships)

Boeing Airplane Company, Seattle, Wash.  
Burgess Battery Company, Freeport, Ill.  
(4 memberships)  
C & D Batteries, Inc., Conshohocken, Pa.  
Canadian Industries Ltd., Montreal, Que.,  
Canada  
Carborundum Company, Niagara Falls, N. Y.  
Catalyst Research Corporation, Baltimore,  
Md.  
Chrysler Corporation, Detroit, Mich.  
Ciba Pharmaceutical Products, Inc., Summit,  
N. J.  
Columbian Carbon Company, New York,  
N. Y.  
Columbia-Southern Chemical Corporation,  
Pittsburgh, Pa.  
Consolidated Mining & Smelting Company of  
Canada, Ltd., Trail, B. C., Canada  
(2 memberships)  
Continental Can Company, Inc., Chicago, Ill.  
Cooper Metallurgical Associates, Cleveland,  
Ohio  
Corning Glass Works, Corning, N. Y.  
Crane Company, Chicago, Ill.  
Diamond Alkali Company, Painesville, Ohio  
(2 memberships)  
Dow Chemical Company, Midland, Mich.  
Wilbur B. Driver Company, Newark, N. J.  
(2 memberships)  
E. I. du Pont de Nemours & Company, Inc.,  
Wilmington, Del.  
Eagle-Picher Company, Chemical Division,  
Joplin, Mo.  
Eastman Kodak Company, Rochester, N. Y.  
Electric Auto-Lite Company, Toledo, Ohio  
Electric Storage Battery Company,  
Philadelphia, Pa.  
The Eppley Laboratory, Inc., Newport, R. I.  
(2 memberships)  
Federal Telecommunication Laboratories,  
Nutley, N. J.  
Food Machinery & Chemical Corporation  
Becco Chemical Division, Buffalo, N. Y.  
Westvaco Chlor-Alkali Division, South  
Charleston, W. Va.  
Ford Motor Company, Dearborn, Mich.  
General Electric Company, Schenectady,  
N. Y.  
Chemistry & Chemical Engineering  
Component, General Engineering  
Laboratory  
Chemistry Research Department

(Sustaining Members cont'd)

- General Electric Company (cont'd)  
Metallurgy & Ceramics Research  
Department
- General Motors Corporation  
Brown-Lipe-Chapin Division, Syracuse,  
N. Y. (2 memberships)  
Guide Lamp Division, Anderson, Ind.  
Research Laboratories Division, Detroit,  
Mich.
- Gillette Safety Razor Company, Boston, Mass.
- Gould-National Batteries, Inc., Depew, N. Y.
- Great Lakes Carbon Corporation, New York,  
N. Y.
- Hanson-Van Winkle-Munning Company,  
Matawan, N. J. (3 memberships)
- Harshaw Chemical Company, Cleveland,  
Ohio (2 memberships)
- Hercules Powder Company, Wilmington, Del.
- Hooker Electrochemical Company, Niagara  
Falls, N. Y. (3 memberships)
- Houdaille-Hershey Corporation, Detroit,  
Mich.
- Hughes Aircraft Company, Culver City,  
Calif.
- International Business Machines Corporation,  
Poughkeepsie, N. Y.
- International Minerals & Chemical  
Corporation, Chicago, Ill.
- Jones & Laughlin Steel Corporation,  
Pittsburgh, Pa.
- K. W. Battery Company, Skokie, Ill.
- Kaiser Aluminum & Chemical Corporation  
Chemical Research Department,  
Permanente, Calif.  
Division of Metallurgical Research,  
Spokane, Wash.
- Keokuk Electro-Metals Company, Keokuk,  
Iowa
- Libbey-Owens-Ford Glass Company, Toledo,  
Ohio
- P. R. Mallory & Company, Indianapolis, Ind.
- McGean Chemical Company, Cleveland, Ohio
- Merk & Company, Inc., Rahway, N. J.
- Metal & Thermit Corporation, Detroit, Mich.
- Minnesota Mining & Manufacturing  
Company, St. Paul, Minn.
- Monsanto Chemical Company, St. Louis, Mo.
- Motorola, Inc., Chicago, Ill.
- National Cash Register Company, Dayton,  
Ohio
- National Lead Company, New York, N. Y.
- National Research Corporation, Cambridge,  
Mass.
- Norton Company, Worcester, Mass.
- Olin Mathieson Chemical Corporation,  
Niagara Falls, N. Y.  
High Energy Fuels Organization  
(2 memberships)
- Pennsalt Chemicals Corporation,  
Philadelphia, Pa.
- Philips Laboratories, Inc., Irvington-on-  
Hudson, N. Y.
- Pittsburgh Metallurgical Company, Inc.,  
Niagara Falls, N. Y.
- Poor & Company, Promat Division,  
Waukegan, Ill.
- Potash Company of America,  
Carlsbad, N. Mex.
- Radio Corporation of America, Harrison, N. J.
- Ray-O-Vac Company, Madison, Wis.
- Raytheon Manufacturing Company,  
Waltham, Mass.
- Reynolds Metals Company, Richmond, Va.  
(2 memberships)
- Schering Foundation, Inc., Bloomfield, N. J.
- Shawinigan Chemicals Ltd., Montreal, Que.,  
Canada
- Speer Carbon Company  
International Graphite & Electrode  
Division, St. Marys, Pa. (2 memberships)
- Sprague Electric Company, North Adams,  
Mass.
- Stackpole Carbon Company, St. Marys, Pa.  
(2 memberships)
- Stauffer Chemical Company, Henderson,  
Nev., and New York, N. Y. (2 memberships)
- Sumner Chemical Company, Division of  
Miles Laboratories, Inc., Elkhart, Ind.
- Superior Tube Company, Norristown, Pa.
- Sylvania Electric Products Inc., Bayside,  
N. Y. (2 memberships)
- Sarkes Tarzian, Inc., Bloomington, Ind.
- Tennessee Products & Chemical Corporation,  
Nashville, Tenn.
- Texas Instruments, Inc., Dallas, Texas
- Titanium Metals Corporation of America,  
Henderson, Nev.
- Udylite Corporation, Detroit, Mich.  
(4 memberships)
- Upjohn Company, Kalamazoo, Mich.
- Victor Chemical Works, Chicago, Ill.
- Wagner Brothers, Inc., Detroit, Mich.
- Weirton Steel Company, Weirton, W. Va.
- Western Electric Company, Inc., Chicago, Ill.
- Wyandotte Chemicals Corporation,  
Wyandotte, Mich.
- Yardney Electric Corporation, New York,  
N. Y.

**How to make metal blackening an exact science:** What metal do you have to blacken? Steel, copper, brass, zinc? There are seven Ebonol<sup>®</sup> compounds in Enthone's specially developed series of blackeners for you to call on for jet blackness, maximum wear resistance and adhesion. Enthone is exceptionally well equipped and qualified to assist you in all phases of metal finishing. Years of practical experience, extensive research and service laboratory facilities manned by a team of specialists in the finishing field are at your service. Write us about your needs or problems. Send a sample of your product in question, if possible. Enthone, Inc., 442 Elm St., New Haven 11, Conn.



ENTHONE, INC. IS A SUBSIDIARY OF AMERICAN SMELTING AND REFINING COMPANY

# ENTHONE